# Investigating the Role of ER Stress on Mouse Pancreatic Beta-Cell Function

Irina X. Zhang

A dissertation submitted in partial fulfillment
of the requirements for the degree of
Doctor of Philosophy
(Pharmacology)
in the University of Michigan
2020

Doctoral Committee:

Professor Leslie S. Satin, Chair
Professor Peter R. Arvan
Professor Ronald W. Holz
Professor Yoichi Osawa

“Never refuse an invitation,

never resist the unfamiliar,

never fail to be polite and

never outstay the welcome.”

-- Alex Garland

Irina X. Zhang

xiaoxue@umich.edu

ORCID ID: 0000-0003-0078-1225

## Dedication

*To mom and dad, grandma and grandpa*
*thank you for your unconditional love and unwavering support*

*To Yuzhong and Lucas,*
*Thank you for your love, care, support and company*

## Acknowledgements

First and foremost, I would like to express my sincere gratitude to my mentor, Dr. Leslie S. Satin, for his continuous support of my Ph.D. study, for his inspiration, patience, dedication, and immense knowledge. I like the analogy that being a graduate student is like becoming all of the *Seven Dwarves*. During the first two years, I was *Dopey* and *Bashful*. You taught me knowledge, trained me in scientific thinking and public speaking, provided a nourishing environment for me to master a variety of techniques and skills, and helped build up my confidence. During the middle two years, I was *Sneezy*, *Sleepy*, *and Grumpy*. I lost myself in the journey, but you did not give up on me. You encouraged and directed me to come out of the jungle. In the final two years, I was *Happy*. I started to enjoy writing manuscripts. You have been very patient and helpful. I have become more and more comfortable in writing. Thank you for tirelessly editing. In the end, I will soon be called *Doc*. You might not be the best advisor for all graduate students, as not everybody is suitable for your mentoring style. You give freedom to choosing projects, prioritizing experiments, and room for creativity and exploration. However, to me, I could not have imagined having a better advisor for my Ph.D. study.

Besides my advisor, I would like to thank the rest of my thesis committee: Dr. Peter R. Arvan, Dr. Ronald W. Holz and Dr. Yoichi Osawa for their insightful comments, suggestions, feedback and encouragement. My sincere thanks also go to Dr. Malini Raghavan, Dr. Arthur Sherman, Dr. Richard Bertram and Dr. Scott Soleimanpour for paper reviews and comments. I additionally thank Dr. Arthur Sherman and Dr. Richard Bertram for guidance on statistical questions.

I am incredibly grateful to the entire Satin lab- past and present- for technical assistance and stimulating discussions. In particular, I am thankful to Dr. Suryakiran Vadrevu for enlightening me and coaching me on all the techniques I needed for this research. My study would have been impossible without you. I also would like to acknowledge Dr. Jim Ren, who is the best patch clamper on Earth, for his help on the electrophysiology studies and his contribution to the publication. You are indeed a genius on patch-clamp. I am also thankful to Benjamin Thompson for keeping the lab running smoothly and for being the best go-to person on rig issues. I have also been fortunate to work with Juan Leon in summer 2018. I truly appreciate your effort and endurance and thank you for giving me the opportunity to practice my teaching skills.

I would like to extend my appreciation to Dr. Lori L. Isom for her kindness and advice. Elizabeth Oxford, Dar-Weia Liao, Josh Daniels and Lisa Garber all offered their assistance as well. I am grateful to have had the privilege of pursuing a Ph.D. in the Department of Pharmacology.

Last but not least, no words can adequately express my gratitude towards my parents and my husband. Thank you for letting me dream big and encouraging me to pursue my dreams. Lucas, my beloved son, you have made me stronger, better and more fulfilled than ever. I love you to the moon and back.

# Table of Contents

**Dedication** ..... ii

**Acknowledgements** ..... iii

**List of Figures** ..... ix

**List of Tables** ..... xii

**List of Abbreviations** ..... xiii

**Abstract** ..... xv

**Chapter 1 Introduction: The Endoplasmic Reticulum and Calcium Homeostasis in Pancreatic Beta Cells** ..... 1

- **Abstract** ..... 1
- **Introduction** ..... 2
- **The ER and UPR activation in beta cells** ..... 3
- **Beta-cell survival and apoptosis** ..... 6
- **The UPR and loss of ER homeostasis in T1DM and T2DM** ..... 9
- **ER $Ca^{2+}$ regulation** ..... 11
- **$Ca^{2+}$ uptake and sequestration into the ER can filter $Ca^{2+}$ signaling in beta cells** ..... 14
- **ER $Ca^{2+}$ efflux channels: RyRs, IP3Rs, and the Translocon** ..... 16
- **ER membrane localized $K^{+}$ channels** ..... 19

**Store-operated $Ca^{2+}$ entry [SOCE]** ..... **20**

**Conclusions and future perspectives** ..... **21**

**Dissertation Project Preview** ..... **22**

**Figures and legends** ..... **23**

**References** ..... **27**

**Chapter 2 ER Stress Increases Store-Operated $Ca^{2+}$ Entry (SOCE) and Augments Basal Insulin Secretion in Pancreatic Beta Cells** ..... **41**

**Abstract** ..... **41**

**Introduction** ..... **42**

**Experimental procedures** ..... **44**

**Results** ..... **49**

**Discussion** ..... **57**

**Figures and Legends** ..... **64**

**References** ..... **80**

**Chapter 3 Differential Roles of Beta-cell IP3R and RyR ER $Ca^{2+}$ Channels in Tunicamycin-Induced Disruption of Beta-cell $Ca^{2+}$ Homeostasis** ..... **87**

**Abstract** ..... **87**

**Introduction** ..... **88**

**Materials and Methods** ..... **90**

**Results** ..... **94**

**Discussion** ..... **98**

**Figures and legends** ..... **103**

**References** ..... **113**

**Chapter 4 ER Stress Activates $K_{ir}2.1$ and Enhances Free $Ca^{2+}$ Oscillations in Pancreatic Beta Cells** ..... **117**

**Abstract** ..... **117**

**Introduction** ..... **118**

**Materials and Methods** ..... **120**

**Results** ..... **123**

**Discussion** ..... **126**

**Figures and legends** ..... **129**

**References** ..... **139**

**Chapter 5 Concluding Remarks, Limitations and Future Directions** ..... **142**

**Conclusions** ..... **142**

**Limitations and future directions** ..... **144**

**References** ..... **150**

# List of Figures

Figure 1.1 UPR activation mediates beta-cell survival ..... 23

Figure 1.2 UPR activation can also mediate beta-cell apoptosis ..... 24

Figure 1.3 ER $Ca^{2+}$ regulation in beta cells in the presence and absence of ER stress ..... 25

Figure 1.4 Beta-cell schematic ..... 26

Figure 2.1 Tunicamycin induced the ER stress response ..... 64

Figure 2.2 Tunicamycin triggered apoptosis ..... 65

Figure 2.3 Tunicamycin treatment decreased basal ER $Ca^{2+}$ level ..... 66

Figure 2.4 Tunicamycin increased cytosolic free $Ca^{2+}$ under sub-threshold glucose conditions . 67

Figure 2.5 Cytosolic free $Ca^{2+}$ imaging analysis ..... 68

Figure 2.6 Tunicamycin treatment resulted in the appearance of electrical activity under sub-threshold glucose conditions ..... 69

Figure 2.7 Tunicamycin increased the amount of insulin secreted under sub-threshold glucose conditions ..... 70

Figure 2.8 Increased cytosolic $Ca^{2+}$, membrane potential oscillations and insulin secretion observed after tunicamycin treatment were mediated by store-operated $Ca^{2+}$ entry (SOCE) ..... 71

Figure 2.9 STIM1 knockdown inhibited TM-triggered cytosolic $Ca^{2+}$ transients ..... 72

Figure 2.10 Effect of alternative SOCE inhibitors on cytosolic $Ca^{2+}$ oscillations ..... 73

Figure 2.11 Increased beta-cell death seen after tunicamycin treatment was not mediated by store-operated $Ca^{2+}$ entry (SOCE) ..... 74

Figure 2.12 Tunicamycin did not affect cytosolic free $Ca^{2+}$ under above-threshold glucose conditions ..... 75
Figure 2.13 Alternative ER stress inducers also increased cytosolic free $Ca^{2+}$ under sub-threshold glucose conditions ..... 76
Figure 2.14 The effect of tunicamycin on gene expression ..... 77
Figure 2.15 Tunicamycin did not affect GLUT2 expression after 6 hours of TM exposure ..... 77
Figure 2.16 Scheme of beta-cell death and increasing insulin secretion mediated by tunicamycin ..... 78
Figure 3.1 Tunicamycin altered IP3Rs and RyRs expression ..... 103
Figure 3.2 Inhibiting IP3Rs or RyRs did not prevent UPR activation ..... 104
Figure 3.3 Xestospongin C treatment restored basal ER $Ca^{2+}$ level ..... 105
Figure 3.4 Dantrolene treatment increased basal ER $Ca^{2+}$ level ..... 106
Figure 3.5 Xestospongin C did not affect cytosolic free $Ca^{2+}$ oscillations under sub-threshold glucose conditions ..... 107
Figure 3.6 Dantrolene suppressed cytosolic free $Ca^{2+}$ oscillations under sub-threshold glucose conditions ..... 108
Figure 3.7 Differential effects of xestospongin C and dantrolene on mitochondrial $Ca^{2+}$ oscillations under sub-threshold glucose conditions ..... 109
Figure 3.8 Differential effects of xestospongin C and dantrolene on beta-cell apoptosis under sub-threshold glucose conditions ..... 110
Figure 3.9 Increased mitochondrial $Ca^{2}$ was mediated by store-operated $Ca^{2+}$ entry (SOCE) .. 111
Figure 3.10 Scheme of beta-cell death and increasing insulin secretion mediated by tunicamycin ..... 111

Figure 4.1 Tunicamycin decreased $K_{ir}2.1$ expression..... 129

Figure 4.2 ML133 prevented tunicamycin-induced increased cytosolic free $Ca^{2+}$ under sub-threshold glucose conditions..... 130

Figure 4.3 Cytosolic free $Ca^{2+}$ imaging analysis ..... 131

Figure 4.4 $BaCl_2$ prevented tunicamycin-induced increased cytosolic free $Ca^{2+}$ under sub-threshold glucose conditions..... 132

Figure 4.5 Acute effect of ML133 on cytosolic free $Ca^{2+}$ under sub-threshold glucose conditions ..... 133

Figure 4.6 Tunicamycin or ML133 did not affect cytosolic free $Ca^{2+}$ under suprathreshold glucose conditions..... 134

Figure 4.7 Cytosolic free $Ca^{2+}$ imaging analysis under suprathreshold glucose conditions..... 135

Figure 4.8 Effects of $K_{ir}2.1$ inhibitor on UPR activation..... 136

Figure 4.9 ML133 prevented tunicamycin-induced beta-cell apoptosis..... 137

Figure 4.10 ER stress inducers decreased SUR1 expression on the plasma membrane..... 137

# List of Tables

Table 1. Material table ..... 79

Table 2 Oligonucleotide primers ..... 112

Table 3 Primer sequences ..... 138

## List of Abbreviations

| | |
|---|---|
| ATF6 | activating transcription factor 6 |
| CaMKII | $Ca^{2+}$/CaM-dependent protein kinase II |
| CHOP | CCAAT/enhancer-binding protein homologous protein |
| CICR | $Ca^{2+}$-induced $Ca^{2+}$ -release |
| CPA | cyclopiazonic acid |
| CPVT | catecholaminergic polymorphic ventricular tachycardia |
| DTT | dithiothreitol |
| ER | endoplasmic reticulum |
| ERAD | ER-associated protein degradation |
| ERO1–α | ER oxidoreductase 1α |
| FBS | fetal bovine serum |
| GADD | DNA damage-inducible 34 |
| GLUT2 | type 2 glucose transporters |
| GPCR | G protein-coupled receptor |
| GSIS | Glucose-stimulated insulin secretion assay |
| HFD | high-fat diet |
| HRP | horseradish peroxidase |
| IAPP | islet amyloid polypeptide |
| IMM | inner mitochondrial membrane |
| IMS | inner membrane space |
| INS | insulin-secreting |
| IP3R | inositol 1,4,5-triphosphate receptor |
| IRE1α | inositol-requiring kinase-1 |
| JNK | c-Jun N-terminal kinase |
| $K_{ATP}$ | ATP-gated $K^+$ channel |
| KHE | proton-K+ exchanger |
| LCMV | lymphocytic choriomeningitis virus |
| MAM | mitochondria-associated membranes |
| MCU | mitochondrial $Ca^{2+}$ uniporter |
| MICU | mitochondrial $Ca^{2+}$ uptake |
| MODY | maturity-onset diabetes of young |

| | |
|---|---|
| NCLX | electrogenic mitochondrial $Na^{+}/Ca^{2+}$ exchanger |
| OMM | outer mitochondrial membrane |
| ORAI1 | $Ca^{2+}$ release-activated $Ca^{2+}$ channel protein 1 |
| PARP | Poly(ADP-ribose) Polymerase |
| PDI | protein disulfide isomerases |
| PERK | PRKR-like ER kinase |
| PF | plateau fraction |
| PI | propidium iodide |
| SERCA | Sarco-endoplasmic Reticulum Calcium ATPase |
| SOCE | store-operated $Ca^{2+}$ entry |
| STIM1 | STromal Interaction Molecule 1 |
| STZ | streptozotocin |
| TG | thapsigargin |
| TM | tunicamycin |
| TUDCA | tauroursodeoxycholate |
| TXNIP | thioredoxin-interacting protein |
| UCUCA | Use and Care of Animals |
| UPR | unfolded protein response |
| VDAC | voltage-dependent anion-selective channel |
| VGCC | voltage-gated-$Ca^{2+}$ channels |
| WRS | Wolcott-Rallison Syndrome |

# Abstract

Type 2 diabetes mellitus (T2DM) is a chronic disease characterized by impaired glucose-stimulated insulin secretion in the setting of increased insulin resistance, a condition in which the body fails to respond to insulin properly. The endoplasmic reticulum (ER) serves as an essential quality control organelle and a $Ca^{2+}$ reservoir. ER stress has been proposed to cause T2DM, but the specific effects of ER stress on beta-cell function are incompletely understood. To determine the interrelationship between ER stress and beta-cell function, the work in this dissertation primarily used the well-known ER stress inducer tunicamycin (TM) to trigger ER stress in insulin-secreting INS-1(832/13) cells or isolated mouse pancreatic islets. Beta-cell function, as exemplified by the tight regulation of ER or cytosolic [$Ca^{2+}$], or membrane potential oscillations and insulin secretion, and beta-cell apoptosis were quantified at various time points, in parallel with well-established ER stress response markers. We observed that the induction of ER stress resulted in decreased ER [$Ca^{2+}$], increased cytosolic free $Ca^{2+}$ oscillations, membrane potential oscillations and increased insulin secretion, even under sub-threshold glucose conditions (e.g. 5 mM glucose) that are typically associated with only minimal insulin release. As ER $Ca^{2+}$ depletion is generally known to activate store-operated $Ca^{2+}$ entry (SOCE) in many cell types, we then used YM58483, a selective SOCE blocker. We found that the cytosolic $Ca^{2+}$ and membrane potential oscillations and increased insulin secretion we observed resulted from increased SOCE, as these were all acutely blocked by the application of YM58483.

Further dissection of TM-triggered ER [$Ca^{2+}$] loss was carried out by studying the effect of TM on the ER $Ca^{2+}$ channels, inositol 1,4,5-triphosphate receptors (IP3Rs) and ryanodine receptors (RyRs), and how their activity was tied to subsequent alterations in beta-cell $Ca^{2+}$ homeostasis. Mouse islets were treated with dantrolene (Dan, a RyR1 isoform inhibitor) or xestospongin C (XeC, an IP3Rs inhibitor) along with TM overnight. We found that TM-induced ER $Ca^{2+}$ depletion, cytosolic $Ca^{2+}$ and mitochondrial $Ca^{2+}$ oscillations were inhibited by co-treatment with Dan, whereas XeC was without effect on the oscillations. While RyR1 transcript was increased after TM exposure, transcripts corresponding to IP3R1 and IP3R2 were decreased by TM. Taken together, TM appeared to deplete ER [$Ca^{2+}$] by increasing RyR1 level and triggering the subsequent activation of SOCE, resulting in increased cytosolic $Ca^{2+}$ oscillations occurring despite the presence of sub-threshold glucose concentration.

Finally, we characterized the role of an inward rectifier $K^+$ channel, $K_{ir}2.1$, in the beta-cell. Our lab previously published data supporting the hypothesis that $K_{ir}2.1$ channels compensated for the loss of functional $K_{ATP}$ channels in islets from $K_{ATP}$ (SUR1) deficient mice in the production of cytosolic $Ca^{2+}$ oscillations. We tested here whether $K_{ir}2.1$ channels might also be involved in ER stress-induced beta-cell dysfunction, by using the selective $K_{ir}2.1$ channels inhibitor ML133. We found that overnight exposure of beta cells to ML133 suppressed TM-triggered cytosolic $Ca^{2+}$ oscillations in 5 mM glucose solution, likely due to ML133's inhibitory effect on the activation of the ER stress response marker spliced XBP1.

In summary, this dissertation maps the complex process of ER stress altering beta-cell function. In the process, we identified several novel mechanisms, including SOCE, RyR1 and $K_{ir}2.1$ channels, that may augment insulin secretion in T2DM patients, and their clinical potentials as drug targets.

# Chapter 1 Introduction: The Endoplasmic Reticulum and Calcium Homeostasis in Pancreatic Beta Cells

Irina X. Zhang, Malini Raghavan and Leslie S. Satin

This article was originally published in 2020 in *Endocrinology*, 161(2):1-14

***Abstract***

The ER (endoplasmic reticulum) mediates the first steps of protein assembly within the secretory pathway and is the site where protein folding and quality control are initiated. The storage and release of $Ca^{2+}$ are critical physiological functions of the ER. Disrupted ER homeostasis activates the UPR (for Unfolded Protein Response), a pathway which attempts to restore cellular equilibrium in the face of ER stress. Unremitting ER stress, and insufficient compensation for it results in beta-cell apoptosis, a process that has been linked to both T1DM (Type 1 diabetes mellitus) and T2DM (Type 2 diabetes mellitus). Both types are characterized by progressive beta-cell failure and a loss of beta-cell mass, although the underlying causes are different. The reduction of mass occurs secondary to apoptosis in the case of T2DM, while beta cells undergo autoimmune destruction in T1DM. In this review, we examine recent findings that link the UPR pathway and ER $Ca^{2+}$ to beta-cell dysfunction. We also discuss how UPR activation in beta cells favors cell survival versus apoptosis and death, and how ER protein chaperones are involved in regulating ER $Ca^{2+}$ levels.

## *Introduction*

Diabetes mellitus is currently a global epidemic, with T2DM accounting for over 90 percent of diabetes cases worldwide (1). T2DM is a chronic metabolic disorder characterized by impaired glucose-stimulated insulin secretion from islet beta cells in the setting of increased insulin resistance (2–4). It is now widely accepted that reduced secretion in T2DM reflects a loss of beta-cell function and possibly reduced beta-cell mass, collectively referred to sometimes as functional beta-cell mass (2,3,5,6). Understanding the loss of functional mass is critical to develop better treatments for the disease. Immunologic and stress-induced factors, in contrast, mediate the loss of beta cells in T1DM (or autoimmune diabetes) (7,8), and the further understanding of such factors is also critical.

The ER is an intracellular organelle that plays important roles in protein folding and quality control, lipid synthesis and $Ca^{2+}$ storage and release (9). Disrupted ER homeostasis and ER stress due to environmental factors have been proposed as potential causes of T2DM (10–12), and there is increasing evidence that the UPR becomes activated in pancreatic islets isolated from T2DM patients or animal models of diabetes (12–14). A loss of ER homeostasis has also been observed in beta cells during the induction of autoimmunity in T1DM, and the association between T1DM and UPR activation and consequent beta-cell death has been reviewed by several groups (12,15,16). Our understanding of the relationship between ER $Ca^{2+}$, ER stress, and beta-cell death, while the subject of considerable attention in the literature is, however, incomplete and there are many competing hypotheses as to the exact mechanisms involved. In this review, we will discuss recent findings concerning ER $Ca^{2+}$

regulation and its possible role in beta dysfunction and compromised cell survival in the context of diabetes.

### *The ER and UPR activation in beta cells*

A properly functioning ER is needed to maintain the health and survival of beta cells. Single beta cells synthesize ~1 million insulin molecules/minute (17), about half of the total amount of protein they synthesize (18). The beta-cell thus requires a very well developed and highly functional ER to support the production and secretion of insulin in response to a rise in glucose. A number of studies have suggested that a malfunctioning ER contributes to the development of both T2DM and T1DM (10–12,15,19–21).

Proteins fail to fold correctly, resulting in UPR activation. In the UPR pathway, three canonical ER membrane transducer proteins are activated once they dissociate from BiP (Binding immunoglobulin Protein, also known as HSP70 or GRP78). BiP is a molecular chaperone that binds to unfolded/misfolded proteins in the ER lumen by attaching to their hydrophobic regions and then releasing the client proteins once they are folded properly (22,23). The three transducers that are activated by BiP dissociation are PERK (PRKR-like ER kinase), ATF6 (activating transcription factor 6) and IRE1α (inositol-requiring kinase-1) (23) (Figure 1.1). In healthy cells, these transducers are occupied by BiP on the lumenal side of the ER membrane. However, when ER stress develops in response to the accumulation of misfolded proteins in the ER lumen, these proteins act as a sink for BiP, resulting in its dissociation from the transducers and subsequently, UPR activation. To avoid excessive overlap with other excellent reviews (18–20,24–28), an schematic overview of the UPR

cascade is provided in Figures 1-1 and 1-2, and we will only briefly summarize the UPR, as well as highlight new findings.

Upon dissociating from BiP, IRE1α is activated by dimerizing and then becoming autophosphorylated. Activated IRE1α splices Xbp1 (X-box binding protein 1) mRNA, removing a premature stop codon. Spliced Xbp1 (sXbp1) in turn induces the transcription of genes encoding chaperones, components of the ERAD pathway (ER-associated protein degradation), autophagy and lipid synthesis (29–31) (Figure 1.1). Additionally, sXbp1 enhances proinsulin folding by directly binding to promoter regions of five PDI (protein disulfide isomerases) family genes encoding PDI, PDIR, P5, ERp44 and ERp46 and regulating their expression (32). IRE1α cleaves other mRNAs as well, including insulin mRNA, to alleviate the ER's synthetic workload (33,34). Mice harboring a null mutation in one of the Xbp1 alleles become insulin resistant, demonstrating a key role of UPR responses in insulin action (35).

The transducer of the Xbp1 arm of the pathway, IRE1α is also complex as it has both kinase and RNase activity (31). *Transiently* exposing beta cells to high glucose enhances insulin biosynthesis in a manner that is dependent on the kinase activity of IRE1α but independent of BiP dissociation or Xbp1 splicing (36). In contrast, *chronic* high glucose suppresses insulin biosynthesis and induces ER stress (36), as reduced insulin transcript has been observed in INS-1 cells treated chronically with high glucose. Obviously then, the various possible outcomes that can result from activation of the IRE1α arm of the UPR in beta cells

require that a higher order of regulation must also be involved, although this regulation is not well understood.

In terms of the PERK arm of the UPR, after BiP dissociates from it, PERK also undergoes oligomerization and autophosphorylation, as for IRE1α, leading to the phosphorylation of eIF2α (eukaryotic initiation factor 2 α subunit) (37). Phosphorylated eIF2α represses the initiation of global protein translation and activates ATF4 (activating transcription factor 4), which in turn increases the expression of chaperones, oxidoreductases, and genes involved in ERAD and autophagy (27,38–40), as described for sXbp1. PERK-deficient mice suffer a loss of beta cells and develop diabetes in their early weeks of life (41).

As mentioned, insulin resistance is an important characteristic of T2DM and normal beta cells compensate for it by increasing their insulin-secretory capacity and their cell number if they are genetically endowed to do so. Several mechanisms underlie the expansion of beta-cell mass that is needed in order to cope with augmented insulin demand, including changes in the expression of cell cycle proteins and transcription factors (42). UPR activation is required to hasten beta-cell proliferation that occurs in response to glucose (43). Thus, an elevation of glucose *in vivo* or *in vitro* increases beta-cell proliferation, especially in rodent models, while chemical agents that reduce ER stress decrease it (43). In human islets exposed to high glucose or in islets from the *db/db* mouse, a model of T2DM, beta-cell proliferation occurs simultaneously with UPR activation (43). Within the UPR pathway, ATF6, rather than PERK or IRE1, has been shown to contribute to the beta-cell proliferation that occurs in response to increased insulin demand (43) (Figure 1.1). In addition to high

glucose exposure, or the addition of chemical stressors such as thapsigargin or tunicamycin (see below), other physiological challenges can lead to ER stress in beta cells. For example, hyperlipidemia, a common feature of patients with type 2 diabetes that is linked to insulin resistance, or exposure to saturated fatty acids such as palmitate have been shown to induce ER stress by activating the PERK and IRE1a pathways (44). Palmitate also increases the saturated lipid content of the ER, resulting in ER dilation (a marker of ER stress), trafficking of the ER chaperones GRP70 and PDI from the ER to the cytosol, and the depletion of ER $Ca^{2+}$ (45).

Mutations in proinsulin, the protein precursor of insulin that normally accounts for 30-50% of the total protein synthesis of the beta-cell (46) can also lead to ER stress. *Akita* and *Munich* mice carry a mutation in the *Ins2* (insulin 2) gene (C96Y in *Akita* and C95S in *Munich*) that disrupts disulfide bond formation leading to misfolded proinsulin (47,48). These mouse models show that misfolded proteins in the ER can sometimes lead to ER stress-induced diabetes in the whole animal (48,49). IAPP (islet amyloid polypeptide), a protein that is normally co-secreted with insulin from beta cells can, under certain conditions, form toxic oligomers in the cell that can also trigger ER stress (50). It has been reported that transgenic mice expressing hIAPP (human islet amyloid polypeptide) fed a high-fat diet become glucose-intolerant and insulin-resistant (50,51). It has also been shown that hIAPP transgenics exhibit hIAPP aggregation and misfolding that in turn triggers ER stress, presumably by making ER membrane leaky to $Ca^{2+}$ (50,52).

***Beta-cell survival and apoptosis***

The UPR exists in two states—an adaptive state of low ER stress, maintained ER homeostasis and beta-cell pro-survival and an apoptotic state where apoptosis is initiated and cell death ensues in response to pathological conditions (53). To maintain or activate the pro-survival state when the cell faces stressful conditions, IRE1, PERK and ATF6 become activated in order to generate a 'stress' signal that is transmitted from the ER lumen to the cytosol and nucleus. Transmission of this stress signal re-establishes normal protein homeostasis by inhibiting global gene transcription, increasing the degradation of misfolded proteins through ERAD, and increasing the degradation of dysfunctional cellular components through autophagy (Figure 1.1). Additionally, an increase in the protein-folding capacity of the cell occurs due to increased chaperone expression.

Prolonged and unmitigated ER stress, in contrast, activates cellular pathways that favor apoptosis (12,13,19,20,25,54,55) (Figure 1.2). Apoptosis then decreases beta-cell mass, which increases the stress experienced by the remaining beta cells as they try to compensate for the reduced insulin levels and experience increased secretory demand, resulting in additional beta-cell death.

IRE1α triggers cell death by inducing the degradation of many ER-localized mRNAs (33), as well as cleaving miRNAs that normally repress caspase 2 mRNA translation; this increases caspase 2-mediated apoptosis (56) (Figure 1.2). Additionally, IRE1α couples to TRAF2 (tumor necrosis factor receptor-associated factor 2) localized to the ER membrane, which recruits ASK1 (apoptosis signal-regulating kinase 1). ASK1 phosphorylates and concomitantly activates JNK (c-Jun N-terminal kinase) to stimulate apoptosis (20). Moreover,

the IRE1α-TRAF2 interaction with procaspase 12 promotes its cleavage to active caspase 12, which in turn cleaves caspase 3 to induce apoptosis (20,57,58).

Recent studies also implicate the ABL family of tyrosine kinases in the enhancement of ER stress-mediated apoptosis through the hyperactivation of IRE1α RNase activity (59). TXNIP (thioredoxin-interacting protein) is a newly discovered pro-apoptotic protein that is part of the ER stress pathway (60). The IRE1α and PERK pathways, via TXNIP, lead to an increase in the production of IL-1β, a highly pro-inflammatory and cell-death inducing cytokine (61,62). Cytokine treated INS-1 cells thus have upregulated TXNIP and increased cell death. Interestingly, suppressing TXNIP with the diabetes drug sitagliptin prevents TXNIP-mediated cell death (63).

PERK promotes beta-cell survival by attenuating global translation while upregulating AATF (apoptosis antagonizing transcription factor) through eIF2α phosphorylation. AATF activates AKT1 via STAT3, and AKT1 is reported to suppress apoptosis (64) (Figure 1.1). Activated eIF2α also upregulates ATF4, which promotes cell death through CHOP (CCAAT/enhancer-binding protein homologous protein) (20) (Figure 1.2). In contrast, ATF6 promotes beta-cell survival by increasing the protein-folding capacity of the cell as well as the components of ERAD (Figure 1.1). For example, BiP is a major target of ATF6. On the other hand, ATF6 favors cell death through CHOP (20) (Figure 1.2). Again, it is clear that these signaling pathways are complex in the outcomes they promote require a balancing of competing factors.

CHOP induces apoptosis through several different mechanisms. CHOP activates ERO1-α (ER oxidoreductase 1α) leading to ER hyperoxidation, and disruption of the interaction between the chaperone ERp44 and IP3R1 (inositol 1,4,5-trisphosphate receptor type 1), causing IP3R1 hypersensitivity and concomitantly increased ER $Ca^{2+}$ release (65–67). ER $Ca^{2+}$ depletion can trigger in turn activate calpain 2, leading to beta-cell apoptosis (68) by activating caspase 12 and JNK (69,70). Moreover, CHOP downregulates anti-apoptotic Bcl-2 and Trb3 levels and induces pro-apoptotic Bim to favor apoptosis (24,25,65–67). CHOP upregulates DNA damage-inducible 34 (GADD34), a protein involved in cell growth arrest and DNA damage, leading to apoptosis (24,25,65–67). Studies in model systems have shown that Bcl-2 can directly interact with both IP3Rs and RyRs (ryanodine receptors) to suppress ER $Ca^{2+}$ release (71,72). Bcl-2 is known to preserve the integrity of mitochondrial membranes and has been shown to inhibit the release of proapoptotic cytochrome C from the mitochondrion (73) (Figure 1.2).

### *The UPR and loss of ER homeostasis in T1DM and T2DM*

Recent studies provide additional evidence for UPR dysregulation in both T1DM and T2DM. Dysregulated UPR exhibiting decreased ATF6 and Xbp1 has been observed in two different mouse models of T1DM (NOD mice, a model of autoimmune diabetes, and mice expressing the LCMV gene (lymphocytic choriomeningitis virus)). ATF6 and Xbp1 are also decreased in islets taken from human T1DM patients (74). The chemical chaperone TUDCA (tauroursodeoxycholate) prevents the loss of ATF6 and Xbp1, reduces the incidence of diabetes and elevates plasma insulin levels and islet insulin content without altering the immune cell populations of the pancreases of T1DM mouse models (74).

Proinflammatory cytokines such as TNF-α, IL-1β and IFN-γ have been implicated in T1DM and T2DM (75,76) and have been shown to alter $Ca^{2+}$ handling, induce UPR dysregulation, and alter glucose-induced insulin release in beta cells (76,77). The proinflammatory cytokines, IL-1β, TNF-α and IFN-γ in combination, IL-1β and IFN-γ in combination, or IL-1β or IFN-γ presented alone increase PERK/eIF2α phosphorylation, JNK phosphorylation, and CHOP expression in beta cells (78). In one study, IL-1β increased Xbp1 splicing and ATF4 and CHOP expression (79). In contrast, in a separate report, IFN-γ alone decreased Xbp1 splicing and BiP expression, while having no effect on CHOP and ATF4 expression (80). Therefore, cytokine may preferentially affect different arms of the UPR pathway when applied individually.

The loss of ER homeostasis also affects autoantigen production in T1DM. Post-translational modifications of proteins such as deamidation and citrullination are known to be induced in diabetes, and the modified peptides that result can become targets of immune cell recognition and activation (81). $Ca^{2+}$-dependent enzymes that mediate such post-translational modifications, such as tTG2 (tissue transglutaminade2) are activated after thapsigargin-mediated ER $Ca^{2+}$ depletion (82). Additionally, the cytokine IL-1β has been shown to convert specific arginine residues of BiP, a diabetes-related autoantigen, into citrulline (83,84). Such mechanisms can link ER $Ca^{2+}$ dysregulation and elevated cytokine levels to the generation of autoimmune epitopes in T1DM.

In T2DM human pancreas, CHOP nuclear localization was found to be six times higher than in non-diabetic human pancreas, but nuclear CHOP was not detected in T1DM human pancreas (85). In addition, BiP, ATF4, ATF6, eIF2α phosphorylation and Xbp1 splicing are all upregulated in islets isolate from *db/db* diabetic mice (86). In contrast, other studies demonstrate reduced ATF6 and Xbp1 levels in T2DM (87,88).

UPR regulation has also been observed in studies on WRS (Wolcott-Rallison Syndrome) and MODY (maturity-onset diabetes of young). WRS is a rare autosomal recessive syndrome (89). A deficiency of PERK in humans is the cause of WRS, and it associates permanent neonatal diabetes (89). PERK deficient mice exhibit increased expression of BiP, IRE1α, Xbp1 splicing and processed ATF6 (90,91). MODY is a rare inherited form of diabetes that runs strongly in families (92). There are at least 14 types of MODY caused by mutations in one of 14 genes which disrupt insulin production (92). For example, MODY4 is caused by heterozygous variants in the *Pdx1* (pancreatic duodenal homeobox 1) gene (93). Heterozygous mutations in *Pdx1* are associated with T2DM. *Pdx1* heterozygous mice exhibit elevated BiP transcripts (93).

### *ER $Ca^{2+}$ regulation*

Glucose-dependent insulin secretion is a $Ca^{2+}$ dependent process. In beta cells, exposure to elevated glucose triggers closure of the ATP-gated $K^+$ channel (KATP) to inhibit $K^+$ efflux and this results in plasma membrane depolarization. The voltage-gated $Ca^{2+}$ channel then opens and allows $Ca^{2+}$ influx (94,95). The ER plays an important role in intracellular $Ca^{2+}$ signaling and it can help coordinates various intracellular signaling pathways that affect beta-

cell function and insulin secretion (9,10,96). $Ca^{2+}$ ions are sequestered within the ER due to activity of the SERCA pump (Sarco/Endoplasmic Reticulum $Ca^{2+}$-ATPases, see below) and are released into the cytosol in response to various physiological triggers. For example, $Ca^{2+}$ ions are released from the ER following the activation of RyRs or IP3Rs by increased cytosolic $Ca^{2+}$, a process referred to as CICR ($Ca^{2+}$-induced $Ca^{2+}$ -release) mechanism (97,98). RyRs and IP3Rs are $Ca^{2+}$ channels that are resident in the ER membrane to mediate $Ca^{2+}$ efflux from the organelle. Of course, a rise in cytosolic $Ca^{2+}$ resulting from either $Ca^{2+}$ influx or ER release results in the triggered fusion and exocytosis of insulin-containing granules to release insulin into the extracellular space. It is crucial for the cell to maintain a concerted regulation of ER $Ca^{2+}$ uptake and release in order to preserve normal $Ca^{2+}$ signaling. As noted above, unresolved ER stress can result in the depletion of $Ca^{2+}$ from the ER and subsequent apoptosis (Figure 1.2). Conversely, there are UPR-independent routes to decrease ER free $Ca^{2+}$ under different pathological conditions, which in turn can result in a loss of ER homeostasis and cell death (99–101).

ER $Ca^{2+}$ is regulated by three classes of handling proteins: (i) SERCAs, which are pumps that transport free $Ca^{2+}$ from the cytosol to the ER lumen in an ATP-requiring manner; (ii) ER $Ca^{2+}$-binding proteins, which can bind significant amounts of $Ca^{2+}$ in the ER lumen, and (iii) ER $Ca^{2+}$ channels, the RyRs, the IP3Rs and the translocon, which all can potentially release $Ca^{2+}$ into the cytosol (Figure 1.3A). Dysfunction manifested in any of the three classes of ER proteins can disrupt ER homeostasis.

The genes encoding the SERCAs (e.g. SERCA1, 2 and 3) generate more than 14 different isoforms by alternative splicing (102). SERCA 2b (110 kDa) is the predominant isoform expressed in beta cells (103), and is downregulated in islets from the *db/db* mouse, cytokine treated beta cells and islets from T2DM donors (79,104) (Figure 1.3B). Interestingly, this loss was alleviated by the application of pioglitazone, an agonist of PPAR-$\gamma$ (peroxisome proliferator-activated receptor) that regulates SERCA2b transcription (104). Increasing SERCA2b expression improves insulin secretion and reduces apoptosis in response to inflammatory cytokines or high glucose in INS-1 cells (104). Other studies also support the hypothesis altered SERCA expression can contribute to diabetes (105). In addition, islets isolated from whole-body SERCA2 haploinsufficient mice exhibited lower ER $Ca^{2+}$ levels, reduced insulin secretion and increased ER stress and beta-cell death in mice that were fed a high fat diet (103).

PERK and calcineurin have been shown to be important to insulin secretion and glucose homeostasis through regulating SERCA activity and ER $Ca^{2+}$ uptake. In addition to regulating the UPR, PERK is also essential for normal beta-cell function. Similar to human WRS, PERK deficient mice rapidly become hyperglycemic and exhibit reduced insulin content and beta cells apoptosis beginning fourth postnatal weeks (41). Calcineurin (protein phosphatase 3), a $Ca^{2+}$ and calmodulin dependent protein phosphatase, regulates human beta-cell survival, as its inhibition induces apoptosis (106). Cavener and his group members have shown that acute inhibition of PERK or calcineurin impairs glucose-stimulated insulin secretion and $Ca^{2+}$ influx through SOCE (store-operated $Ca^{2+}$ entry, see below) in beta cells (107). PERK inhibition decreases ER $Ca^{2+}$ reuptake via SERCA by reducing the interaction

of SERCA and calnexin, which binds to SERCA and suppresses the SERCA activity. Calcineurin interacts with PERK and dephosphorylates calnexin. Therefore, PERK and calcineurin act together to regulate SERCA activity (107).

***$Ca^{2+}$ uptake and sequestration into the ER can filter $Ca^{2+}$ signaling in beta cells***

ER $Ca^{2+}$, uptake in beta cells during glucose-induced $Ca^{2+}$ oscillations, filters and shapes the waveforms of the cytosolic $Ca^{2+}$ oscillations by introducing a slow time constant (3). Thus, as $Ca^{2+}$ initially rises in the cytosol, its slower uptake into the ER via SERCA alters the dynamics of the $Ca^{2+}$ rise (reduced SERCA activity increases the rate of rise of cytosolic $Ca^{2+}$ in response to $Ca^{2+}$ influx into the cell) and seen in the cytosol. In addition, once the ER is filled with $Ca^{2+}$ by the end of the oscillation active phase, the ER will begin to passively release $Ca^{2+}$, giving rise to a secondary (and slower) phase of decay at the end of the oscillation. This filtering of cytosolic $Ca^{2+}$ transients has been modeled by Sherman and colleagues who showed that it can have a profound effect on the time courses of $Ca^{2+}$-dependent processes in the beta-cell (108). Of interest is that experimental studies of the ER $Ca^{2+}$ uptake and release processes failed to establish the identity of the ion channel(s) or pathway(s) mediating slow ER $Ca^{2+}$ leak (109). However, it was clearly *not* mediated by either IP3Rs or RyRs, as it was insensitive to drugs known to block these channels. As unconventional ER $Ca^{2+}$ channels such as Sec61 (see below) may fulfill this role, more investigations seem warranted.

The ER contains approximately 2 mM total $Ca^{2+}$, and only a fraction of this is free. The majority of ER $Ca^{2+}$ is thought to be bound to various $Ca^{2+}$-binding proteins including,

calreticulin, BiP, PDI and GP94 (110). Calreticulin has a highly acidic C-terminal domain that contains multiple low affinity $Ca^{2+}$-binding sites (111,112). These sites bind $Ca^{2+}$ with a $K_D$ in the ER $Ca^{2+}$ range (113,114), and a number of studies indicate that the overexpression of calreticulin increases the $Ca^{2+}$ storage capacity of the ER (115,116). UPR activation induced by high glucose or HFD treatment in mice shows increased expression of calreticulin (43,117,118). In addition to increasing ER $Ca^{2+}$ storage, calreticulin is a chaperone for nascent ER glycoproteins, that contains monoglucosylated glycans, the key structural elements of glycoproteins that are recognized by calreticulin. Via this function, calreticulin could contribute to the enhanced maintenance of ER homeostasis in a stressed ER (119).

BiP is suggested to play a role in ER $Ca^{2+}$ storage in some studies (120), whereas other studies support the hypothesis that $Ca^{2+}$ binding by BiP primarily regulates its interactions with nucleotides and other factors (121). Structural studies of truncated BiP constructs indicate the presence of two $Ca^{2+}$ binding sites in the vicinity of the nucleotide binding/catalytic site of BiP (122). Further studies are required to understand whether BiP contains low affinity $Ca^{2+}$ binding sites that contribute to ER $Ca^{2+}$ storage, and if so, where such sites are located.

While a number of reviews indicate that reduced ER $Ca^{2+}$ levels impair the conformation and function of ER $Ca^{2+}$-binding chaperones, there have been relatively few studies of this. In fact, in one study, decreasing the $Ca^{2+}$ concentration in the 1-0.1 mM range increased the ATPase activity of recombinant BiP (123). Additionally, the binding of calreticulin to

monoglucosylated glycans was shown to be independent of $Ca^{2+}$ concentration (124). On the other hand, low affinity $Ca^{2+}$ binding influences the structure of calreticulin (114,125) and mediates its phospholipid binding (126). Moreover, the ER retention of several $Ca^{2+}$-binding chaperones at least partly depends on the maintenance of normal ER $Ca^{2+}$ levels (127–131) and/or the presence of their $Ca^{2+}$-binding domains (132). Thus, by interfering with their proper localization, ER $Ca^{2+}$ depletion is predicted to interfere with the proper function of $Ca^{2+}$-binding chaperones.

### *ER $Ca^{2+}$ efflux channels: RyRs, IP3Rs, and the Translocon*

$Ca^{2+}$ exits the ER down its concentration gradient via RyRs or IP3Rs, or the translocon as mentioned previously. $Ca^{2+}$ release through RyRs is primarily triggered by increased cytosolic $Ca^{2+}$ through the process of CICR. The advantage of CICR is that it can occur rapidly and regeneratively, as $Ca^{2+}$ released into the cytosol then facilitates the further release of more $Ca^{2+}$, a positive feedback process (97,133). RyRs are the largest known ion channel proteins. There are three RyR isoforms, each having a molecular mass of 565 kDa (134,135). RyR1 and RyR2 are primarily expressed in skeletal and cardiac muscle, respectively, and RyR3 is expressed at rather low levels in various other tissues (134). In beta cells, RyR2 is the predominant isoform, but RyR1 is also expressed, albeit at a comparatively low level (136). RyR3 appears to be minimally expressed in beta cells (136). However, the existence of RyRs and their significance for beta-cell function has been the subject of considerable controversy given their relatively low level of expression (137) and whether or not there is an important role for cyclic ADP-ribose as a stimulator of $Ca^{2+}$ release via RyRs (138,139).

RyR activity can be increased by ATP, CaMKII ($Ca^{2+}$/CaM-dependent protein kinase II) (135,140)) or PKA (135,140,141). The drug ryanodine, a classic blocker of RyRs has a complicated pharmacology as it has both agonist and antagonist actions on RyRs depending on the dose used (142). Thus, RyRs are activated by ryanodine at nanomolar concentrations, where ryanodine binding to the RyR keeps it in an open state that allows ER $Ca^{2+}$ release into the cytosol. In contrast, at >100 μM, ryanodine inhibits RyRs (140). Another well-known RyR blocker is the muscle relaxant dantrolene (143). Dantrolene selectively blocks RyR1 and RyR3 but not RyR2 (143). Evans-Molina and colleges have proposed that tunicamycin-induced ER stress increases RyR activity and ER $Ca^{2+}$ release without altering RyR2 expression and results in increased spontaneous cytosolic $Ca^{2+}$ transients in response to elevated extracellular $Ca^{2+}$ levels in INS 1 cells and dispersed cadaveric human islets. Islets isolated from Akita mice exhibit cytosolic $Ca^{2+}$ oscillations stimulated by 5 mM glucose, whereas wildtype littermate mice do not have the same sensitivity (136). Ryanodine suppresses the glucose-stimulated $Ca^{2+}$ oscillations in Akita mice and decreases tunicamycin-induced spontaneous $Ca^{2+}$ transients in INS 1 cells and human islets. They also suggest RyR2 as the isoform gains function in response to ER stress. In addition to the fact that RyR2 is the predominant isoform of RyR, knock-in mice with a mutation of chronic activation of RyR2 mimicking constitutive CaMKII- phosphorylation develops glucose intolerance and exhibits diminished $Ca^{2+}$ responses and impaired glucose-induced insulin secretion (136,144). However, in this study dantrolene (at 1 μM) failed to restore ER $Ca^{2+}$ when applied to tunicamycin-treated INS-1 cells. In a separate study, on the other hand, 30 μM dantrolene decreased thapsigargin-triggered apoptosis in MIN6 cells, an insulin secreting mouse cell

line (145). These findings indicate that ER stress can cause complex and cell-type dependent modulation of ER $Ca^{2+}$ efflux channels.

Calstabin (a $Ca^{2+}$ channel stabilizing binding protein) binds to RyRs and prevents ER $Ca^{2+}$ leak by stabilizing the closed states of the RyRs (134). Calstabin 2 is a subunit of the RyR2 macromolecular complex and its dissociation from RyR2 causes increased ER $Ca^{2+}$ leak (134). Human patients and mice harboring mutations that alter the binding of calstabin2 to RyR2 (for example, CPVT (catecholaminergic polymorphic ventricular tachycardia)) are glucose intolerant and have decreased glucose-stimulated insulin secretion due to increased ER $Ca^{2+}$ leakage. Islets from T2DM donors or diabetic mouse islets have oxidation/nitrosylation of RyR2 and a depletion of calstabin2. Inhibiting the dissociation of calstabin2 from RyR2 using the drug Rycal S107 reverses glucose intolerance and improves insulin secretion in both human and murine islets, indicating that the proper functioning of RyR2 channels is critically important for beta cells (134).

IP3Rs contain an IP3 binding-core domain near their N-termini. Upon binding IP3, the binding-core rearranges and then dissociates from its associated suppressor domain, resulting in IP3R activation. IP3Rs become less sensitive to IP3 when the ER $Ca^{2+}$ level is low in order to protect the ER from becoming too $Ca^{2+}$ depleted. RyRs and IP3Rs share 40% homology (135), and as for RyRs, IP3Rs are also regulated by cytosolic $Ca^{2+}$, ATP, and protein phosphorylation, and they also interact with other proteins (135,146–148). Three IP3R isoforms (IP3R1, IP3R2 and IP3R3) exist and each has a molecular weight about 300 kDa (135,149). IP3R2 is most highly expressed in cardiac and skeletal muscle, as well as

liver and kidney (150), while IP3R3 is expressed in both endocrine and exocrine pancreas, as well as other tissues (150). While genetic variation within IP3R3 has been linked to T1DM (151), IP3R1 is the most abundant isoform in beta cells (152).

Many proteins interact with IP3R1. As noted above (Figure 1.2), the chaperone ERp44 inhibits IP3R1 when ER $Ca^{2+}$ levels are low (67), and BiP helps assemble IP3R1 into tetramers and is required for $Ca^{2+}$ release by the receptor (67) (Figure 1.3A). ERp44 competes with BiP for the same site on IP3R1 (67). In the face of ER stress, ERp44 upregulation causes BiP to dissociate from IP3R1, leading to decreased $IP_3$-induced $Ca^{2+}$ release (Figure 1.3B).

In contrast to RyRs and IP3Rs, the translocon is a $Ca^{2+}$ 'leak channel' (153,154), but it is not regulated by cytosolic $Ca^{2+}$ or by GPCR (G protein-coupled receptor) activation. Sec61, a core component of the translocon, is located on the ER membrane (153), along with other protein components. The Sec61 complex forms a protein-conducting channel to translocate nascent polypeptide chains from the cytosol to the ER during translation. The translocon complex has also been proposed to mediate ER $Ca^{2+}$ leak (154). Mice with Sec61 gene point mutation fed on HFD are hyperglycemic and hypoinsulinemic compared to their wildtype littermates. After feeding these mice HFD for a week, the islets isolated from these mice show upregulation of BiP and CHOP as well as an increase in apoptosis (155).

***ER membrane localized $K^+$ channels***

The ER $Ca^{2+}$ concentration is greater (e.g. 300-700 μM) than that of the cytosol (e.g. 50 – 100 nM) and the activity of ATP-fueled SERCA pumps is largely responsible for maintaining this ER $Ca^{2+}$ gradient in the absence of an ER potential difference or a $K^+$ concentration gradient (156). SERCA pumping of $Ca^{2+}$ from the cytosol to the ER is associated with a proton ejection and a proton-$K^+$ exchanger (KHE) operates to reclaim these ejected protons (156–159). Various $K^+$ channels in the ER can in turn mediate $K^+$ reuptake by the ER.

TALK-1 and TASK-1 are two ER-located $K^+$ channels (Figure 1.3) that likely help mediate these ER $K^+$ fluxes (160). Mouse beta cells lacking TALK-1 have been reported to have elevated ER $Ca^{2+}$ and reduced ER $Ca^{2+}$ release (160,161). Therefore, TALK-1 modulates ER $Ca^{2+}$ homeostasis. TALK-1 deficient mice have decreased expression of BiP after a prolonged high-fat diet (HFD), which implicates that maintaining ER $Ca^{2+}$ may prevent UPR activation in islets (161). TALK-1 deficient mice also have decreased mRNA encoding SERCA 2b and 3 after a prolonged HFD, which perhaps suggests they may prevent ER $Ca^{2+}$ overload (161). Much remains to be understood about changes to TALK-1 and TASK-1 expression and their functional roles under ER stress conditions in beta cells.

***Store-operated $Ca^{2+}$ entry [SOCE]***

A reduction in ER $Ca^{2+}$ is sensed by an ER $Ca^{2+}$ sensor called STIM1 (STromal Interaction Molecule 1) which multimerizes and then redistributes to the ER-plasma membrane junction. Here, STIM1 binds to and subsequently opens ORAI1 ion channels which are $Ca^{2+}$ permeable, triggering $Ca^{2+}$ entry into the cytoplasm as part of a process called SOCE (162).

This mechanism was originally proposed by Putney and colleagues based on data from inexcitable cells, and they called the mechanism 'capacitative $Ca^{2+}$ entry'. This is in reference to the fact that the release of $Ca^{2+}$ from the ER and subsequent ER $Ca^{2+}$ depletion concomitantly increased the uptake of extracellular $Ca^{2+}$ and ER $Ca^{2+}$ repletion (163), much like a capacitor that can store charge but then discharge it. Recent studies show that treating human and mouse islets with a cocktail of TNF-α, IL-1β and IFN-γ or glucolipotoxicity-inducing agents reduce levels of STIM1 protein (77). STIM1 expression is also reduced in STZ (streptozotocin)-treated mice and islets from T2DM donors. Restoration of STIM1 expression in islets from T2DM donors was found to improve insulin secretion (77).

Mutations in the components comprising SOCE have been linked to several major diseases, including severe combined immunodeficiency (164). Precise regulation of SOCE is critical for maintaining normal glucose-stimulated insulin secretion in beta cells (165). In these cells, SOCE also helps maintain ER $Ca^{2+}$ and provides an extra $Ca^{2+}$ influx mechanism to help depolarize beta cells in response to GPCR agonists such as GLP-1 and acetylcholine (166). In pancreatic alpha cells, Gylfe and colleagues have proposed that SOCE plays an essential role in the stimulus secretion coupling mechanism that links low glucose to increased glucagon secretion (167), although this remains controversial (168).

### *Conclusions and future perspectives*

Overall, there has been remarkable progress in our understanding of how the UPR and $Ca^{2+}$ handling become dysregulated in diabetes. Genetic mutations, membrane lipid and glucose induced alterations as well as inflammatory mediators influence the induction of the UPR, as

well as the expression or activity of key regulators of ER $Ca^{2+}$. In turn, a loss of ER homeostasis has important consequences for insulin secretion and glucose intolerance in T2DM and for the generation of autoimmune epitopes in T1DM. However, many gaps remain in our understanding of the detailed molecular mechanisms involved in the loss of ER homeostasis and also $Ca^{2+}$ dysregulation in diabetes, which may be important for identifying new drug targets. Further studies thus are needed to apply our current level of knowledge to design of new therapeutics.

### *Dissertation Project Preview*

In this thesis, we aim to investigate the interrelationship between ER stress and pancreatic beta-cell function and beta-cell apoptosis. The function of a beta-cell includes cytosolic $Ca^{2+}$ oscillations, membrane potential oscillations, mitochondrial $Ca^{2+}$ oscillations and insulin secretion (Figure 1.4, beta-cell cartoon). We begin by demonstrating how beta-cell function and viability are affected as a consequence of ER stress (Chapter 2). Chapter 3 focuses on the mechanism of ER stress-inducing ER $Ca^{2+}$ loss. Next, chapter 4 characterizes the inward rectifier $K^+$ channel $K_{ir}2.1$ in beta cells under ER stress conditions. Finally, section 5 concludes significant findings, discusses limitations and proposes future directions.

***Figures and legends***

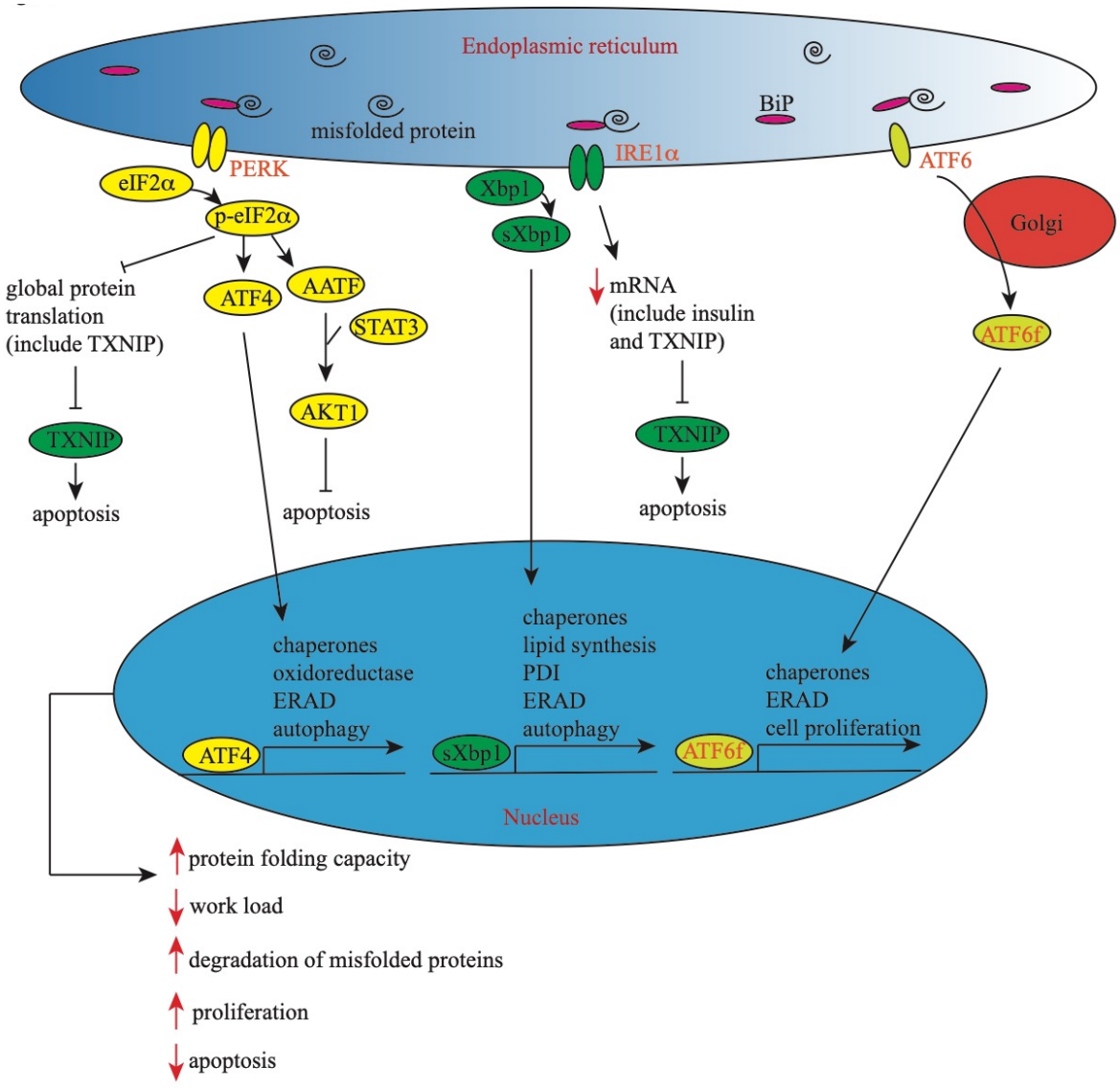


*Figure 1.1 UPR activation mediates beta-cell survival*

BiP is sequestered by binding to ER stress-inducing unfolded/misfolded protein in the ER lumen, leading to its dissociation from PERK, IRE1α and ATF6, which are ER membrane-localized stress transducers. Activated PERK phosphorylates eIF2α, which inhibits global protein translation and activates ATF4. ATF4 mediates the transcription of genes that encode chaperones, oxidoreductases, ERAD and autophagy. IRE1α cleaves Xbp1 mRNA, and spliced Xbp1 (sXbp1) mRNA in turn mediates gene transcription of chaperones, lipid synthesis, and ERAD and autophagy. In addition, sXbp1 promotes proinsulin folding through various PDI family genes. When ATF6 is released from BiP, it translocates to the Golgi complex, where ATF6 is cleaved to generate ATF6f. ATF6f activates the transcription of genes encoding protein chaperones and ERAD. ATF6f also triggers beta-cell proliferation. When mild or tolerable levels of UPR are

activated in beta cells, the UPR transducers PERK, IRE1α and ATF6 mediate the transcription of genes for chaperones, ERAD components and autophagy in an attempt to restore ER homeostasis. UPR activation also triggers mRNA decay and attenuates global gene translation to reduce the workload on the ER. Finally, the induction of AKT1 and reduction of TXNIP serve to inhibit cell death. Elements of the UPR pathway are essential to maintaining beta-cell homeostasis under normal conditions, due to the high secretory workload placed on the beta-cell.

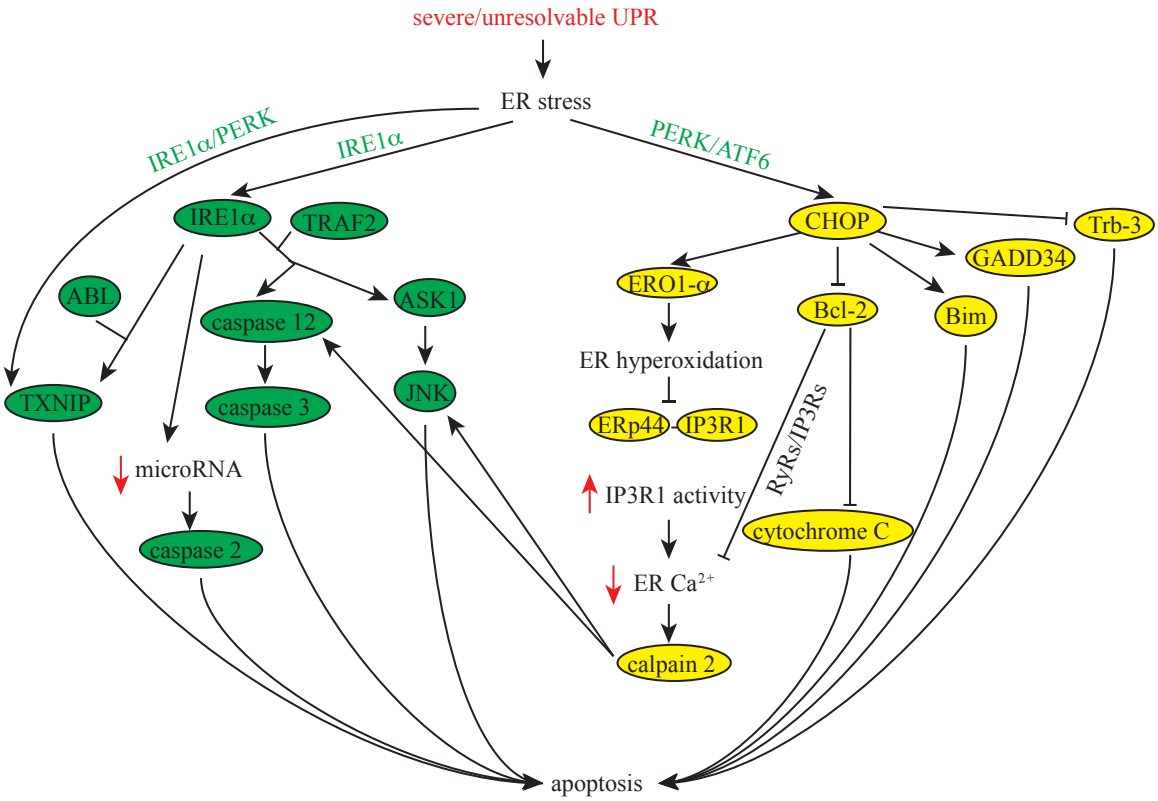


*Figure 1.2 UPR activation can also mediate beta-cell apoptosis*

Prolonged and unresolvable ER stress and concomitant UPR activation can trigger the activation of apoptotic pathways like the ASK1-JNK and CHOP mediated apoptosis pathways. ER stress also upregulates caspases and TXNIP, proteins that are involved in apoptosis. IRE1α cleaves microRNA that suppresses caspase 2 translation. IRE1α also couples to TRAF2 and triggers apoptosis. PERK and ATF6 activation upregulate CHOP and leads to apoptosis by upregulating GADD34, Bim and ERO1-α and by downregulating Trb-3 and Bcl-2. ERO1-α causes ER hyperoxidation that disrupts ERp44-IP3R1 interaction, causing IP3R1 hypersensitivity and increases ER $Ca^{2+}$ release. Bcl-2 suppresses IP3Rs and RyRs-mediated ER $Ca^{2+}$ release. ER $Ca^{2+}$ depletion leads to beta-cell apoptosis through the activation of calpain 2, which activates caspase 12 and JNK.

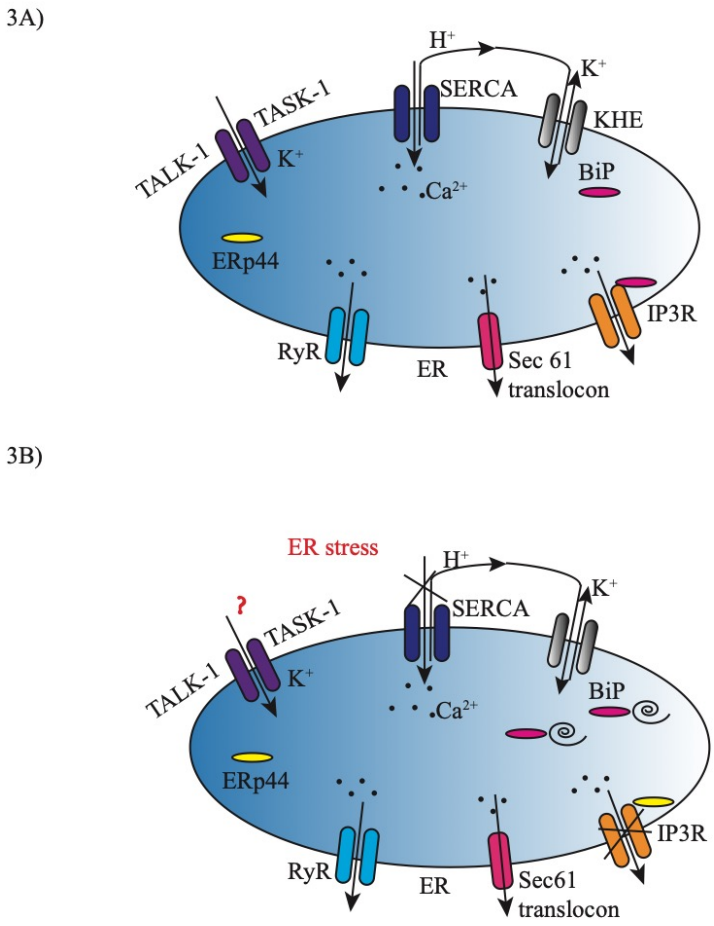


*Figure 1.3 ER $Ca^{2+}$ regulation in beta cells in the presence and absence of ER stress*

ER $Ca^{2+}$ is regulated by SERCAs, RyRs, IP3Rs and possibly the translocon. SERCA pumping of $Ca^{2+}$ to the ER is concomitant with a proton ejection and a KHE operates to reclaim these ejected protons. BiP is required for IP3R1 tetrameric assembly and $Ca^{2+}$ release from the ER. ERp44 competes with BiP binding to IP3R1 at the same site and inhibits IP3R1-mediated ER $Ca^{2+}$ release. To maintain ER $Ca^{2+}$ homeostasis, two members of the twin-pore $K^+$ channel family, TALK-1 and TASK-1 come together to form a $K^+$ channel mediating $K^+$ influx that can help promote ER $Ca^{2+}$ release. In response to ER stress conditions, BiP is sequestered by misfolded proteins, ERp44 becomes upregulated and competes with BiP binding to IP3R1 which results in decreased $IP_3$-induced $Ca^{2+}$ release.

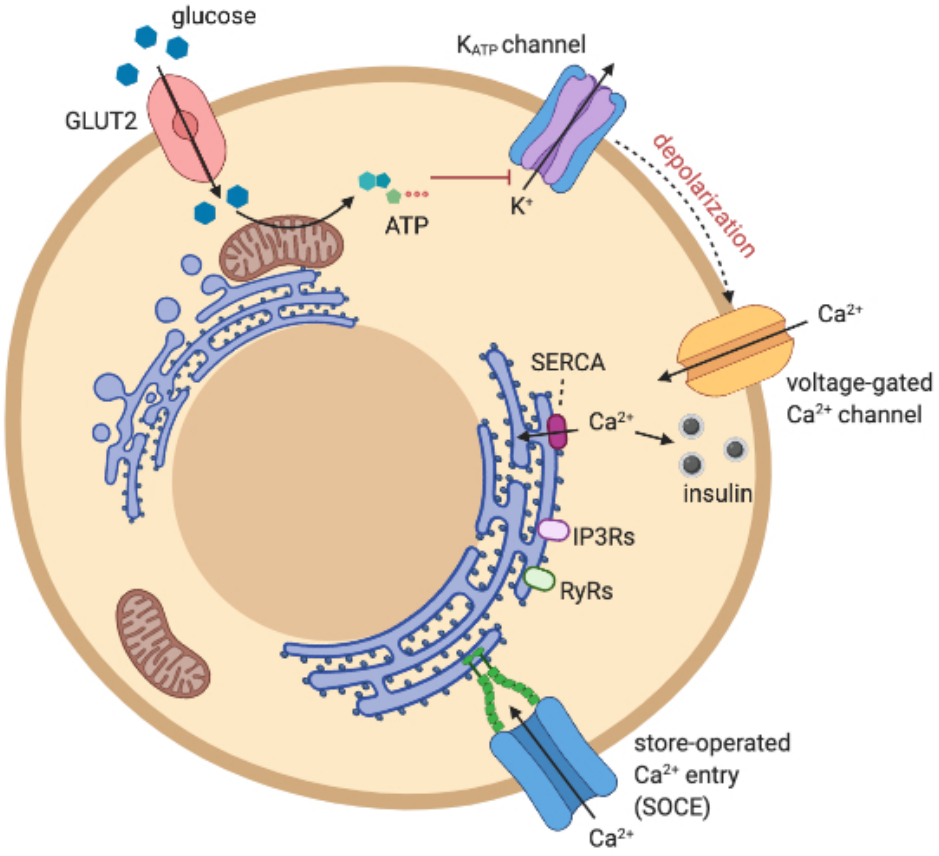


*Figure 1.4 Beta-cell schematic*

In response to rising glucose concentration, glucose enters the beta-cell via type 2 glucose transporters (GLUT2) and is then metabolized to generate ATP. Increased ATP/ADP causes the ATP-sensitive potassium channel ($K_{ATP}$) to close, depolarizing the beta-cell. Voltage-gated-$Ca^{2+}$ channels (VGCC) are activated by depolarization, and $Ca^{2+}$ then flows into the beta-cell and drives insulin secretion. The ER serves as a $Ca^{2+}$ reservoir. $Ca^{2+}$ is pumped into the ER lumen via sarco/endoplasmic reticulum $Ca^{2+}$-ATPases (SERCA pumps) and released to the cytosol through the triggered activation of inositol 1,4,5-triphosphate receptors (IP3Rs) and ryanodine receptors (RyRs). ER $Ca^{2+}$ depletion results in the opening of the store-operated $Ca^{2+}$ entry (SOCE) of the plasma membrane.

***References***


1. **CDC.** National diabetes statistics report, 2017. Available at: https://www.cdc.gov/diabetes/data/statistics/statistics-report.html.

2. **Topp BG, Atkinson LL, Finegood DT.** Dynamics of insulin sensitivity, β-cell function, and β-cell mass during the development of diabetes in *fa* / *fa* rats. *Am. J. Physiol.-Endocrinol. Metab.* 2007;293(6):E1730–E1735.

3. **Satin LS, Butler PC, Ha J, Sherman AS.** Pulsatile insulin secretion, impaired glucose tolerance and type 2 diabetes. *Mol. Aspects Med.* 2015;42:61–77.

4. **Kahn SE.** The relative contributions of insulin resistance and beta-cell dysfunction to the pathophysiology of Type 2 diabetes. *Diabetologia* 2003;46(1):3–19.

5. **Meier JJ, Bonadonna RC.** Role of Reduced -Cell Mass Versus Impaired -Cell Function in the Pathogenesis of Type 2 Diabetes. *Diabetes Care* 2013;36(Supplement_2):S113–S119.

6. **Kahn SE.** Quantifying -Cells in Health and Disease: The Past, the Present, and the Need. *Diabetes Care* 2013;36(1):4–5.

7. **Liston A, Todd JA, Lagou V.** Beta-Cell Fragility As a Common Underlying Risk Factor in Type 1 and Type 2 Diabetes. *Trends Mol. Med.* 2017;23(2):181–194.

8. **Rodriguez-Calvo T, Zapardiel-Gonzalo J, Amirian N, Castillo E, Lajevardi Y, Krogvold L, Dahl-Jørgensen K, von Herrath MG.** Increase in Pancreatic Proinsulin and Preservation of β-Cell Mass in Autoantibody-Positive Donors Prior to Type 1 Diabetes Onset. *Diabetes* 2017;66(5):1334–1345.

9. **Berridge MJ.** The endoplasmic reticulum: a multifunctional signaling organelle. *Cell Calcium* 2002;32(5–6):235–249.

10. **Sabatini PV, Speckmann T, Lynn FC.** Friend and foe: β-cell Ca2+ signaling and the development of diabetes. *Mol. Metab.* 2019;21:1–12.

11. **Hetz C, Papa FR.** The Unfolded Protein Response and Cell Fate Control. *Mol. Cell* 2018;69(2):169–181.

12. **Meyerovich K, Ortis F, Allagnat F, Cardozo AK.** Endoplasmic reticulum stress and the unfolded protein response in pancreatic islet inflammation. *J. Mol. Endocrinol.* 2016;57(1):R1–R17.

13. **Sano R, Reed JC.** ER stress-induced cell death mechanisms. *Biochim. Biophys. Acta BBA - Mol. Cell Res.* 2013;1833(12):3460–3470.

14. **Cunha DA, Hekerman P, Ladriere L, Bazarra-Castro A, Ortis F, Wakeham MC, Moore F, Rasschaert J, Cardozo AK, Bellomo E, Overbergh L, Mathieu C, Lupi R, Hai**

**T, Herchuelz A, Marchetti P, Rutter GA, Eizirik DL, Cnop M.** Initiation and execution of lipotoxic ER stress in pancreatic -cells. *J. Cell Sci.* 2008;121(14):2308–2318.

15. **Clark AL, Urano F.** Endoplasmic reticulum stress in beta cells and autoimmune diabetes. *Curr. Opin. Immunol.* 2016;43:60–66.

16. **Engin F.** ER stress and development of type 1 diabetes. *J. Investig. Med.* 2016;64(1):2–6.

17. **Acosta-Montaño P, García-González V.** Effects of Dietary Fatty Acids in Pancreatic Beta Cell Metabolism, Implications in Homeostasis. *Nutrients* 2018;10(4):393.

18. **Fonseca SG, Gromada J, Urano F.** Endoplasmic reticulum stress and pancreatic β-cell death. *Trends Endocrinol. Metab.* 2011;22(7):266–274.

19. **Back SH, Kaufman RJ.** Endoplasmic Reticulum Stress and Type 2 Diabetes. *Annu. Rev. Biochem.* 2012;81(1):767–793.

20. **Rojas J, Bermudez V, Palmar J, Martínez MS, Olivar LC, Nava M, Tomey D, Rojas M, Salazar J, Garicano C, Velasco M.** Pancreatic Beta Cell Death: Novel Potential Mechanisms in Diabetes Therapy. *J. Diabetes Res.* 2018;2018:1–19.

21. **Sun J, Cui J, He Q, Chen Z, Arvan P, Liu M.** Proinsulin misfolding and endoplasmic reticulum stress during the development and progression of diabetes. *Mol. Aspects Med.* 2015;42:105–118.

22. **Pobre KFR, Poet GJ, Hendershot LM.** The endoplasmic reticulum (ER) chaperone BiP is a master regulator of ER functions: Getting by with a little help from ERdj friends. *J. Biol. Chem.* 2019;294(6):2098–2108.

23. **Preissler S, Ron D.** Early Events in the Endoplasmic Reticulum Unfolded Protein Response. *Cold Spring Harb. Perspect. Biol.* 2019;11(4). doi:10.1101/cshperspect.a033894.

24. **Malhotra JD, Kaufman RJ.** ER Stress and Its Functional Link to Mitochondria: Role in Cell Survival and Death. *Cold Spring Harb. Perspect. Biol.* 2011;3(9):a004424–a004424.

25. **Oslowski CM, Urano F.** The binary switch that controls the life and death decisions of ER stressed β cells. *Curr. Opin. Cell Biol.* 2011;23(2):207–215.

26. **Scheuner D, Kaufman RJ.** The Unfolded Protein Response: A Pathway That Links Insulin Demand with β-Cell Failure and Diabetes. *Endocr. Rev.* 2008;29(3):317–333.

27. **Tabas I, Ron D.** Integrating the mechanisms of apoptosis induced by endoplasmic reticulum stress. *Nat. Cell Biol.* 2011;13(3):184–190.

28. **Wang S, Kaufman RJ.** The impact of the unfolded protein response on human disease. *J. Cell Biol.* 2012;197(7):857–867.

29. **Yoshida H, Matsui T, Yamamoto A, Okada T, Mori K.** XBP1 mRNA Is Induced by ATF6 and Spliced by IRE1 in Response to ER Stress to Produce a Highly Active Transcription Factor. *Cell* 2001;107(7):881–891.

30. **Calfon M, Zeng H, Urano F, Till JH, Hubbard SR, Harding HP, Clark SG, Ron D.** IRE1 couples endoplasmic reticulum load to secretory capacity by processing the XBP-1 mRNA. *Nature* 2002;415(6867):92–96.

31. **Abdullah A, Ravanan P.** The unknown face of IRE1α - Beyond ER stress. *Eur. J. Cell Biol.* 2018;97(5):359–368.

32. **Tsuchiya Y, Saito M, Kadokura H, Miyazaki J, Tashiro F, Imagawa Y, Iwawaki T, Kohno K.** IRE1–XBP1 pathway regulates oxidative proinsulin folding in pancreatic β cells. *J. Cell Biol.* 2018;217(4):1287–1301.

33. **Han D, Lerner AG, Vande Walle L, Upton J-P, Xu W, Hagen A, Backes BJ, Oakes SA, Papa FR.** IRE1alpha kinase activation modes control alternate endoribonuclease outputs to determine divergent cell fates. *Cell* 2009;138(3):562–575.

34. **Lipson KL, Ghosh R, Urano F.** The Role of IRE1α in the Degradation of Insulin mRNA in Pancreatic β-Cells. Maedler K, ed. *PLoS ONE* 2008;3(2):e1648.

35. **Ozcan U, Cao Q, Yilmaz E, Lee A-H, Iwakoshi NN, Ozdelen E, Tuncman G, Gorgun C, Glimcher LH, Hotamisligil GS.** Endoplasmic Reticulum Stress Links Obesity, Insulin Action, and Type 2 Diabetes. *Science* 2004;306(5695):457–461.

36. **Lipson KL, Fonseca SG, Ishigaki S, Nguyen LX, Foss E, Bortell R, Rossini AA, Urano F.** Regulation of insulin biosynthesis in pancreatic beta cells by an endoplasmic reticulum-resident protein kinase IRE1. *Cell Metab.* 2006;4(3):245–254.

37. **Harding HP, Zhang Y, Ron D.** Protein translation and folding are coupled by an endoplasmic-reticulum-resident kinase. *Nature* 1999;397(6716):271–274.

38. **B'chir W, Maurin A-C, Carraro V, Averous J, Jousse C, Muranishi Y, Parry L, Stepien G, Fafournoux P, Bruhat A.** The eIF2α/ATF4 pathway is essential for stress-induced autophagy gene expression. *Nucleic Acids Res.* 2013;41(16):7683–7699.

39. **Clemens MJ.** Initiation Factor eIF2α Phosphorylation in Stress Responses and Apoptosis. In: Rhoads RE, ed. *Signaling Pathways for Translation*.Vol 27. Berlin, Heidelberg: Springer Berlin Heidelberg; 2001:57–89.

40. **Harding HP, Novoa I, Zhang Y, Zeng H, Wek R, Schapira M, Ron D.** Regulated Translation Initiation Controls Stress-Induced Gene Expression in Mammalian Cells. *Mol. Cell* 2000;6(5):1099–1108.

41. **Zhang P, McGrath B, Li S 'a., Frank A, Zambito F, Reinert J, Gannon M, Ma K, McNaughton K, Cavener DR.** The PERK Eukaryotic Initiation Factor 2 Kinase Is Required

for the Development of the Skeletal System, Postnatal Growth, and the Function and Viability of the Pancreas. *Mol. Cell. Biol.* 2002;22(11):3864–3874.

42. **Sachdeva MM, Stoffers DA.** Minireview: Meeting the Demand for Insulin: Molecular Mechanisms of Adaptive Postnatal ß-Cell Mass Expansion. *Mol. Endocrinol.* 2009;23(6):747–758.

43. **Sharma RB, O'Donnell AC, Stamateris RE, Ha B, McCloskey KM, Reynolds PR, Arvan P, Alonso LC.** Insulin demand regulates β cell number via the unfolded protein response. *J. Clin. Invest.* 2015;125(10):3831–3846.

44. **Karaskov E, Scott C, Zhang L, Teodoro T, Ravazzola M, Volchuk A.** Chronic Palmitate But Not Oleate Exposure Induces Endoplasmic Reticulum Stress, Which May Contribute to INS-1 Pancreatic β-Cell Apoptosis. *Endocrinology* 2006;147(7):3398–3407.

45. **Borradaile NM, Han X, Harp JD, Gale SE, Ory DS, Schaffer JE.** Disruption of endoplasmic reticulum structure and integrity in lipotoxic cell death. *J. Lipid Res.* 2006;47(12):2726–2737.

46. **Back SH, Kang S-W, Han J, Chung H-T.** Endoplasmic Reticulum Stress in the *β* -Cell Pathogenesis of Type 2 Diabetes. *Exp. Diabetes Res.* 2012;2012:1–11.

47. **Herbach N, Rathkolb B, Kemter E, Pichl L, Klaften M, de Angelis MH, Halban PA, Wolf E, Aigner B, Wanke R.** Dominant-Negative Effects of a Novel Mutated Ins2 Allele Causes Early-Onset Diabetes and Severe -Cell Loss in Munich Ins2C95S Mutant Mice. *Diabetes* 2007;56(5):1268–1276.

48. **Riahi Y, Israeli T, Cerasi E, Leibowitz G.** Effects of proinsulin misfolding on β-cell dynamics, differentiation and function in diabetes. *Diabetes Obes. Metab.* 2018;20:95–103.

49. **Liu M, Sun J, Cui J, Chen W, Guo H, Barbetti F, Arvan P.** INS-gene mutations: from genetics and beta cell biology to clinical disease. *Mol. Aspects Med.* 2015;42:3–18.

50. **Haataja L, Gurlo T, Huang CJ, Butler PC.** Islet Amyloid in Type 2 Diabetes, and the Toxic Oligomer Hypothesis. *Endocr. Rev.* 2008;29(3):303–316.

51. **Höppener JWM, Jacobs HM, Wierup N, Sotthewes G, Sprong M, de Vos P, Berger R, Sundler F, Ahrén B.** Human Islet Amyloid Polypeptide Transgenic Mice: In Vivo and Ex Vivo Models for the Role of hIAPP in Type 2 Diabetes Mellitus. *Exp. Diabetes Res.* 2008;2008:1–8.

52. **Montemurro C, Nomoto H, Pei L, Parekh VS, Vongbunyong KE, Vadrevu S, Gurlo T, Butler AE, Subramaniam R, Ritou E, Shirihai OS, Satin LS, Butler PC, Tudzarova S.** IAPP toxicity activates HIF1α/PFKFB3 signaling delaying β-cell loss at the expense of β-cell function. *Nat. Commun.* 2019;10(1):2679.

53. **Chan JY, Luzuriaga J, Maxwell EL, West PK, Bensellam M, Laybutt DR.** The balance between adaptive and apoptotic unfolded protein responses regulates β-cell death

under ER stress conditions through XBP1, CHOP and JNK. *Mol. Cell. Endocrinol.* 2015;413:189–201.

54. **Hetz C.** The unfolded protein response: controlling cell fate decisions under ER stress and beyond. *Nat. Rev. Mol. Cell Biol.* 2012;13(2):89–102.

55. **Woehlbier U, Hetz C.** Modulating stress responses by the UPRosome: A matter of life and death. *Trends Biochem. Sci.* 2011;36(6):329–337.

56. **Upton J-P, Wang L, Han D, Wang ES, Huskey NE, Lim L, Truitt M, McManus MT, Ruggero D, Goga A, Papa FR, Oakes SA.** IRE1 Cleaves Select microRNAs During ER Stress to Derepress Translation of Proapoptotic Caspase-2. *Science* 2012;338(6108):818–822.

57. **Yoneda T, Imaizumi K, Oono K, Yui D, Gomi F, Katayama T, Tohyama M.** Activation of Caspase-12, an Endoplastic Reticulum (ER) Resident Caspase, through Tumor Necrosis Factor Receptor-associated Factor 2-dependent Mechanism in Response to the ER Stress. *J. Biol. Chem.* 2001;276(17):13935–13940.

58. **Hitomi J, Katayama T, Taniguchi M, Honda A, Imaizumi K, Tohyama M.** Apoptosis induced by endoplasmic reticulum stress depends on activation of caspase-3 via caspase-12. *Neurosci. Lett.* 2004;357(2):127–130.

59. **Morita S, Villalta SA, Feldman HC, Register AC, Rosenthal W, Hoffmann-Petersen IT, Mehdizadeh M, Ghosh R, Wang L, Colon-Negron K, Meza-Acevedo R, Backes BJ, Maly DJ, Bluestone JA, Papa FR.** Targeting ABL-IRE1α Signaling Spares ER-Stressed Pancreatic β Cells to Reverse Autoimmune Diabetes. *Cell Metab.* 2017;25(4):883-897.e8.

60. **Thielen L, Shalev A.** Diabetes pathogenic mechanisms and potential new therapies based upon a novel target called TXNIP. *Curr. Opin. Endocrinol. Diabetes Obes.* 2018;25(2):75–80.

61. **Oslowski CM, Hara T, O'Sullivan-Murphy B, Kanekura K, Lu S, Hara M, Ishigaki S, Zhu LJ, Hayashi E, Hui ST, Greiner D, Kaufman RJ, Bortell R, Urano F.** Thioredoxin-Interacting Protein Mediates ER Stress-Induced β Cell Death through Initiation of the Inflammasome. *Cell Metab.* 2012;16(2):265–273.

62. **Lerner AG, Upton J-P, Praveen PVK, Ghosh R, Nakagawa Y, Igbaria A, Shen S, Nguyen V, Backes BJ, Heiman M, Heintz N, Greengard P, Hui S, Tang Q, Trusina A, Oakes SA, Papa FR.** IRE1α Induces Thioredoxin-Interacting Protein to Activate the NLRP3 Inflammasome and Promote Programmed Cell Death under Irremediable ER Stress. *Cell Metab.* 2012;16(2):250–264.

63. **Clark AL, Kanekura K, Lavagnino Z, Spears LD, Abreu D, Mahadevan J, Yagi T, Semenkovich CF, Piston DW, Urano F.** Targeting Cellular Calcium Homeostasis to Prevent Cytokine-Mediated Beta Cell Death. *Sci. Rep.* 2017;7(1):5611.

64. **Ishigaki S, Fonseca SG, Oslowski CM, Jurczyk A, Shearstone JR, Zhu LJ, Permutt MA, Greiner DL, Bortell R, Urano F.** AATF mediates an antiapoptotic effect of the unfolded protein response through transcriptional regulation of AKT1. *Cell Death Differ.* 2010;17(5):774–786.

65. **Oslowski CM, Urano F.** A switch from life to death in endoplasmic reticulum stressed β-cells. *Diabetes Obes. Metab.* 2010;12:58–65.

66. **Li G, Mongillo M, Chin K-T, Harding H, Ron D, Marks AR, Tabas I.** Role of ERO1-α–mediated stimulation of inositol 1,4,5-triphosphate receptor activity in endoplasmic reticulum stress–induced apoptosis. *J. Cell Biol.* 2009;186(6):783–792.

67. **Kiviluoto S, Vervliet T, Ivanova H, Decuypere J-P, De Smedt H, Missiaen L, Bultynck G, Parys JB.** Regulation of inositol 1,4,5-trisphosphate receptors during endoplasmic reticulum stress. *Biochim. Biophys. Acta BBA - Mol. Cell Res.* 2013;1833(7):1612–1624.

68. **Hara T, Mahadevan J, Kanekura K, Hara M, Lu S, Urano F.** Calcium Efflux From the Endoplasmic Reticulum Leads to β-Cell Death. *Endocrinology* 2014;155(3):758–768.

69. **Tan Y, Dourdin N, Wu C, De Veyra T, Elce JS, Greer PA.** Ubiquitous Calpains Promote Caspase-12 and JNK Activation during Endoplasmic Reticulum Stress-induced Apoptosis. *J. Biol. Chem.* 2006;281(23):16016–16024.

70. **Nakagawa T, Yuan J.** Cross-Talk between Two Cysteine Protease Families: Activation of Caspase-12 by Calpain in Apoptosis. *J. Cell Biol.* 2000;150(4):887–894.

71. **Rong Y-P, Bultynck G, Aromolaran AS, Zhong F, Parys JB, De Smedt H, Mignery GA, Roderick HL, Bootman MD, Distelhorst CW.** The BH4 domain of Bcl-2 inhibits ER calcium release and apoptosis by binding the regulatory and coupling domain of the IP3 receptor. *Proc. Natl. Acad. Sci.* 2009;106(34):14397–14402.

72. **Vervliet T, Decrock E, Molgo J, Sorrentino V, Missiaen L, Leybaert L, De Smedt H, Kasri NN, Parys JB, Bultynck G.** Bcl-2 binds to and inhibits ryanodine receptors. *J. Cell Sci.* 2014;127(12):2782–2792.

73. **Tait SWG, Green DR.** Mitochondria and cell death: outer membrane permeabilization and beyond. *Nat. Rev. Mol. Cell Biol.* 2010;11(9):621–632.

74. **Engin F, Yermalovich A, Nguyen T, Hummasti S, Fu W, Eizirik DL, Mathis D, Hotamisligil GS.** Restoration of the Unfolded Protein Response in Pancreatic Cells Protects Mice Against Type 1 Diabetes. *Sci. Transl. Med.* 2013;5(211):211ra156-211ra156.

75. **Cnop M, Welsh N, Jonas J-C, Jorns A, Lenzen S, Eizirik DL.** Mechanisms of Pancreatic -Cell Death in Type 1 and Type 2 Diabetes: Many Differences, Few Similarities. *Diabetes* 2005;54(Supplement 2):S97–S107.

76. **Ramadan JW, Steiner SR, O'Neill CM, Nunemaker CS.** The central role of calcium in the effects of cytokines on beta-cell function: Implications for type 1 and type 2 diabetes. *Cell Calcium* 2011;50(6):481–490.

77. **Kono T, Tong X, Taleb S, Bone RN, Iida H, Lee C-C, Sohn P, Gilon P, Roe MW, Evans-Molina C.** Impaired Store-Operated Calcium Entry and STIM1 Loss Lead to Reduced Insulin Secretion and Increased Endoplasmic Reticulum Stress in the Diabetic β-Cell. *Diabetes* 2018;67(11):2293–2304.

78. **Chan JY, Cooney GJ, Biden TJ, Laybutt DR.** Differential regulation of adaptive and apoptotic unfolded protein response signalling by cytokine-induced nitric oxide production in mouse pancreatic beta cells. *Diabetologia* 2011;54(7):1766–1776.

79. **Cardozo AK, Ortis F, Storling J, Feng Y-M, Rasschaert J, Tonnesen M, Van Eylen F, Mandrup-Poulsen T, Herchuelz A, Eizirik DL.** Cytokines Downregulate the Sarcoendoplasmic Reticulum Pump Ca2+ ATPase 2b and Deplete Endoplasmic Reticulum Ca2+, Leading to Induction of Endoplasmic Reticulum Stress in Pancreatic -Cells. *Diabetes* 2005;54(2):452–461.

80. **Pirot P, Eizirik DL, Cardozo AK.** Interferon-γ potentiates endoplasmic reticulum stress-induced death by reducing pancreatic beta cell defence mechanisms. *Diabetologia* 2006;49(6):1229–1236.

81. **Babon JAB, DeNicola ME, Blodgett DM, Crèvecoeur I, Buttrick TS, Maehr R, Bottino R, Naji A, Kaddis J, Elyaman W, James EA, Haliyur R, Brissova M, Overbergh L, Mathieu C, Delong T, Haskins K, Pugliese A, Campbell-Thompson M, Mathews C, Atkinson MA, Powers AC, Harlan DM, Kent SC.** Erratum: Corrigendum: Analysis of self-antigen specificity of islet-infiltrating T cells from human donors with type 1 diabetes. *Nat. Med.* 2017;23(8):1004–1004.

82. **Marre ML, McGinty JW, Chow I-T, DeNicola ME, Beck NW, Kent SC, Powers AC, Bottino R, Harlan DM, Greenbaum CJ, Kwok WW, Piganelli JD, James EA.** Modifying Enzymes Are Elicited by ER Stress, Generating Epitopes That Are Selectively Recognized by CD4 $^{+}$ T Cells in Patients With Type 1 Diabetes. *Diabetes* 2018;67(7):1356–1368.

83. **Buitinga M, Callebaut A, Marques Câmara Sodré F, Crèvecoeur I, Blahnik-Fagan G, Yang M-L, Bugliani M, Arribas-Layton D, Marré M, Cook DP, Waelkens E, Mallone R, Piganelli JD, Marchetti P, Mamula MJ, Derua R, James EA, Mathieu C, Overbergh L.** Inflammation-Induced Citrullinated Glucose-Regulated Protein 78 Elicits Immune Responses in Human Type 1 Diabetes. *Diabetes* 2018;67(11):2337–2348.

84. **Rondas D, Crèvecoeur I, D'Hertog W, Ferreira GB, Staes A, Garg AD, Eizirik DL, Agostinis P, Gevaert K, Overbergh L, Mathieu C.** Citrullinated Glucose-Regulated Protein 78 Is an Autoantigen in Type 1 Diabetes. *Diabetes* 2015;64(2):573–586.

85. **Huang C, Lin C, Haataja L, Gurlo T, Butler AE, Rizza RA, Butler PC.** High Expression Rates of Human Islet Amyloid Polypeptide Induce Endoplasmic Reticulum

Stress–Mediated β-Cell Apoptosis, a Characteristic of Humans With Type 2 but Not Type 1 Diabetes. *Diabetes* 2007;56(8):2016–2027.

86. **Laybutt DR, Preston AM, Åkerfeldt MC, Kench JG, Busch AK, Biankin AV, Biden TJ.** Endoplasmic reticulum stress contributes to beta cell apoptosis in type 2 diabetes. *Diabetologia* 2007;50(4):752–763.

87. **Engin F, Nguyen T, Yermalovich A, Hotamisligil GS.** Aberrant islet unfolded protein response in type 2 diabetes. *Sci. Rep.* 2015;4(1):4054.

88. **Yang L, Calay ES, Fan J, Arduini A, Kunz RC, Gygi SP, Yalcin A, Fu S, Hotamisligil GS.** S-Nitrosylation links obesity-associated inflammation to endoplasmic reticulum dysfunction. *Science* 2015;349(6247):500–506.

89. **Senee V, Vattem KM, Delepine M, Rainbow LA, Haton C, Lecoq A, Shaw NJ, Robert J-J, Rooman R, Diatloff-Zito C, Michaud JL, Bin-Abbas B, Taha D, Zabel B, Franceschini P, Topaloglu AK, Lathrop GM, Barrett TG, Nicolino M, Wek RC, Julier C.** Wolcott-Rallison Syndrome: Clinical, Genetic, and Functional Study of EIF2AK3 Mutations and Suggestion of Genetic Heterogeneity. *Diabetes* 2004;53(7):1876–1883.

90. **Gupta S, McGrath B, Cavener DR.** PERK (EIF2AK3) Regulates Proinsulin Trafficking and Quality Control in the Secretory Pathway. *Diabetes* 2010;59(8):1937–1947.

91. **Gao Y, Sartori DJ, Li C, Yu Q-C, Kushner JA, Simon MC, Diehl JA.** PERK is required in the adult pancreas and is essential for maintenance of glucose homeostasis. *Mol. Cell. Biol.* 2012;32(24):5129–5139.

92. **Firdous P, Nissar K, Ali S, Ganai BA, Shabir U, Hassan T, Masoodi SR.** Genetic Testing of Maturity-Onset Diabetes of the Young Current Status and Future Perspectives. *Front. Endocrinol.* 2018;9:253.

93. **Sachdeva MM, Claiborn KC, Khoo C, Yang J, Groff DN, Mirmira RG, Stoffers DA.** Pdx1 ( *MODY4* ) regulates pancreatic beta cell susceptibility to ER stress. *Proc. Natl. Acad. Sci.* 2009;106(45):19090–19095.

94. **Khan FA, Goforth PB, Zhang M, Satin LS.** Insulin Activates ATP-Sensitive K+ Channels in Pancreatic -Cells Through a Phosphatidylinositol 3-Kinase-Dependent Pathway. *Diabetes* 2001;50(10):2192–2198.

95. **Ashcroft FM, Rorsman P.** KATP channels and islet hormone secretion: new insights and controversies. *Nat. Rev. Endocrinol.* 2013;9(11):660–669.

96. **Görlach A, Klappa P, Kietzmann DrT.** The Endoplasmic Reticulum: Folding, Calcium Homeostasis, Signaling, and Redox Control. *Antioxid. Redox Signal.* 2006;8(9–10):1391–1418.

97. **Graves TK, Hinkle PM.** $Ca^{2+}$ -Induced $Ca^{2+}$ Release in the Pancreatic β-Cell: Direct Evidence of Endoplasmic Reticulum $Ca^{2+}$ Release. *Endocrinology* 2003;144(8):3565–3574.

98. **Dyachok O, Tufveson G, Gylfe E.** Ca2+-induced Ca2+ release by activation of inositol 1,4,5-trisphosphate receptors in primary pancreatic β-cells. *Cell Calcium* 2004;36(1):1–9.

99. **Mekahli D, Bultynck G, Parys JB, De Smedt H, Missiaen L.** Endoplasmic-Reticulum Calcium Depletion and Disease. *Cold Spring Harb. Perspect. Biol.* 2011;3(6):a004317–a004317.

100. **Sano R, Annunziata I, Patterson A, Moshiach S, Gomero E, Opferman J, Forte M, d'Azzo A.** GM1-ganglioside accumulation at the mitochondria-associated ER membranes links ER stress to Ca(2+)-dependent mitochondrial apoptosis. *Mol. Cell* 2009;36(3):500–511.

101. **Korkotian E, Schwarz A, Pelled D, Schwarzmann G, Segal M, Futerman AH.** Elevation of intracellular glucosylceramide levels results in an increase in endoplasmic reticulum density and in functional calcium stores in cultured neurons. *J. Biol. Chem.* 1999;274(31):21673–21678.

102. **Periasamy M, Kalyanasundaram A.** SERCA pump isoforms: Their role in calcium transport and disease. *Muscle Nerve* 2007;35(4):430–442.

103. **Tong X, Kono T, Anderson-Baucum EK, Yamamoto W, Gilon P, Lebeche D, Day RN, Shull GE, Evans-Molina C.** SERCA2 Deficiency Impairs Pancreatic β-Cell Function in Response to Diet-Induced Obesity. *Diabetes* 2016;65(10):3039–3052.

104. **Kono T, Ahn G, Moss DR, Gann L, Zarain-Herzberg A, Nishiki Y, Fueger PT, Ogihara T, Evans-Molina C.** PPAR-γ Activation Restores Pancreatic Islet SERCA2 Levels and Prevents β-Cell Dysfunction under Conditions of Hyperglycemic and Cytokine Stress. *Mol. Endocrinol.* 2012;26(2):257–271.

105. **Zarain-Herzberg A, García-Rivas G, Estrada-Avilés R.** Regulation of SERCA pumps expression in diabetes. *Cell Calcium* 2014;56(5):302–310.

106. **Soleimanpour SA, Crutchlow MF, Ferrari AM, Raum JC, Groff DN, Rankin MM, Liu C, De León DD, Naji A, Kushner JA, Stoffers DA.** Calcineurin Signaling Regulates Human Islet β-Cell Survival. *J. Biol. Chem.* 2010;285(51):40050–40059.

107. **Wang R, McGrath BC, Kopp RF, Roe MW, Tang X, Chen G, Cavener DR.** Insulin Secretion and $Ca^{2+}$ Dynamics in β-Cells Are Regulated by PERK (EIF2AK3) in Concert with Calcineurin. *J. Biol. Chem.* 2013;288(47):33824–33836.

108. **Bertram R, Sherman A.** Filtering of Calcium Transients by the Endoplasmic Reticulum in Pancreatic β-Cells. *Biophys. J.* 2004;87(6):3775–3785.

109. **Arredouani A, Henquin J-C, Gilon P.** Contribution of the endoplasmic reticulum to the glucose-induced $[Ca^{2+}]_c$ response in mouse pancreatic islets. *Am. J. Physiol.-Endocrinol. Metab.* 2002;282(5):E982–E991.

110. **Coe H, Michalak M.** Calcium binding chaperones of the endoplasmic reticulum. *Gen Physiol Biophys* 2009;28:F96–F103.

111. **Fliegel L, Burns K, Reithmeier R, Michalak M.** Molecular cloning of the high affinity calcium-binding protein (calreticulin) of skeletal muscle sarcoplasmic reticulum. *J. Biol. Chem.* 1989;264:21522–21528.

112. **Treves S, De Mattei M, Landfredi M, Villa A, Green NM, MacLennan DH, Meldolesi J, Pozzan T.** Calreticulin is a candidate for a calsequestrin-like function in $Ca^{2+}$-storage compartments (calciosomes) of liver and brain. *Biochem. J.* 1990;271(2):473–480.

113. **Baksh S, Michalak M.** Expression of calreticulin in Escherichia coli and identification of its Ca2+ binding domains. *J. Biol. Chem.* 1991;266(32):21458–65.

114. **Wijeyesakere SJ, Gafni AA, Raghavan M.** Calreticulin Is a Thermostable Protein with Distinct Structural Responses to Different Divalent Cation Environments. *J. Biol. Chem.* 2011;286(11):8771–8785.

115. **Bastianutto C, Clementi E, Codazzi F, Podini P, Giorgi FD, Rizzuto R, Meldolesi J, Pozzan T.** Overexpression of calreticulin increases the Ca2+ capacity of rapidly exchanging Ca2+ stores and reveals aspects of their lumenal microenvironment and function. *J. Cell Biol.* 1995;130(4):847–855.

116. **Mery L, Mesaeli N, Michalak M, Opas M, Lew DP, Krause K-H.** Overexpression of Calreticulin Increases Intracellular Ca Storage and Decreases Store-operated Ca Influx. *J. Biol. Chem.* 1996;271(16):9332–9339.

117. **Omikorede O, Qi C, Gorman T, Chapman P, Yu A, Smith DM, Herbert TP.** ER stress in rodent islets of Langerhans is concomitant with obesity and β-cell compensation but not with β-cell dysfunction and diabetes. *Nutr. Diabetes* 2013;3(10):e93–e93.

118. **Gupta D, Jetton TL, LaRock K, Monga N, Satish B, Lausier J, Peshavaria M, Leahy JL.** Temporal characterization of β cell-adaptive and -maladaptive mechanisms during chronic high-fat feeding in C57BL/6NTac mice. *J. Biol. Chem.* 2017;292(30):12449–12459.

119. **Raghavan M, Wijeyesakere SJ, Peters LR, Del Cid N.** Calreticulin in the immune system: ins and outs. *Trends Immunol.* 2013;34(1):13–21.

120. **Lièvremont J-P, Rizzuto R, Hendershot L, Meldolesi J.** BiP, a Major Chaperone Protein of the Endoplasmic Reticulum Lumen, Plays a Direct and Important Role in the Storage of the Rapidly Exchanging Pool of $Ca^{2+}$. *J. Biol. Chem.* 1997;272(49):30873–30879.

121. **Lamb HK, Mee C, Xu W, Liu L, Blond S, Cooper A, Charles IG, Hawkins AR.** The Affinity of a Major $Ca^{2+}$ Binding Site on GRP78 Is Differentially Enhanced by ADP and ATP. *J. Biol. Chem.* 2006;281(13):8796–8805.

122. **Sriram M, Osipiuk J, Freeman B, Morimoto R, Joachimiak A.** Human Hsp70 molecular chaperone binds two calcium ions within the ATPase domain. *Structure* 1997;5(3):403–414.

123. **Wei J, Hendershot LM.** Characterization of the nucleotide binding properties and ATPase activity of recombinant hamster BiP purified from bacteria. *J. Biol. Chem.* 1995;270(44):26670–26676.

124. **Conte IL, Keith N, Gutiérrez-Gonzalez C, Parodi AJ, Caramelo JJ.** The interplay between calcium and the in vitro lectin and chaperone activities of calreticulin. *Biochemistry* 2007;46(15):4671–4680.

125. **Villamil Giraldo AM, Lopez Medus M, Gonzalez Lebrero M, Pagano RS, Labriola CA, Landolfo L, Delfino JM, Parodi AJ, Caramelo JJ.** The structure of calreticulin C-terminal domain is modulated by physiological variations of calcium concentration. *J. Biol. Chem.* 2010;285(7):4544–4553.

126. **Wijeyesakere SJ, Bedi SK, Huynh D, Raghavan M.** The C-Terminal Acidic Region of Calreticulin Mediates Phosphatidylserine Binding and Apoptotic Cell Phagocytosis. *J. Immunol. Baltim. Md 1950* 2016;196(9):3896–3909.

127. **Booth C, Koch GL.** Perturbation of cellular calcium induces secretion of luminal ER proteins. *Cell* 1989;59(4):729–737.

128. **Tufi R, Panaretakis T, Bianchi K, Criollo A, Fazi B, Di Sano F, Tesniere A, Kepp O, Paterlini-Brechot P, Zitvogel L, Piacentini M, Szabadkai G, Kroemer G.** Reduction of endoplasmic reticulum Ca2+ levels favors plasma membrane surface exposure of calreticulin. *Cell Death Differ.* 2008;15(2):274–282.

129. **Zhang Y, Liu R, Ni M, Gill P, Lee AS.** Cell surface relocalization of the endoplasmic reticulum chaperone and unfolded protein response regulator GRP78/BiP. *J. Biol. Chem.* 2010;285(20):15065–15075.

130. **Jeffery E, Peters LR, Raghavan M.** The polypeptide binding conformation of calreticulin facilitates its cell-surface expression under conditions of endoplasmic reticulum stress. *J. Biol. Chem.* 2011;286(4):2402–2415.

131. **Peters LR, Raghavan M.** Endoplasmic reticulum calcium depletion impacts chaperone secretion, innate immunity, and phagocytic uptake of cells. *J. Immunol.* 2011;187(2):919–931.

132. **Sönnichsen B, Füllekrug J, Nguyen Van P, Diekmann W, Robinson DG, Mieskes G.** Retention and retrieval: both mechanisms cooperate to maintain calreticulin in the endoplasmic reticulum. *J. Cell Sci.* 1994;107 ( Pt 10):2705–2717.

133. **Laver DR.** Regulation of the RyR channel gating by Ca2+ and Mg2+. *Biophys. Rev.* 2018;10(4):1087–1095.

134. **Santulli G, Pagano G, Sardu C, Xie W, Reiken S, D'Ascia SL, Cannone M, Marziliano N, Trimarco B, Guise TA, Lacampagne A, Marks AR.** Calcium release channel RyR2 regulates insulin release and glucose homeostasis. *J. Clin. Invest.* 2015;125(5):1968–1978.

135. **Santulli G, Nakashima R, Yuan Q, Marks AR.** Intracellular calcium release channels: an update: RyRs *vs* . IP $_3$ Rs. *J. Physiol.* 2017;595(10):3041–3051.

136. **Yamamoto WR, Bone RN, Sohn P, Syed F, Reissaus CA, Mosley AL, Wijeratne AB, True JD, Tong X, Kono T, Evans-Molina C.** Endoplasmic reticulum stress alters ryanodine receptor function in the murine pancreatic β cell. *J. Biol. Chem.* 2019;294(1):168–181.

137. **Islam MS.** The Ryanodine Receptor Calcium Channel of -Cells: Molecular Regulation and Physiological Significance. *Diabetes* 2002;51(5):1299–1309.

138. **Mészáros LG, Bak J, Chu A.** Cyclic ADP-ribose as an endogenous regulator of the non-skeletal type ryanodine receptor Ca2+ channel. *Nature* 1993;364(6432):76–79.

139. **Rutter GA, Theler J-M, Li G, Wollheim CB.** Ca2+ stores in insulin-secreting cells: lack of effect of cADP ribose. *Cell Calcium* 1994;16(2):71–80.

140. **Van Petegem F.** Ryanodine Receptors: Structure and Function. *J. Biol. Chem.* 2012;287(38):31624–31632.

141. **Holz GG, Leech CA, Heller RS, Castonguay M, Habener JF.** cAMP-dependent Mobilization of Intracellular Ca $^{2+}$ Stores by Activation of Ryanodine Receptors in Pancreatic β-Cells: A Ca $^{2+}$ SIGNALING SYSTEM STIMULATED BY THE INSULINOTROPIC HORMONE GLUCAGON-LIKE PEPTIDE-1-(7–37). *J. Biol. Chem.* 1999;274(20):14147–14156.

142. **Thomas NL, Williams AJ.** Pharmacology of ryanodine receptors and Ca2+-induced Ca2+ release. *Wiley Interdiscip. Rev. Membr. Transp. Signal.* 2012;1(4):383–397.

143. **Zhao F, Li P, Chen SRW, Louis CF, Fruen BR.** Dantrolene Inhibition of Ryanodine Receptor Ca $^{2+}$ Release Channels: MOLECULAR MECHANISM AND ISOFORM SELECTIVITY. *J. Biol. Chem.* 2001;276(17):13810–13816.

144. **Dixit SS, Wang T, Manzano EJQ, Yoo S, Lee J, Chiang DY, Ryan N, Respress JL, Yechoor VK, Wehrens XHT.** Effects of CaMKII-Mediated Phosphorylation of Ryanodine Receptor Type 2 on Islet Calcium Handling, Insulin Secretion, and Glucose Tolerance. Alquier T, ed. *PLoS ONE* 2013;8(3):e58655.

145. **Luciani DS, Gwiazda KS, Yang T-LB, Kalynyak TB, Bychkivska Y, Frey MHZ, Jeffrey KD, Sampaio AV, Underhill TM, Johnson JD.** Roles of IP3R and RyR Ca2+ Channels in Endoplasmic Reticulum Stress and -Cell Death. *Diabetes* 2009;58(2):422–432.

146. **Ivanova H, Vervliet T, Missiaen L, Parys JB, De Smedt H, Bultynck G.** Inositol 1,4,5-trisphosphate receptor-isoform diversity in cell death and survival. *Biochim. Biophys. Acta BBA - Mol. Cell Res.* 2014;1843(10):2164–2183.

147. **Saleem H, Tovey SC, Molinski TF, Taylor CW.** Interactions of antagonists with subtypes of inositol 1,4,5-trisphosphate ($IP_3$) receptor: $IP_3$ receptor antagonists. *Br. J. Pharmacol.* 2014;171(13):3298–3312.

148. **Fedorenko OA, Popugaeva E, Enomoto M, Stathopulos PB, Ikura M, Bezprozvanny I.** Intracellular calcium channels: Inositol-1,4,5-trisphosphate receptors. *Eur. J. Pharmacol.* 2014;739:39–48.

149. **Mataragka S, Taylor CW.** All three $IP_3$ receptor subtypes generate $Ca^{2+}$ puffs, the universal building blocks of $IP_3$-evoked $Ca^{2+}$ signals. *J. Cell Sci.* 2018;131(16):jcs220848.

150. **Ye R, Ni M, Wang M, Luo S, Zhu G, Chow RH, Lee AS.** Inositol 1,4,5-trisphosphate receptor 1 mutation perturbs glucose homeostasis and enhances susceptibility to diet-induced diabetes. *J. Endocrinol.* 2011;210(2):209–217.

151. **Roach JC, Deutsch K, Li S, Siegel AF, Bekris LM, Einhaus DC, Sheridan CM, Glusman G, Hood L, Lernmark Å, Janer M.** Genetic Mapping at 3-Kilobase Resolution Reveals Inositol 1,4,5-Triphosphate Receptor 3 as a Risk Factor for Type 1 Diabetes in Sweden. *Am. J. Hum. Genet.* 2006;79(4):614–627.

152. **Lee B, Laychock SG.** Inositol 1,4,5-trisphosphate receptor isoform expression in mouse pancreatic islets: effects of carbachol. *Biochem. Pharmacol.* 2001;61(3):327–336.

153. **Lang S, Pfeffer S, Lee P-H, Cavalié A, Helms V, Förster F, Zimmermann R.** An Update on Sec61 Channel Functions, Mechanisms, and Related Diseases. *Front. Physiol.* 2017;8:887.

154. **Van Coppenolle F, Abeele F, Slomianny C, Flourakis M, hesketh J, Dewailly E, Prevarskaya N.** Ribosome-translocon complex mediates calcium leakage from endoplasmic reticulum stores. *J. Cell Sci.* 2004;117(18):4135–4142.

155. **Lloyd DJ, Wheeler MC, Gekakis N.** A Point Mutation in Sec61 1 Leads to Diabetes and Hepatosteatosis in Mice. *Diabetes* 2010;59(2):460–470.

156. **Xu H, Martinoia E, Szabo I.** Organellar channels and transporters. *Cell Calcium* 2015;58(1):1–10.

157. **Kuum M, Veksler V, Liiv J, Ventura-Clapier R, Kaasik A.** Endoplasmic reticulum potassium-hydrogen exchanger and small conductance calcium-activated potassium channel activities are essential for ER calcium uptake in neurons and cardiomyocytes. *J. Cell Sci.* 2012;125(3):625–633.

158. **Kuum M, Veksler V, Kaasik A.** Potassium fluxes across the endoplasmic reticulum and their role in endoplasmic reticulum calcium homeostasis. *Cell Calcium* 2015;58(1):79–85.

159. **Espinoza-Fonseca LM.** The $Ca^{2+}$-ATPase pump facilitates bidirectional proton transport across the sarco/endoplasmic reticulum. *Mol. Biosyst.* 2017;13(4):633–637.

160. **Graff SM, Dadi P, Ibsen CE, Dickerson M, Jordan KL, Jacobson D.** 40-OR: The Role of TALK-1 $K^+$ Channels in Pancreatic ß-Cell Insulin Secretion, Mitochondrial Function, and the ER Stress Response. *Diabetes* 2019;68(Supplement 1):40-OR.

161. **Vierra NC, Dadi PK, Milian SC, Dickerson MT, Jordan KL, Gilon P, Jacobson DA.** TALK-1 channels control β cell endoplasmic reticulum $Ca^{2+}$ homeostasis. *Sci. Signal.* 2017;10(497):eaan2883.

162. **Qiu R, Lewis RS.** Structural features of STIM and Orai underlying store-operated calcium entry. *Curr. Opin. Cell Biol.* 2019;57:90–98.

163. **Takemur H, Hughes AR, Thastrup O, Putney JW.** Activation of Calcium Entry by the Tumor Promoter Thapsigargin in Parotid Acinar Cells. *J. Biol. Chem.* 1989;264(21):12266–12271.

164. **Lacruz RS, Feske S.** Diseases caused by mutations in *ORAI1* and *STIM1*: Mutations in *ORAI1* and *STIM1*. *Ann. N. Y. Acad. Sci.* 2015;1356(1):45–79.

165. **Sabourin J, Le Gal L, Saurwein L, Haefliger J-A, Raddatz E, Allagnat F.** Store-operated $Ca^{2+}$ Entry Mediated by Orai1 and TRPC1 Participates to Insulin Secretion in Rat β-Cells. *J. Biol. Chem.* 2015;290(51):30530–30539.

166. **Malli R, Frieden M, Hunkova M, Trenker M, Graier WF.** Ca2+ refilling of the endoplasmic reticulum is largely preserved albeit reduced Ca2+ entry in endothelial cells. *Cell Calcium* 2007;41(1):63–76.

167. **Liu Y-J, Vieira E, Gylfe E.** A store-operated mechanism determines the activity of the electrically excitable glucagon-secreting pancreatic α-cell. *Cell Calcium* 2004;35(4):357–365.

168. **Briant L, Salehi A, Vergari E, Zhang Q, Rorsman P.** Glucagon secretion from pancreatic α-cells. *Ups. J. Med. Sci.* 2016;121(2):113–119.

# Chapter 2 ER Stress Increases Store-Operated $Ca^{2+}$ Entry (SOCE) and Augments Basal Insulin Secretion in Pancreatic Beta Cells

Irina X. Zhang, Jianhua Ren, Suryakiran Vadrevu, Malini Raghavan and Leslie S. Satin

This article was originally published in 2020 in Journal of Biological Chemistry.

jbc.RA120.012721

***Abstract***

Type 2 diabetes mellitus (T2DM) is characterized by impaired glucose-stimulated insulin secretion and increased peripheral insulin resistance. Unremitting ER stress can lead to beta-cell apoptosis and has been linked to type 2 diabetes. Although many studies have attempted to link ER stress and T2DM, the specific effects of ER stress on beta-cell function remain incompletely understood. To determine the interrelationship between ER stress and β-cell function, here we treated insulin-secreting INS-1(832/13) cells or isolated mouse islets with the ER stress inducer tunicamycin (TM). TM induced ER stress as expected, as evidenced by activation of the unfolded protein response (UPR). Beta cells treated with TM also exhibited concomitant alterations in their electrical activity and cytosolic free $Ca^{2+}$ oscillations. As ER stress is known to reduce ER $Ca^{2+}$ levels, we tested the hypothesis that the observed increase in $Ca^{2+}$ oscillations occurred because of reduced ER $Ca^{2+}$ levels and, in turn, increased store-operated $Ca^{2+}$ entry (or SOCE). TM-induced cytosolic $Ca^{2+}$ and membrane electrical oscillations were acutely inhibited by YM58483, which blocks store-operated $Ca^{2+}$ channels. Significantly, TM-treated cells

secreted increased insulin under conditions normally associated with only minimal release, e.g. 5 mM glucose, YM58483 blocked this secretion. Taken together, these results support a critical role for ER $Ca^{2+}$ depletion-activated $Ca^{2+}$ current in mediating $Ca^{2+}$-induced insulin secretion in response to ER stress.

### *Introduction*

Type 2 diabetes mellitus (T2D) is characterized by impaired glucose-stimulated insulin secretion in the setting of insulin resistance (1–3). Insulin secretion from pancreatic beta cells is triggered by glucose-induced $Ca^{2+}$ entry triggered by the closure of K(ATP) channels (4–6). In many preparations, $Ca^{2+}$ entry is manifested by regular oscillations in cytosolic $Ca^{2+}$, where each oscillation in turn provokes the release of insulin granules (4, 7–10). Maintaining intracellular $Ca^{2+}$ homeostasis is critical for proper insulin secretion and for retaining beta-cell fitness. In mammalian cells, such as the pancreatic beta-cell, the ER is the intracellular organelle where proteins of the secretory pathway are synthesized and initially packaged for export (11). In addition, the ER maintains protein quality control (12), and serves as a $Ca^{2+}$ reservoir that sequesters but also can release free $Ca^{2+}$ into the cytosol to generate a physiological signal (13–15). $Ca^{2+}$ is pumped into the ER lumen via sarco/endoplasmic reticulum $Ca^{2+}$-ATPases (SERCA pumps) and released to the cytosol through the triggered activation of inositol trisphosphate (IP3) and/or ryanodine receptors in the ER membrane (16–21).

Beta cells undergo apoptosis after sustained exposure to the ER stress inducers tunicamycin (TM), thapsigargin, dithiothreitol (DTT), high-glucose or saturated fatty acid (22–27). These conditions activate the unfolded protein response (UPR) through various mechanisms to restore

normal proteostasis and preserve beta-cell function and viability (22, 23). For instance, TM inhibits N-acetylglucosamine phosphotransferase, the key enzyme involved in the N-glycosylation of proteins, which in turn leads to the misfolding of glycoproteins in the ER (28). The resulting ER stress causes UPR activation which in turn may restore proper protein folding and trafficking, increase the protein-folding capacity of the cell, and causes the degradation of misfolded proteins. In addition, further activation of the UPR inhibits new protein synthesis to reduce the protein load of the ER during times of increased stress.

Disrupted ER homeostasis has been proposed to be a potential cause of T2DM (14) and increasing evidence has emerged suggesting that the ER stress cascade is activated in islets from T2DM patients and from animal models of diabetes (23, 29, 30). We have recently discussed the potential links between disrupted ER homeostasis and altered beta-cell function in a review article (31). Other groups have also proposed the relevance of UPR signaling to beta-cell loss and the pathology of diabetes (32). We wished to advance the study of ER stress in disrupting specific beta-cell function, such as ER $Ca^{2+}$ handling, cytosolic $Ca^{2+}$ oscillations and insulin secretion, and we also wanted to determine how these changes in turn affected long term beta-cell survival.

In our study, we used TM to experimentally induce ER stress in insulin-secreting INS-1(832/13) cells or isolated mouse islets. ER stress responses in the form of UPR endpoints, ER and cytosolic $Ca^{2+}$ levels, insulin secretion and beta-cell death were measured at various time points after exposing islets or cells to TM to determine the timeline of these events. TM treatment increased cytosolic $Ca^{2+}$ and insulin secretion, even in 5 mM glucose, a level that is below the

normal glucose threshold of insulin secretion and the triggering of cytosolic $Ca^{2+}$ oscillations. We further found that this abnormal $Ca^{2+}$ signaling resulted from the activation of store-operated $Ca^{2+}$ entry (SOCE), most likely due to a stress-induced reduction of ER $Ca^{2+}$ concentration. The possible significance of this novel mechanism for augmenting insulin secretion for patients with T2DM is discussed.

## *Experimental* procedures

### ***Materials***

Tunicamycin (TM), YM58483, thapsigargin (TG), 2-Aminoethoxydiphenyl borate (2APB) and SKF96365 (SKF) were all obtained from Cayman Chemical. Small interfering RNAs (siRNAs) were purchased from ThermoFisher scientific. Supplementary Tables 1A and 1B contain a complete list of PCR primers and antibodies, respectively. ECL reagents was obtained from Bio-Rad Laboratories.

### ***Isolation of pancreatic islets and islet pretreatments***

Pancreatic islets were isolated from male Swiss-Webster mice (3 months of age; 25-35 g) according to the regulations of the University of Michigan Committee on the Use and Care of Animals (UCUCA), using previously described methods (78) and with an approved protocol. Isolated islets from a given mouse were divided into control and experimental groups, and both were cultured in standard RPMI 1640 medium containing 11 mM glucose, 10% fetal bovine serum (FBS), 10 mM HEPES, 1% penicillin/streptomycin and 1% sodium pyruvate. Control islets were incubated with DMSO, while test islets were pretreated with 10 μg/mL tunicamycin.

***Cell culture and transfection***

INS-1(832/13) cells were grown in RPMI 1640 containing 11 mM glucose, 10% fetal bovine serum (FBS), 1% penicillin/streptomycin, 10 mM HEPES and 1% sodium pyruvate. INS-1(832/13) cells were grown in 10 cm culture dishes, 6-well plates or T25 flasks at 37°C in a 5% $CO_2$ humidified atmosphere. Cells obtained ~70% confluence prior to the initiation of experimentation. INS-1(832/13) cells were transfected with STIM1-specific siRNA or negative control siRNA using lipofectamine RNAiMAX reagent as described in the manufacturer's protocol (Invitrogen). The treated cells were assessed by real-time PCR and western blot.

***Real-Time PCR***

Total RNA was extracted from INS-1(832/13) cells or islets using the RNeasy Mini Kit (Qiagen) according to the manufacturer's instructions. One μg of total RNA from INS-1(832/13) cells or 0.4 μg of total islet RNA was reverse-transcribed using Superscript RT II (Invitrogen) according to the manufacturer's instructions. Real-time experiments were carried out using an SYBR Green PCR master mix (Applied Biosystems) with the primers shown in Table 1A. Raw threshold-cycle (CT) values were obtained using the Step One software, and mean CT values were calculated from triplicate PCR reactions for each sample. Data were presented as RQ values ($2^{-\Delta\Delta CT}$) with expression presented relative to an endogenous control, HPRT1.

***Western blotting***

Total protein was obtained by treating INS-1(832/13) cells or mouse islets with KHEN lysis buffer (50 mM KCL, 50 mM HEPES, 10 mM EGTA, 1.92 mM $MgCl_2$; pH 7.2) and then separating proteins using 4-12% SDS-PAGE and transferring them to nitrocellulose membranes.

Membranes were blocked in 5% w/v nonfat dry milk or 5% BSA in 1X TBST containing 50 mM Tris-HCl (pH 7.4), 150 mM NaCl and 0.1% Tween 20. Blots were incubated overnight with primary antibodies diluted in 5% nonfat dry milk in 1X TBST at 4 °C as described in Table 1B. Blots were incubated with horseradish peroxidase (HRP)-conjugated mouse anti-rabbit antibodies or goal anti-mouse antibodies and these were visualized using ECL reagents.

***Fura-2/AM imaging***

Islets were loaded with Fura-2/AM (2.5 μM) for 45 min. in medium containing 5 mM glucose prior to imaging. Islets were then transferred to a 1 mL perfusion chamber containing 5 mM glucose imaging buffer for 6 min, followed by 10 to 30 min perfusion with this solution at approximately 1 mL/min. Imaging buffer contained (in mM): 140 NaCl, 3$CaCl_2$, 5 KCl, 2 $MgCl_2$, 10 HEPES and 5 glucose. Ratiometric Fura-2 imaging was carried out using 340/380 nm excitation and collecting 502 nm emission, as previously described (78). The fluorescence data were acquired using Metafluor.

***FRET measurements***

To measure ER $Ca^{2+}$, we utilized a previously described ER-localized FRET biosensor, D4ER (79). The sensor was selectively expressed in the beta cells of intact mouse islets using an adenovirus and under the control of the rat insulin promoter, as previously described (79). The same system described above for Fura-2/AM imaging was employed here. D4ER imaging was carried out using 430 nm excitation, and 470/535 nm ratiometric emission. The imaging solution used contained (in mM): 140 NaCl, 3 $CaCl_2$, 5 KCl, 2 $MgCl_2$, 10 HEPES, 5 glucose and 0.2 diazoxide (Dz). Dz was included to keep the $K_{ATP}$ channel in its open state to prevent oscillatory

$Ca^{2+}$ activity and improve the signal/noise ratio and stability of the ER $Ca^{2+}$ recordings. FRET ratios were acquired using Metafluor, and mean values were calculated using Prism.

***Analysis of cytosolic $Ca^{2+}$ recordings***

Traces containing cytosolic $Ca^{2+}$ oscillations were analyzed using MATLAB (Mathworks) to obtain the plateau fraction (PF), periods, baseline ratios and relative amplitudes of $Ca^{2+}$ oscillations, as described (50). PF was calculated as the active phase duration divided by the period of each oscillation (50). Only islets displaying oscillations were assigned a PF, and those exhibiting a persistent plateau phase were assigned a PF value of 1.0.

***Electrophysiology***

Islet membrane potential was measured using perforated patch whole cell current clamp as described (53). Electrophysiological recordings were made from single beta cells in intact islets treated with TM for 6, 12 and 16 hours, respectively. Islets treated with vehicle medium were used to make control recordings. Only one beta-cell in each intact islet was patched. Membrane potential of each beta-cell in an intact islet was recorded in current-clamp mode after perforated patch configuration was established. The external recording solution contained (in mM): 140 NaCl, 3 $CaCl_2$, 5 KCl, 2 $MgCl_2$, 10 HEPES and 5 glucose.

***Assays of cell death***

INS-1(832/13) cells were dislodged from T25 flasks with 0.05% trypsin and after gentle shaking, and propidium iodide (PI) was applied to label dead cells, as described in the manufacturer's

protocol (Sigma). The percentage of PI-positive cells was determined using a flow cytometer provided by the Flow Cytometry Core of the University of Michigan.

***Assays of apoptosis***

INS-1(832/13) cells were harvested as described in above cell death assay and fixed in cold 70% ethanol and stored in 4°C. Before measurement, PI was added as described in the manufacturer's protocol (Sigma), and the percentage apoptotic cells was determined by calculating the percentage of sub-G1 cells in the DNA content histogram using a flow cytometer provided by the Flow Cytometry Core of the University of Michigan.

***Glucose-stimulated insulin secretion assay (GSIS)***

Islets were washed with glucose free KRB buffer (115 mM NaCl, 4.7 mM KCl, 1.2 mM $MgSO_4 \bullet 7H_2O$, 1.2 mM $KH_2PO_4$, 20 mM $NaHCO_3$, 16mM HEPES, 2.56 mM $CaCl_2$-$2H_2O$, 0.2% BSA) for 30 min at 37° C, and then incubated with KRB buffer containing 5 mM or more glucose for an additional 30 min. The supernatant and islets were then collected separately to determine insulin content using a mouse insulin ELISA kit according to the manufacturer's instructions (Crystal Chem).

***Statistical analysis***

Data were expressed as means +/- SEM, unless specified, and were analyzed using an unpaired Student's t-test (Prism, GraphPad Software Solutions) when comparing two groups. Differences between two or more groups were analyzed using two-way ANOVA (Prism) with post hoc

multiple comparison by Tukey's procedure. Values of $p < 0.05$ were considered statistically significant.

***Results***

Tunicamycin, a commonly used pharmacological inducer of ER stress in beta cells, inhibits protein glycosylation (22, 33–35). To investigate the relationship between ER stress, ER $Ca^{2+}$ and cytosolic $Ca^{2+}$, we systematically measured the concentration of $Ca^{2+}$ in the cytosol and ER in parallel with UPR markers to establish their respective time courses following TM treatment. Changes in the three canonical ER stress response markers, spliced XBP1, CHOP and BiP were determined at the mRNA or protein level. Mouse islets or insulin secreting INS-1(832/13) cells were treated with vehicle (DMSO) as a control or TM for 6, 12 or 16 hours in 11 mM glucose-containing medium prior to extracting total cell mRNA and making whole cell protein lysates.

As shown in Figures 2.1A and 2.1B, XBP1 splicing increased after 6 hours of TM treatment in both INS-1(832/13) cells and mouse islets, while total XBP1 levels were unchanged. Similarly, as shown in Figure 2.1C, CHOP increased after 6 hours of TM treatment in INS-1(832/13) cells. In contrast, as shown in Figures 2.1D through 2.1G, levels of BiP protein only increased after 12 hours of exposure to TM. XBP1 splicing is known to be an early event in the UPR, while the upregulation of BiP expression has been reported to be more delayed (22, 23, 36, 37).

Apoptosis occurs in a variety of cell types as a consequence of prolonged ER stress (23) and previous studies have shown that TM induces cell death in INS-1(832/13) cells and other cell lines (35, 38–42). To determine the presence of apoptosis, we assayed the level of cleaved PARP

protein, an established marker of apoptosis (43, 44) by western blotting. As shown in Figure 2.2A and 2.2B, a band corresponding to cleaved PARP was visible at 89 kDa in lysates obtained from INS-1(832/13) cells exposed to TM for 12 hours or more. Cleaved PARP was barely detected in any of our cell samples under control conditions or if TM exposure was for 6 hours or less. It thus appeared that TM only triggered significant apoptosis after 12 hours. The percentage of cleaved versus total PARP was monitored and is shown in Figure 2.2B to rule out the effect of uneven protein loading. In addition, the percentage of INS-1(832/13) cells that take up propidium iodide (PI), a dye that is indicative of cell death, only increased after 16 hours of TM treatment, compared to DMSO-treated controls (Figure 2.2C). Cell death as assessed using this marker was not observed at any of the earlier time points studied. Figure 2.2D shows there was a four-fold increase in the number of cells in the sub-G1 phase following 24 hours exposure to TM, indicating they were late stage apoptotic cells compared to DMSO treated controls.

Taken together, TM triggered a classic ER stress response in INS-1(832/13) cells after 6 hours, while apoptosis was only seen after 12 hours. Frank, quantitative beta-cell death, in turn, was evident much later, after about 16 hours of TM treatment, as evidenced by increased propidium iodide uptake.

As mentioned, TM has been used to induce ER stress in several studies of beta cells (22, 23, 33, 35). The ER plays an important role in beta-cell function since it is the site where proteins of the secretory pathway are folded and processed in preparation for transport to the Golgi apparatus (15, 45), and it is the location where proteostasis occurs (45, 46). In terms of cellular $Ca^{2+}$ homeostasis, the ER also has a central role in this process due to its ability to sequester and

buffer cytosolic $Ca^{2+}$, serve as a releasable $Ca^{2+}$ source in response to surface membrane GPCR signaling, and it supplies $Ca^{2+}$ to $Ca^{2+}$-binding ER-resident protein chaperones that act to ensure proper protein folding (47, 48).

To test whether TM altered ER $Ca^{2+}$ level in our system, the ER $Ca^{2+}$ probe D4ER was transiently expressed in islet beta cells using an adenovirus delivering the *D4ER* gene placed behind the rat insulin promoter 2. Islets were then treated with vehicle control (DMSO) or TM (10 μg/ml) for 6, 12 or 16 hours and then ER $Ca^{2+}$ was measured. Figure 2.3A shows ER $Ca^{2+}$ normalized to the initial FRET ratio (F0), expressed in relative units, as a function of time, and the effect of thapsigargin (TG, 1 μM) is shown for both control and TM-treated islets. TG is a SERCA blocker that is well known to deplete ER $Ca^{2+}$ by blocking $Ca^{2+}$ uptake into the ER (49). Only beta cells that responded to TG are shown in Fig. 3A; these constituted approximately 50% of the beta cells tested. As shown in Figure 2.3B, TM caused a decline of steady state ER $Ca^{2+}$ in islets compared to DMSO after 6, 12 and 16h of treatment.

Mouse islets do not typically show oscillations in cytosolic $Ca^{2+}$ or electrical activity when acutely exposed to glucose concentrations < 7 mM (2, 50–52). To determine the relationship between ER stress and cytosolic free $Ca^{2+}$ in our experimental system, mouse islets were exposed to TM or vehicle control (DMSO) in standard RPMI 1640 medium for 6,12 or 16 hours. Following this treatment, cytosolic free $Ca^{2+}$ and islet electrical activity were recorded in parallel studies using an extracellular recording solution containing 5 mM glucose.

As shown in Figure 2.4A, cytosolic free $Ca^{2+}$ in control islets did not display oscillatory activity in 5 mM glucose solution, as expected (2, 50–52). In contrast, islets treated with TM exhibited islet $Ca^{2+}$ oscillations or $Ca^{2+}$ transients when exposed to the TM for 6 hours or more. 40% of islets treated with TM for 6 hours displayed free $Ca^{2+}$ oscillations compared to those treated with DMSO (Figure 2.4B). Treatment with TM for 12 or 16 hours resulted in a greater % of oscillating islets.

The plateau fraction, frequency and amplitude of oscillating islets as well as their baseline $Ca^{2+}$ levels were analyzed and plotted in Figure 2.5. Plateau fraction, oscillation frequency and amplitude were not plotted for control islets as they did not exhibit oscillations. Statistically significant increases in baseline $Ca^{2+}$ levels were observed after 6 and 12 hours of TM exposure (Figures 2.5B).

Our observation that islets treated with TM exhibited cytosolic $Ca^{2+}$ oscillations (Figure 2.6) was next confirmed by separate measurements of islet electrical activity, obtained using perforated patch clamp recording. TM-treated beta cells thus exhibited oscillations in islet membrane potential in 5 mM glucose, which was rarely observed in control islets exposed to the same glucose concentration, as was found for $Ca^{2+}$. However, the occurrence of oscillations was related to the duration of TM treatment. As shown in Figure 2.6, islets subjected to TM for 6 hours showed occasional oscillations in 5 mM glucose, while islets treated for 12 or 16 hours showed regular oscillations having an average period of 5 – 8 minutes. Importantly, the oscillations we observed in TM-treated islets in 5 mM glucose strongly resembled those of normal islets exposed to glucose concentrations >7-8 mM (53).

When beta cells are depolarized, $Ca^{2+}$ influx through voltage-gated $Ca^{2+}$ channels leads to a rise in cytosolic $Ca^{2+}$ concentration that triggers the release of insulin granules from the cell (4, 10, 51, 54). To test whether the changes we observed in islet electrical and cytosolic $Ca^{2+}$ activity in response to TM treatment were sufficient to elicit insulin secretion even under normally sub-threshold conditions, islets were pretreated with DMSO or TM in standard RPMI 1640 medium (including 11 mM glucose) for 6, 12 or 16 hours. After treatment, islets were thoroughly washed, and a static incubation protocol was used to measure insulin secretion in 5 mM glucose. As shown in Figure 2.7A, insulin secreted into the medium was significantly increased after 12 hours or more of TM exposure, while islet insulin content was unchanged. Expressed another way, TM exposure for 12 hours or more resulted in greater insulin secretion as a percent of insulin content, compared to controls (Figure 2.7B). The time course of increased secretion closely paralleled the increase in cytosolic $Ca^{2+}$ or electrical activity depicted in Figures 2.4 through 2.6. They support the hypothesis that the activation of cytosolic $Ca^{2+}$ activity by ER stress in 5 mM glucose was triggered by increased islet electrical activity and was sufficient to release more insulin from the beta-cell. Secreted insulin and percent insulin content were both higher after 6 hours of TM compared to DMSO exposure, but the differences were not statistically significant. The unique aspect of the 6-hour time point will be addressed in the Discussion. We also point out that the magnitude of the secretion response of TM-treated islets in 5 mM glucose is still much lower than that seen in response to 11 mM or more glucose.

Store-operated $Ca^{2+}$ entry (SOCE) links reduced ER $Ca^{2+}$ concentration to the activation of voltage-independent, plasma membrane $Ca^{2+}$ channels that can replenish the depleted ER, with

$Ca^{2+}$ entering the cell from the extracellular space (55–57). To determine whether SOCE played a role in mediating the oscillations we observed following chronic ER stress and ER $Ca^{2+}$ lowering, we tested whether YM58483, a selective blocker of membrane SOCE channels, interfered with our physiological endpoints (58–60). As shown in Figures 2.8A and 2.8B, both cytosolic $Ca^{2+}$ oscillations and the electrical activity observed in TM-treated islets in 5 mM glucose were abruptly abolished by YM58483 treatment. These results show that SOCE, which normally plays little or no role in the genesis of glucose-induced islet electrical oscillations (61), was here facilitated by TM-induced ER stress in beta cells, presumably because TM reduced ER $Ca^{2+}$. Importantly, YM58483 also blocked TM-induced insulin secretion in islets bathed in 5 mM glucose (Figures 2.8C and 2.8D). In contrast, the addition of YM58483 had no effect on insulin secretion, islet electrical activity, or intracellular $Ca^{2+}$ in control islets (Figures 2.8A-D).

At the molecular level, main components of SOCE are stromal interaction molecule-1 (STIM1) and $Ca^{2+}$ release-activated $Ca^{2+}$ channel protein 1 (ORAI1). STIM1 is an ER $Ca^{2+}$ sensor while ORAI1, which is found on the plasma membrane, is the pore-forming subunit of functional SOCE. When STIM1 senses ER $Ca^{2+}$ depletion, STIM1 molecules aggregate and interact with ORAI1 at ER-PM junctions, and this complex mediates $Ca^{2+}$ influx through SOCE (62, 63). To confirm the results, we obtained at the molecular level, siRNA was used to knockdown STIM1 in INS-1(832/13) cells. Transfecting INS-1(832/13) cells with siRNA-STIM1 (siSTIM1) reduced STIM1 mRNA by ~ 80-90% (Figure 2.9A) and STIM1 protein by ~70-75% (Figure 2.9B and 2.9C) compared to treatment with control siRNA (siCon). STIM1 reduction did not result in significant upregulation of ORAI1, suggesting the cells did not compensate for the loss of STIM1 (Figure 2.9B and 2.9C). The percentage of cells showing cytosolic $Ca^{2+}$ transients in 5

mM glucose was decreased in siSTIM-transfected cells (~40%) compared to siCon-transfected control cells (~10%) following 16 hour TM exposure (Figure 2.9D and 2.9E). Even after 16 hours of DMSO exposure, controls showed no change in their $Ca^{2+}$ activities.

As an alternative to blocking SOCE channels with YM58483, we tested whether removing extracellular $Ca^{2+}$ was similarly able to abolish the cytosolic $Ca^{2+}$ oscillations we observed in TM-treated islets in 5 mM glucose. Removing extracellular $Ca^{2+}$ confirmed the results we obtained with YM58483, supporting the hypothesis that the oscillations seen after TM treatment indeed require increased influx of extracellular $Ca^{2+}$ (Figure 2.10A). However, applying other SOCE channel blockers, 2-Aminoethoxydiphenyl borate (2APB) or SKF96365 (SKF) acutely at the end of a $Ca^{2+}$ imaging experiment surprisingly *increased* cytosolic $Ca^{2+}$ levels in both control and experimental groups (Figure 2.10B and 2.10C) (64, 65). 2APB and SKF are nonselective SOCE inhibitors as they also inhibit other channels over a similar concentration range (66).

While ER $Ca^{2+}$ decreased in TM-treated islets compared to controls, blocking SOCE with YM58483 had little or no measurable effect on the ER $Ca^{2+}$ levels of either control or TM-treated beta cells (Figure 2.11A). This finding was unexpected but will be addressed further in the Discussion. Blocking SOCE with YM58483 also did not affect any of the TM-induced UPR endpoints we measured (Figure 2.11B).

Previous reports have shown that elevated cytosolic $Ca^{2+}$ is detrimental to beta cells (67). Thus, preventing excessive cytosolic $Ca^{2+}$ elevation due to overactive SOCE might have at least partly protected beta cells from cell death induced by prolonged exposure to TM. However, as shown

in Figure 2.11C, 24 hour treatment with TM increased cell death in INS-1(832/13) cells, but we found no protection afforded by the inclusion of YM58483.

To maintain glucose homeostasis, beta cells secrete insulin when blood glucose concentration rises. Islets exhibit oscillations in cytosolic free $Ca^{2+}$ when exposed to 7 mM or more glucose (52). After isolated mouse islets were exposed to TM or vehicle control (DMSO), free $Ca^{2+}$ and insulin secretion were measured in parallel in 11 mM glucose. As shown in Figure 2.12A, both control and experimental groups showed $Ca^{2+}$ oscillations in 11 mM glucose. The percentages of oscillating islets we observed were very similar between the two groups (70~80%), while the remaining islets tended to go to a plateau (Figure 2.12B). The frequency of the oscillations observed in TM-treated islets was higher than for controls, while no significant change was observed in plateau fraction, baseline $Ca^{2+}$ or oscillation amplitude (Figure 2.12C-F). In addition, we found no significant change in insulin secretion between experimental and control groups after they were stimulated with 11 mM glucose for 30 minutes (Figure 2.12G and 2.12H).

Besides tunicamycin, ER stress can be induced by treating islets with thapsigargin or high glucose (22, 23). As shown in Figure 2.13A, mouse islets exposed to thapsigargin (200 nM) for 16 hours exhibited oscillatory cytosolic $Ca^{2+}$ levels despite being in 5 mM glucose. Similarly, mouse islets cultured in medium containing 25 mM glucose to induce stress also exhibited cytosolic $Ca^{2+}$ oscillations (Figure 2.13B). These oscillations were also abruptly abolished by YM58483 treatment. DMSO treated or 11 mM glucose cultured islets did not exhibit $Ca^{2+}$ oscillations in 5 mM glucose solution, however, as expected.

As SOCE activated in response to TM treatment in our study, we also assayed the level of STIM1 and ORAI1 expression under these same experimental conditions. As shown in Figure 2.14A, we observed a protein band corresponding to STIM1 as expected, and an additional, smaller molecular weight band in lysates from TM-treated INS-1(832/13) cells after 16 hours of treatment. The intensity of the upper band for STIM1 was not significantly altered in response to TM compared to controls (Figure 2.14B). ORAI1 protein was also unchanged by TM treatment (Figure 2.14A and 2.14B), as reported in another recent study (68). GLUT2 protein was also measured in INS-1(832/13) cells after 6 hours of TM treatment compared to control, and no change in protein expression was found (Figure 2.15A and 2.15B).

***Discussion***

In this study, we sought to delineate the temporal relationship between the induction of ER stress, altered beta-cell function, and altered beta-cell viability, focusing on the role of ER and cytosolic $Ca^{2+}$ in these processes. Studies were carried out by exposing mouse islets or INS-1(832/13) cells to the glycosylation inhibitor tunicamycin for up to 24 hours. We found that UPR activation appeared to be linked to a reduction in ER $Ca^{2+}$ and a phase of increased extracellular $Ca^{2+}$ influx linked to ER $Ca^{2+}$ unloading. The $Ca^{2+}$ oscillations that were triggered by store-operated $Ca^{2+}$ influx were sufficient to trigger the release of insulin, even in normally sub-threshold glucose. Cell death was found to occur much later, e.g. after 16 hours post-treatment and appeared to be independent of the early phase of SOCE-mediated $Ca^{2+}$ influx and concomitant insulin secretion.

Previous research carried out using many types of cells has shown that thapsigargin, a SERCA blocker, which prevents ATP-dependent $Ca^{2+}$ sequestration by the ER, unloads the ER $Ca^{2+}$ store,

triggering SOCE (16, 60). Activated SOCE results in increased cytosolic $Ca^{2+}$, which serves to replenish the ER $Ca^{2+}$ pool (69). The recent findings reported by Yamamoto *et al*. indicate that tunicamycin decreases ER $Ca^{2+}$ by increasing ryanodine receptor 2 activity which in turn elicits spontaneous cytosolic $Ca^{2+}$ transients that are seen after raising extracellular $Ca^{2+}$ concentration (70). We agree with Yamamoto *et al* that ryanodine receptors (RyRs) are likely involved in ER stress induced ER $Ca^{2+}$ lowering, as we observed inhibitory effects of the RyR blocker ryanodine (data not shown). However, we propose a *very different* interpretation in this paper. Our data that ER stress conditions activate a $Ca^{2+}$ current mediated by SOCE channels under low glucose conditions, which likely occurs secondary to ER $Ca^{2+}$ depletion by tunicamycin.

The normal glucose threshold for islet oscillations in our hands is near 7 mM (2, 50), which means that TM-induced ER stress in a sense increased the sensitivity of islets to glucose concentration. In our view, glucose-induced islet $Ca^{2+}$ oscillations are induced despite the low level of glucose by the activation of SOCE-mediated $Ca^{2+}$ current, which depolarizes the beta-cell membrane to threshold despite incomplete closure of beta-cell $K_{ATP}$ channels. The evidence for this interpretation is that (1) the $Ca^{2+}$ oscillations we observed strongly resemble those of control islets exposed to glucose >7 mM, suggesting a common origin; (2) the $Ca^{2+}$ oscillations of stressed islets were completely blocked by the selective SOCE blocker YM58483 (58, 59); and notably this drug had no effect on untreated control islets; (3) patch clamp electrophysiology confirmed the electrical nature of the ER stress-induced oscillations and, as for the $Ca^{2+}$ oscillations, the electrical bursting we observed in 5 mM glucose was similarly abolished by YM58483; and (4) the percentage of $Ca^{2+}$ oscillations were decreased in TM-treated siSTIM1-knockdown INS-1(832/13) cells compared to controls. Taken together these data are in strong

support of a plasma-membrane delimited mechanism, and they rule out intracellular store $Ca^{2+}$ release as the proximal cause of the $Ca^{2+}$ oscillations we observed in TM-treated islets, although we believe ER $Ca^{2+}$ depletion by ER stress indirectly caused the oscillations by triggering SOCE.

Physiologically, when blood glucose rises, $K_{ATP}$ channel closure mediates plasma membrane depolarization, which in turn increases cytosolic $Ca^{2+}$, which then drives insulin secretion (2, 5, 8). Membrane potential changes in mouse beta cells have been shown to precede changes in cytosolic $Ca^{2+}$ under physiological conditions (5). The cytosolic $Ca^{2+}$ oscillations shown in Figures 2.4A occurred in parallel with membrane potential oscillations in 5 mM glucose saline in response to TM treatment, shown in Figure 2.6. In simultaneous measurements of cytosolic $Ca^{2+}$ and insulin secretion, each oscillation in islet $Ca^{2+}$ has been shown to be well synchronized with a pulse of insulin secretion (4, 5, 10).

Although cytosolic $Ca^{2+}$ was increased after 6 hours of TM treatment, the change in insulin secretion and percent insulin (Figure 2.7) we measured at this time point were not statistically significant compared to controls, although the means we obtained were greater than controls. This may be explained by our observation that less than 40% of islets displayed elevated cytosolic $Ca^{2+}$ within 6 hours of TM treatment (Figure 2.4B). Our results at the 6-hour time point may thus underestimate the amount of insulin secretion seen in response to TM because it included both responding and non-responding islets.

YM58483 did not affect the extent of ER $Ca^{2+}$ depletion that followed TM treatment (Figure 2.11A), which was surprising. This could be due to several possible factors: (1) the influx of

$Ca^{2+}$ due to SOCE may have been too small to cause a detectable change in ER $Ca^{2+}$ due to limits in the $Ca^{2+}$ sensitivity of the D4ER $Ca^{2+}$ probe; (2) SERCA expression and/or function might also be reduced by TM treatment, such that under these pathophysiological conditions, SOCE is capable of mediating an electrical current and $Ca^{2+}$ oscillations but not significant ER store refilling. ER stress has in fact been reported to cause reduced SERCA2b expression in beta cells, which supports this idea (18, 71, 72); (3) the ER may become so leaky to $Ca^{2+}$ after TM treatment that a modest activation of SOCE is unable to do enough to measurably refill the ER, like turning on a small hose to refill a very leaky barrel.

Our results support the hypothesis that TM-triggered beta-cell death occurs as a consequence of ER $Ca^{2+}$ depletion, and that SOCE activation is a separate action that is unrelated to the ultimate fate of the cell, as shown in Figure 2.16. Similar observations and conclusions were made in studies of thapsigargin-treated LNCaP, PC3 and MCF7 cells (49). Thapsigargin caused the unloading of ER $Ca^{2+}$ and resulted in cell death despite genetic knockdown of the SOCE components STIM1 and/or ORAI1 in this case. Therefore, ER $Ca^{2+}$ depletion due to ER stress appeared to be an important contributor to thapsigargin-induced cell death, instead of SOCE activation and increased cytosolic $Ca^{2+}$ (49).

As shown in Figures 2.14A-B, we found two bands corresponding to STIM1 protein. The upper band of STIM1 expression at 77 kDa and ORAI1 expression remained unchanged. Both STIM1 and ORAI1 are known to be N-linked glycosylated proteins (62, 63, 73, 74). Other investigators also observed no change in ORAI1 in response to induced ER stress, while STIM1 responded to TM treatment. The slightly smaller molecular weight STIM1 species, representing non-

glycosylated STIM1, were reported. Blocking STIM1 glycosylation led to diminished SOCE (73, 74). Evans-Molina and colleagues have recently reported that STIM1 was downregulated in a diabetes model, while overexpressing STIM1 restored SOCE under high glucose conditions (68). However, Evans-Molina and colleagues propose that SOCE is an essential driver of glucose-induced $Ca^{2+}$ oscillations (15 mM glucose) under normal conditions and that SOCE is impaired in response to proinflammatory cytokines or palmitate mediated stress conditions. In contrast, we propose that SOCE is *not* involved in the triggering or modulation of glucose-induced $Ca^{2+}$ oscillations in untreated control islets, but *is activated* by ER stress, resulting in the appearance of $Ca^{2+}$ oscillations under sub-threshold glucose conditions (5 mM glucose) by virtue of this abnormal triggering mechanism, which in essence shifts the glucose sensitivity of the islet to the left where islet $Ca^{2+}$ activity could then contribute to the production of high basal insulin release. Different glucose conditions may account for the different interpretations.

The justification for our use of insulin secreting INS cells in addition to mouse islets in the present paper relates to the small amount of tissue available for biochemical and molecular studies if just islets were used. For example, analyzing propidium iodide levels with flow cytometry in order to quantify cell death is extremely challenging if primary beta cells are used. INS-1(832/13) cells are one of the most commonly used insulin-secreting cell lines that display many important characteristics of primary beta cells. Importantly, INS-1(832/13) cells are very responsive to glucose (75). According to Figures 2.1A and 2.1B, INS-1(832/13) cells had identical UPR responses as isolated islets. Thus, we believe that the molecular studies done in INS-1(832/13) cells while not perfectly reflecting what we might expect if islets or primary beta cells were used in their place, are reasonable surrogates for the primary cells with regards to

UPR activation and cell death. This is not likely to be true regarding physiology where our methods are well attuned to studying primary islets and their oscillatory and secretory characteristics.

In summary, as shown in Figure 2.16, we propose that TM induced beta-cell death occurs through ER $Ca^{2+}$ depletion, whereas SOCE and concomitant increased cytosolic $Ca^{2+}$ were required for our finding increased insulin secretion under stress conditions. During prediabetes, which is associated with insulin resistance, the pancreatic beta-cell is thought to compensate for rising levels of glucose by increasing insulin secretion and, if that fails, increasing beta-cell mass, provided the cells are capable of doing so (76). However, long-term hyperinsulinemia, and the increased metabolic workload it represents, can potentially exhaust the beta-cell and promote beta-cell death (77). In our results, TM-induced ER stress resulted in increased beta-cell electrical activity, cytosolic $Ca^{2+}$ oscillations and insulin secretion by activating SOCE. Blocking SOCE by applying YM58483 to stressed but not control islets abolished ER stress-triggered increases in electrical activity, cytosolic $Ca^{2+}$ oscillations and insulin secretion (Figures 2.8A-D). Therefore, the increased insulin secretion data not only confirmed that TM increased cytosolic $Ca^{2+}$ oscillations, but it also established SOCE as the key mechanism.

This report shows that SOCE is a key player in ER stress-induced cytosolic $Ca^{2+}$ oscillations and insulin secretion, and we suggest that this pathway must work in parallel with the UPR and cell death pathways. The cytosolic $Ca^{2+}$ oscillations we observed clearly resulted from electrical oscillations and not $Ca^{2+}$ -induced $Ca^{2+}$ release from the ER. Thus, these results suggest the possibility that in T2DM or under pre-diabetic conditions increased secretion due to SOCE

activation may contribute to the increased basal insulin secretion that is a hallmark of type 2 diabetes. Combining our findings with more detailed mechanistic and pharmacological studies on SOCE activity in prediabetes may disclose additional valuable information and perhaps novel treatment strategies.

## *Figures and Legends*

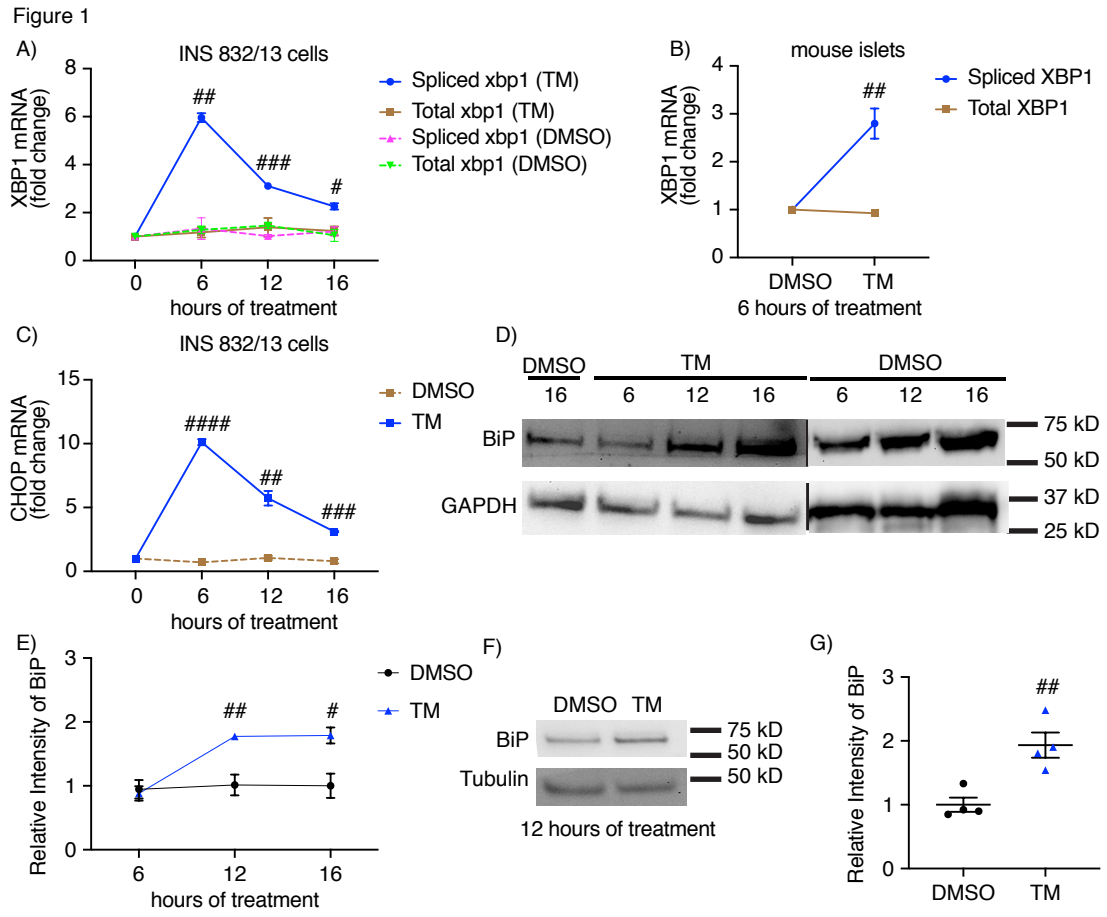


*Figure 2.1 Tunicamycin induced the ER stress response*

INS-1(832/13) cells and isolated mouse pancreatic islets were treated with vehicle control (DMSO) or tunicamycin (TM, 10 µg/ml) for the indicated length of time shown. 1A: Expression levels of spliced XBP1 and total XBP1 mRNA in INS-1(832/13) cells and 1B: Same but in islets. 1C: Expression level of CHOP in INS-1(832/13) cells. 1D: Representative western blot showing the level of BiP in INS-1(832/13) cells and 1F: Same but in islets. GAPDH and tubulin are loading controls. Quantitative protein levels are shown graphically in 1E and 1 G respectively. 1E: Protein levels are all normalized to DMSO 16h. All values shown are means ± SEM. #, $p< 0.05$, ##, $p< 0.01$, ###, $p< 0.0005$, ####, $p< 0.0001$ compared with control conditions; n= at least 3 times repeated per condition.

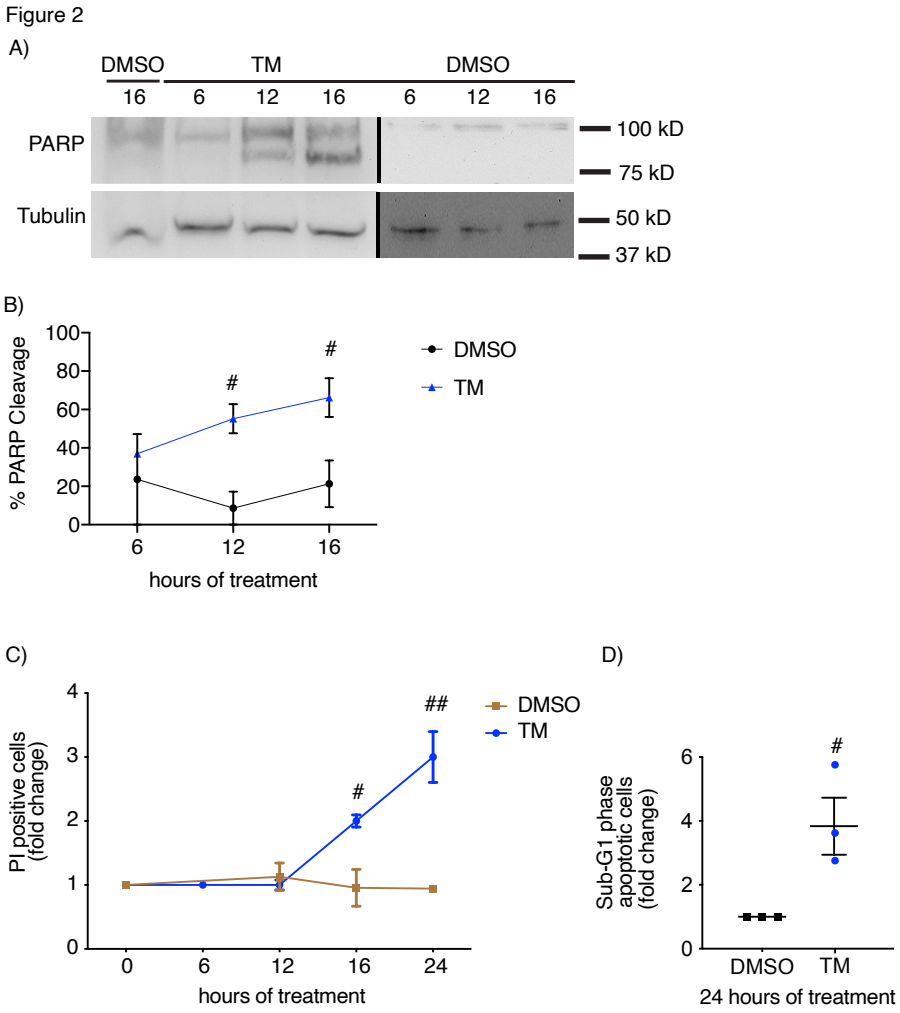


*Figure 2.2 Tunicamycin triggered apoptosis*

INS-1(832/13) cells were treated with vehicle control (DMSO) or tunicamycin (TM, 10 µg/ml) for the indicated length of time shown. 2A: Representative western blot showing the level of total PARP at 116 kDa and cleaved PARP at 89 kDa in INS-1(832/13) cells. Tubulin is shown as loading control. 2B: Quantitative percentage of cleaved PARP out of total PARP are shown graphically. Protein levels are normalized to DMSO 16h. 2C: After various hours of DMSO or TM treatment, cell death in INS-1(832/13) cells is shown by propidium iodide (PI) staining and was quantified using flow cytometry. Fold change was derived by comparing to untreated group. 2D: After 24 hours of DMSO or TM treatment, late stage apoptotic INS-1(832/13) cells is shown using the sub-G1 assay measured by flow cytometry. Fold change was derived by comparing to DMSO group. All values shown are means ± SEM. #, $p < 0.05$, ##, $p < 0.01$, compared with control conditions; n= at least 3 times repeated per condition.

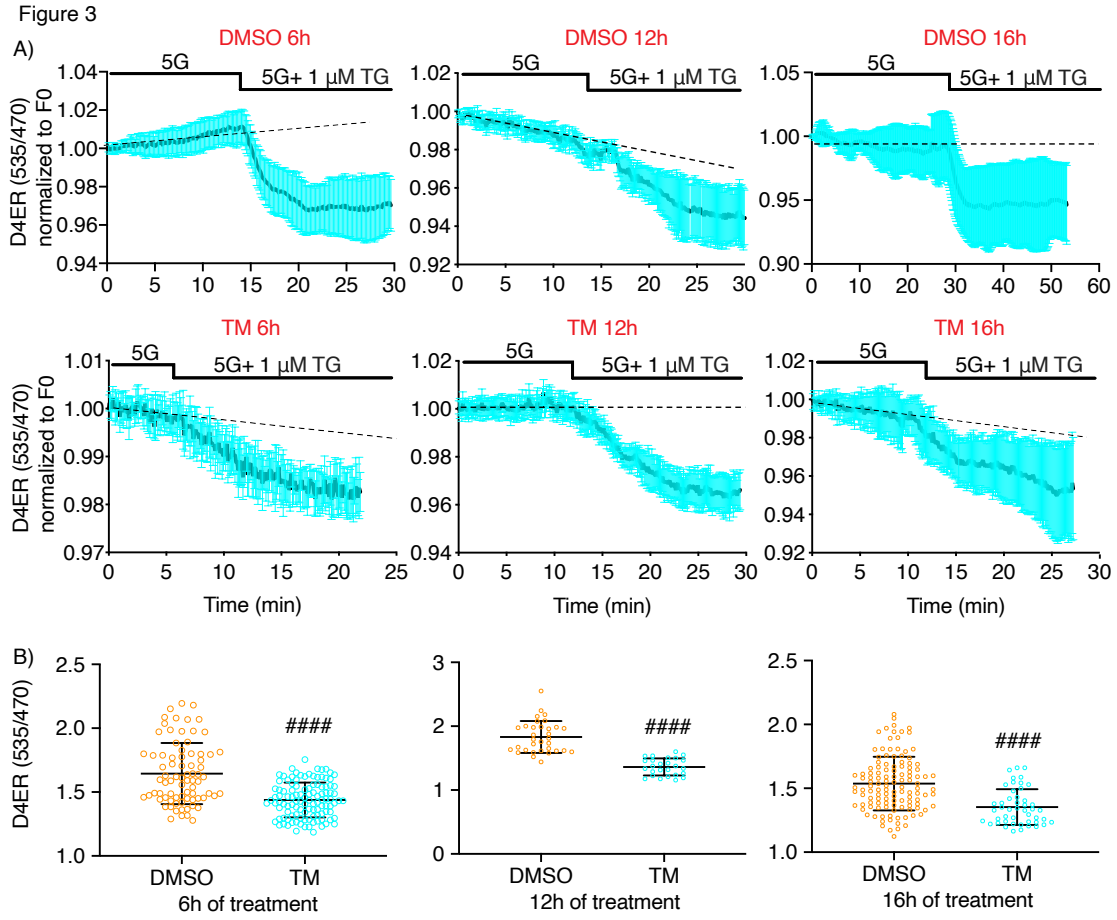


*Figure 2.3 Tunicamycin treatment decreased basal ER $Ca^{2+}$ level*

Mouse pancreatic islets were infected with an adenovirus expressing a beta-cell directed D4ER probe for three hours followed by a 48-hour recovery period. Islets were then treated with vehicle control (DMSO) or tunicamycin (TM, 10 µg/ml) for 6, 12 and 16 hours in 11 mM glucose islet culture medium (RPMI 1640 medium, see Methods). 3A: Basal ER $Ca^{2+}$ (normalized to the initial intensity) traces for each condition obtained in 5 mM glucose solution before and after thapsigargin (TG, 1 µM). 3B: The raw data showing resting ER $Ca^{2+}$ level from mouse islets in 5 mM glucose solution with 200 uM diazoxide present. Each data point shown was a D4ER ratio obtained for one selected region of interest, a single cell or small group of cells. All values shown are means ± SD. ####, $p < 0.0001$; n= at least 5 mice.

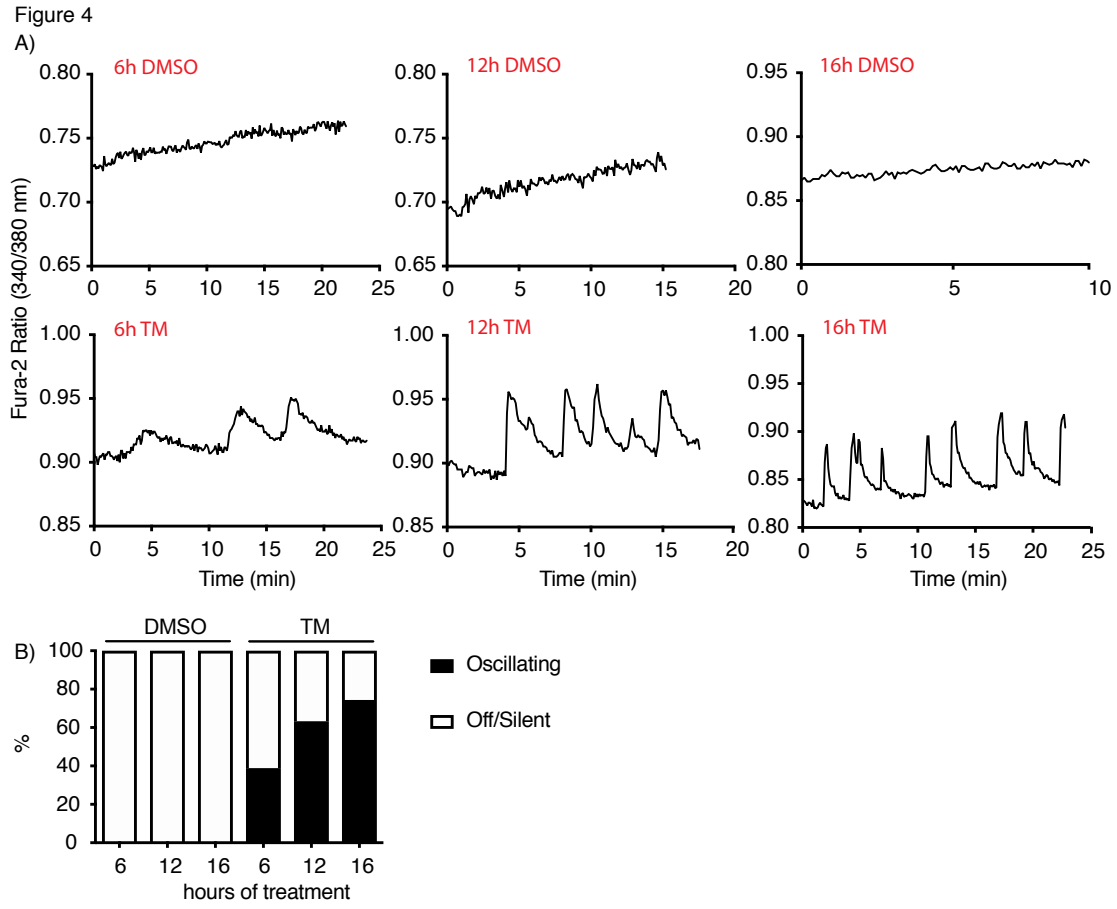


*Figure 2.4 Tunicamycin increased cytosolic free $Ca^{2+}$ under sub-threshold glucose conditions*

Isolated pancreatic mouse islets were treated with a vehicle control (DMSO) or tunicamycin (TM, 10 µg/ml) for 6, 12 and 16 hours in 11 mM glucose. 3A: The responses of cytosolic free $Ca^{2+}$ to solution containing 5 mM glucose under the indicated conditions. 3B: Percentage of oscillating islets; n= at least 3 mice.

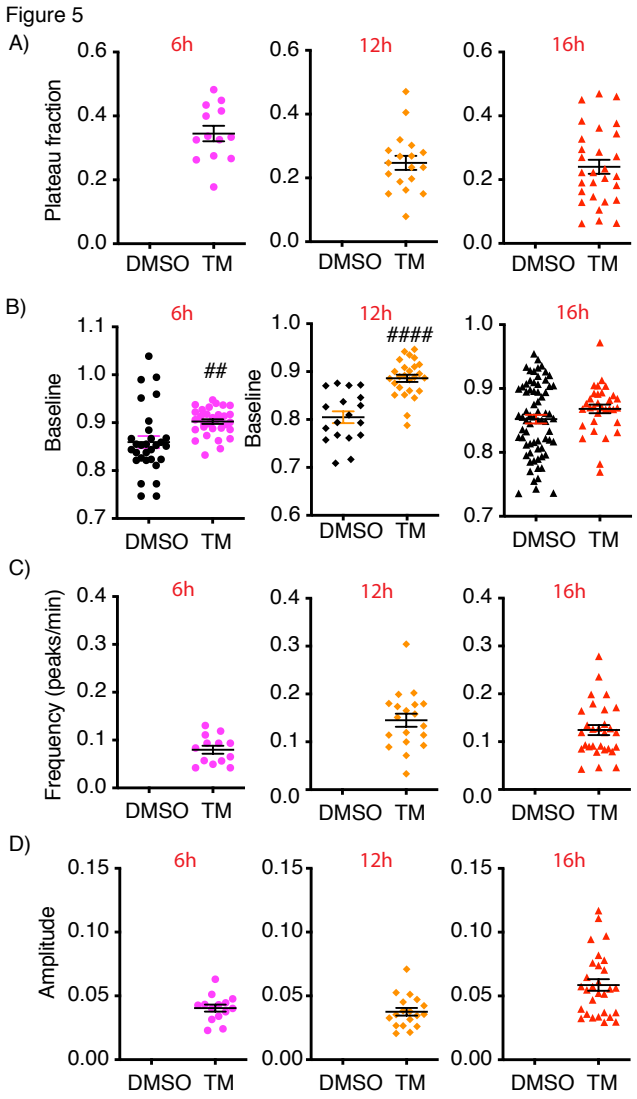


*Figure 2.5 Cytosolic free $Ca^{2+}$ imaging analysis*

Summary findings for the cytosolic free $Ca^{2+}$ traces shown in 4A. 5A: Plateau fraction. 5B: Baseline values. 5C: oscillation frequency. 5D: oscillation amplitude. All values shown are means ± SEM. ##, $p< 0.01$, ####, $p< 0.0001$; n= at least 3 mice.

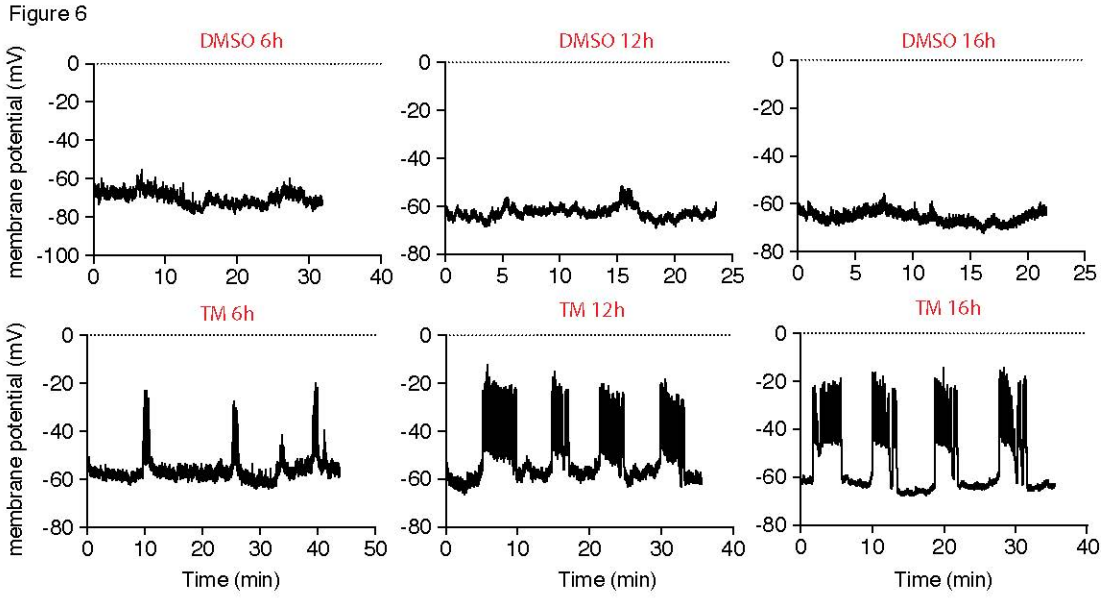


*Figure 2.6 Tunicamycin treatment resulted in the appearance of electrical activity under sub-threshold glucose conditions*

Isolated mouse islets were treated with vehicle control (DMSO) or tunicamycin (TM, 10 μg/ml) for 6, 12 and 16 hours in 11 mM glucose. The acute responses of islet membrane potential to 5 mM glucose solution under the conditions indicated are shown. Details are provided in the text. Consistent results were observed in at least 3 mice.

Figure 7

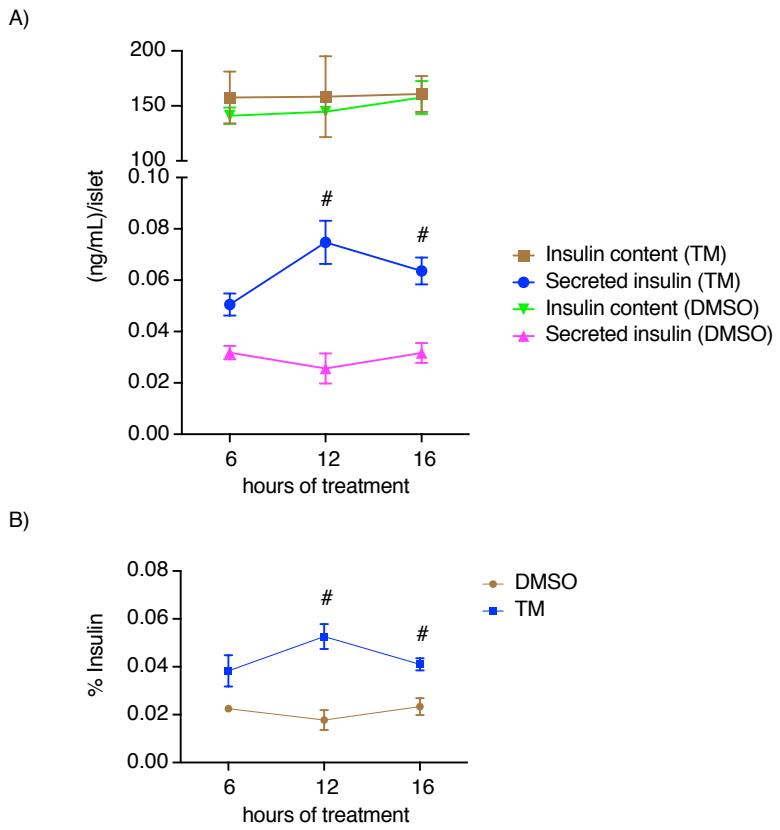


*Figure 2.7 Tunicamycin increased the amount of insulin secreted under sub-threshold glucose conditions*

Isolated mouse islets were treated with vehicle control (DMSO) or tunicamycin (TM, 10 µg/ml) for 6, 12 and 16 hours in 11 mM glucose. Insulin secretion was measured by acutely exposing 10 islets to 5 mM glucose for 30 minutes for each experimental condition. 7A: Both secreted insulin and insulin remaining in the extracted islets were quantified in triplicate by ELISA and normalized to total protein concentration (BCA protein assay). 7B: The percent insulin that was secreted was obtained by dividing the secreted insulin by total insulin (the sum of secreted insulin and insulin in the lysate). Values shown are means ± SEM. #, $p < 0.05$ compared with control conditions; n= 3 mice.

Figure 8

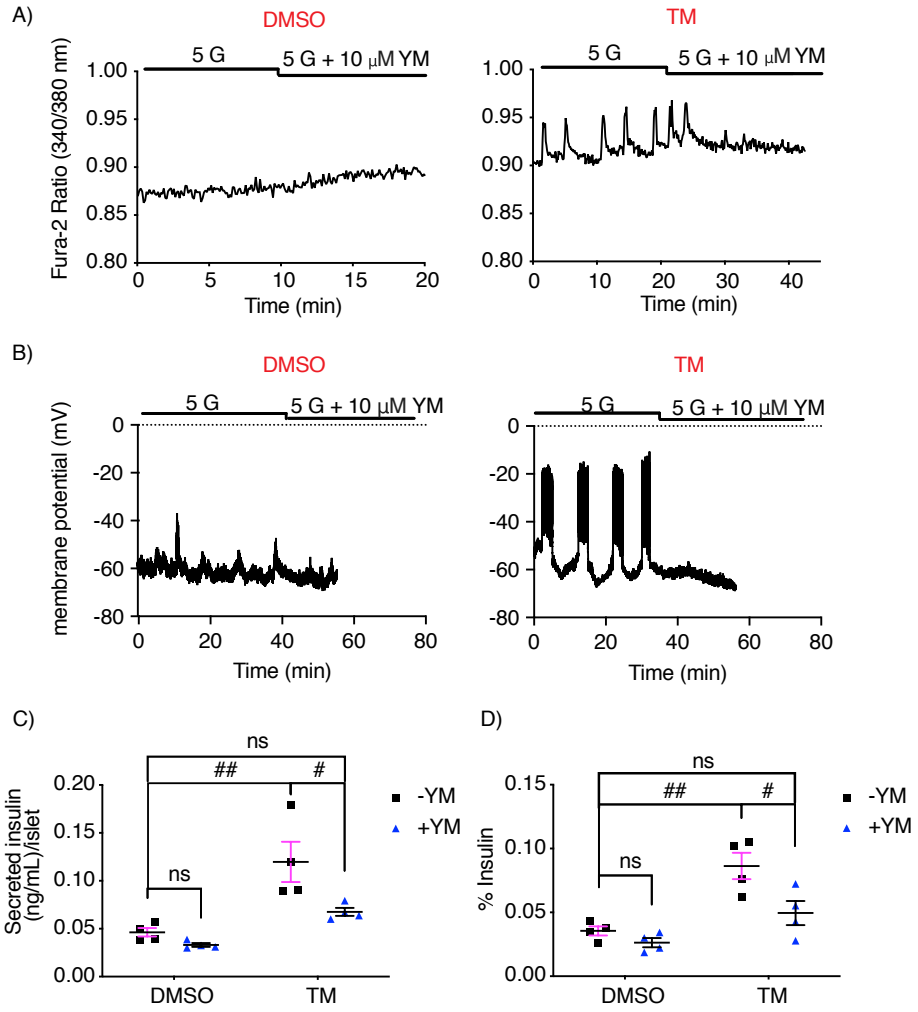


*Figure 2.8 Increased cytosolic $Ca^{2+}$, membrane potential oscillations and insulin secretion observed after tunicamycin treatment were mediated by store-operated $Ca^{2+}$ entry (SOCE)*

Islets were treated with vehicle control (DMSO) or tunicamycin (TM, 10 µg/ml) for 16 hours, and were then acutely exposed to 5 mM glucose containing solution with or without YM58483 (YM, 10 µM). 8A: Cytosolic free $Ca^{2+}$ changes. 8B: Membrane potential changes. 8C: Insulin secretion. Row Factor F(1, 12)= 24.25, p= 0.0004, Column Factor F(1, 12)= 8.923, p=0.0113, Interaction F(1, 12)= 3.170, p= 0.1003, by two-way ANOVA. 8D: Percentage insulin secreted. Row Factor F(1, 12)= 24.75, p= 0.0003, Column Factor F(1, 12)= 9.572, p=0.0093, Interaction F(1, 12)= 3.446, p= 0.0881, by two-way ANOVA. All values shown are means ± SEM. #, p< 0.05, ##, p< 0.01, ns= not significant; n= at least 3 mice, by two-way ANOVA with post hoc multiple comparison by Tukey's procedure.

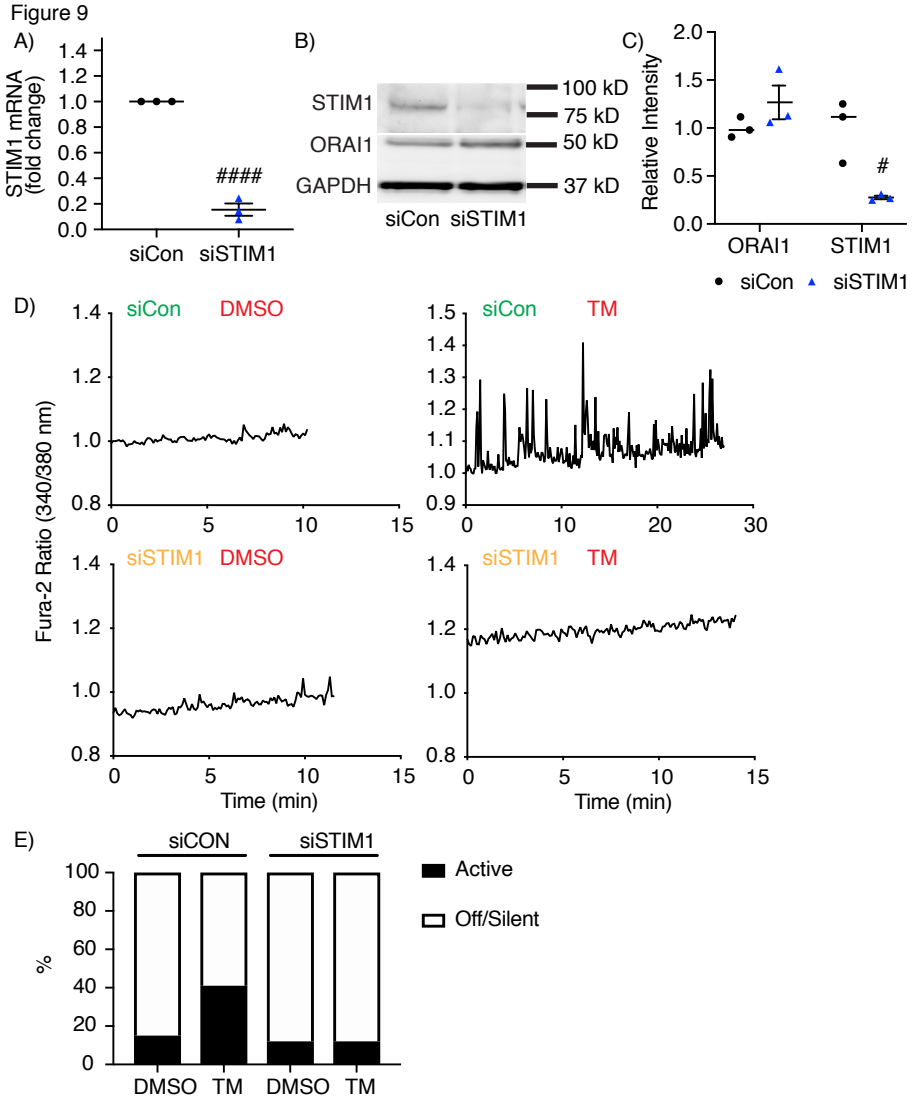


*Figure 2.9 STIM1 knockdown inhibited TM-triggered cytosolic $Ca^{2+}$ transients*

9A: STIM1 siRNA knockdown in INS-1(832/13) cells was assessed by qPCR 48 hours after siRNA transfection. 9B: Representative western blots showing the expression of STIM1 and ORAI1 48 hours after transfection with STIM1 siRNA compared to the negative control siRNA. 9C: Quantitative protein levels of STIM1 and ORAI1 are shown graphically. INS-1(832/13) cells were treated with vehicle control (DMSO) or tunicamycin (TM, 10 µg/ml) for 16 hours after transfecting with STIM1 siRNA or negative control siRNA for 48 hours. 9D: The responses of cytosolic free $Ca^{2+}$ to solution containing 5 mM glucose. 9E: Percentage of active INS-1(832/13) cells showing $Ca^{2+}$ transients. All values shown are means ± SEM. #, $p< 0.05$, ##, $p< 0.01$, ###, $p< 0.0005$, ####, $p< 0.0001$; n= 3 times repeated per condition.

Figure 10

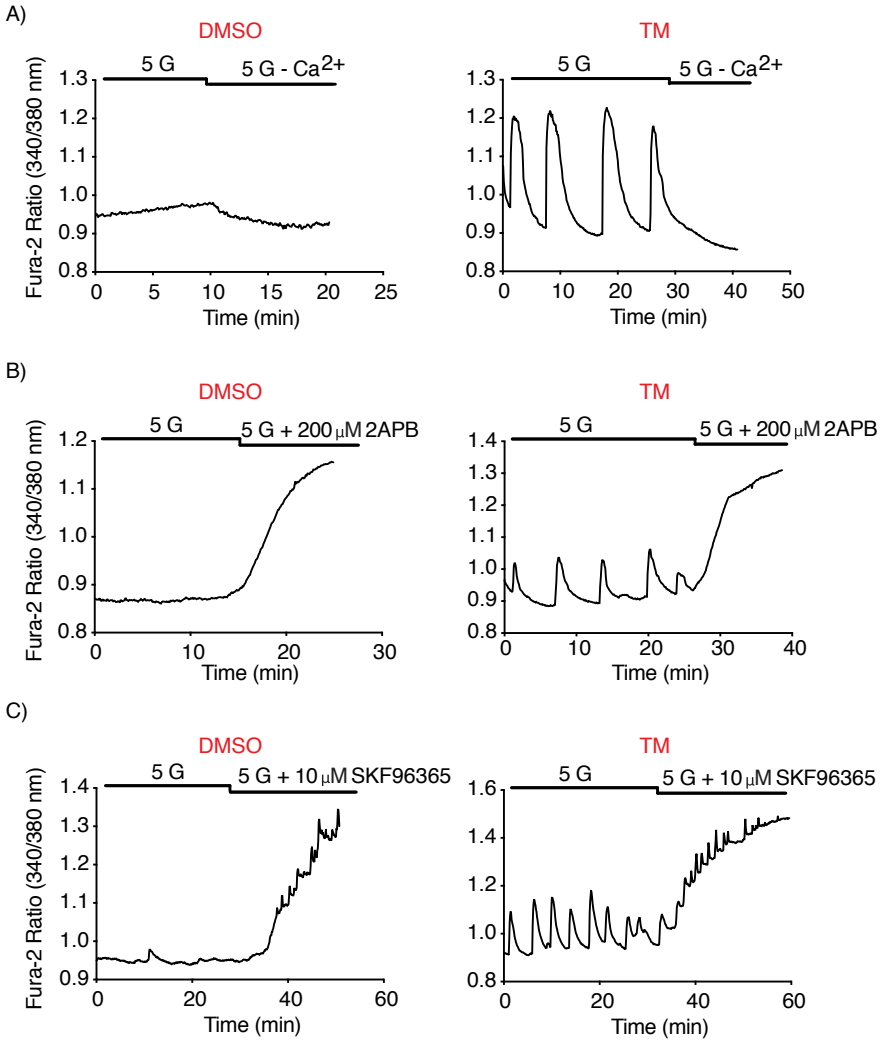


*Figure 2.10 Effect of alternative SOCE inhibitors on cytosolic $Ca^{2+}$ oscillations*

Islets were treated with vehicle control (DMSO) or tunicamycin (TM, 10 µg/ml) for 16 hours. Cytosolic free $Ca^{2+}$ changes were imaged before and after acutely exposed to 5 mM glucose containing solution. 10A: without $Ca^{2+}$, 10B: with 2-Aminoethoxydiphenyl borate (2APB, 200 µM), and 10C: with SKF96365 (10 µM). n= at least 3 mice.

Figure 11

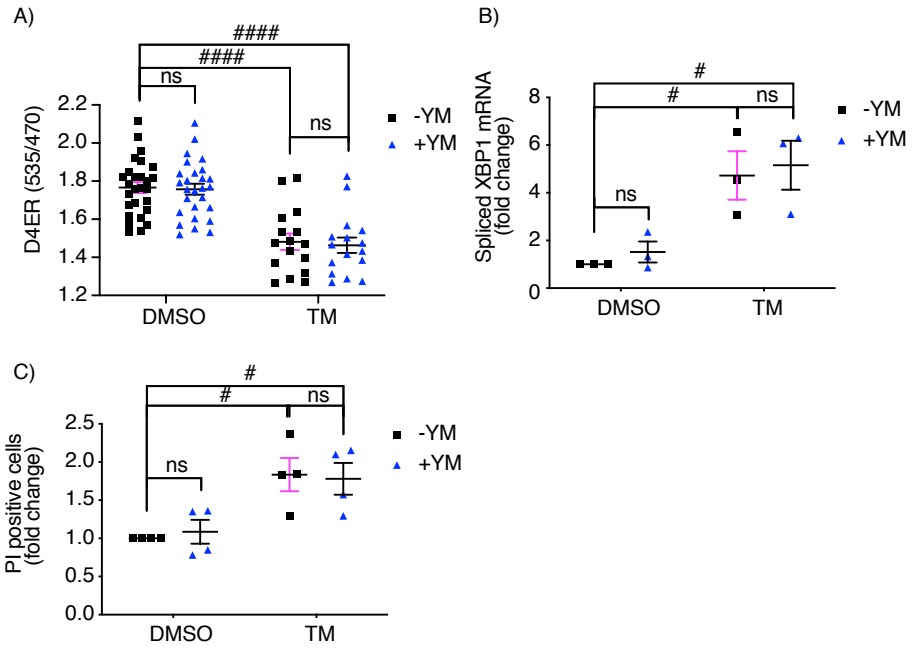


*Figure 2.11 Increased beta-cell death seen after tunicamycin treatment was not mediated by store-operated $Ca^{2+}$ entry (SOCE)*

INS-1(832/13) cells or mouse islets were treated with vehicle control (DMSO), tunicamycin (TM, 10 µg/ml), DMSO+YM58483 (YM, 10 µM) or TM+YM58483 for 11A: 16 hours, 11B: 6 hours and 11C: 24 hours in 11 mM glucose containing culture medium. 11A: Summary of raw data showing basal ER $Ca^{2+}$ ratios obtained from islets of 3 mice. Row Factor F(1, 82)= 69.54, p< 0.0001, Column Factor F(1, 82)= 0.1515, p=0.6981, Interaction F(1, 82)= 0.01884, p= 0.8912, by two-way ANOVA. 11B: Expression level of spliced XBP1 mRNA. Row Factor F(1, 8)= 23.75, p= 0.0012, Column Factor F(1, 8)= 0.3909, p=0.5493, Interaction F(1, 8)= 0.003133, p= 0.9567, by two-way ANOVA. 11C: Cell death observed in INS-1(832/13) cells stained with propidium iodide (PI) and quantified using flow cytometry. Row Factor F(1, 12)= 20.29, p= 0.0007, Column Factor F(1, 12)= 0.008395, p=0.9285, Interaction F(1, 12)= 0.1708, p= 0.6867, by two-way ANOVA. The results were obtained from 3 different batches of INS-1(832/13) cells. All values shown are means ± SEM. #, p< 0.05, ####, p< 0.0001, ns= not significant; n= 3 times repeated per condition, by two-way ANOVA with post hoc multiple comparison by Tukey's procedure.

Figure 12

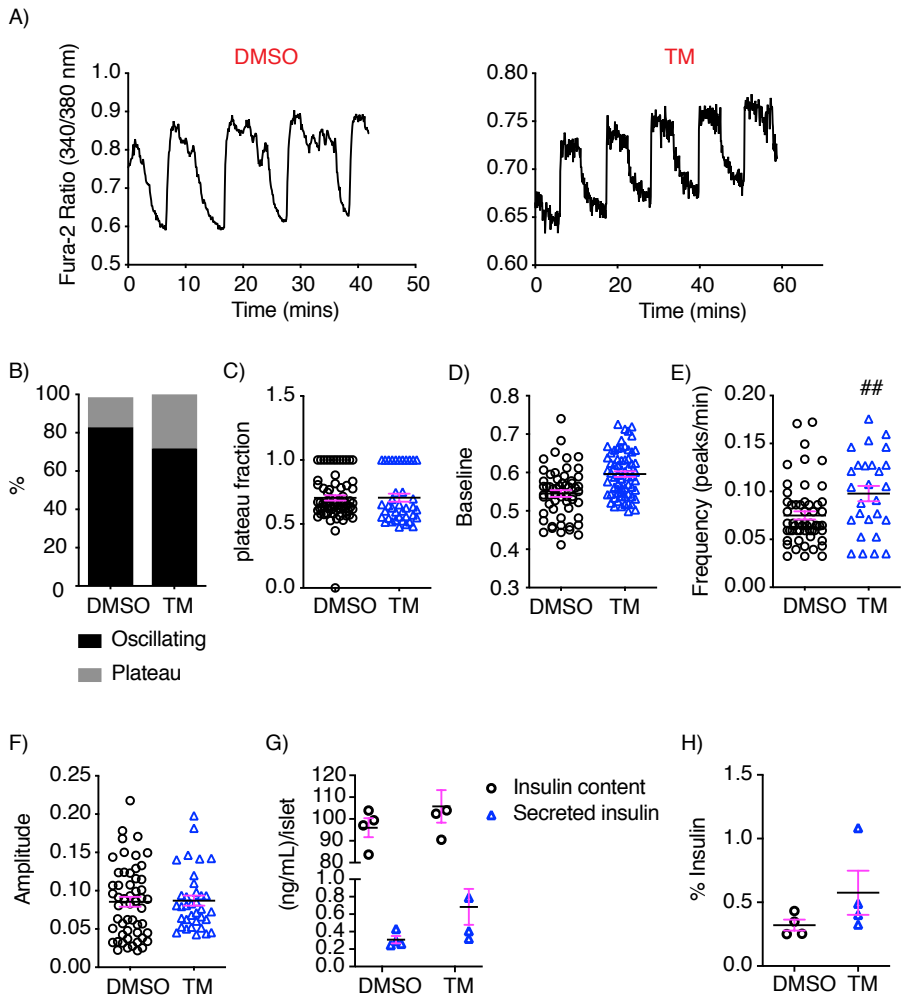


*Figure 2.12 Tunicamycin did not affect cytosolic free $Ca^{2+}$ under above-threshold glucose conditions*

Isolated pancreatic mouse islets were treated with a vehicle control (DMSO) or tunicamycin (TM, 10 µg/ml) for 16 hours in 11 mM glucose. 12A: The responses of cytosolic free $Ca^{2+}$ to solution containing 11 mM glucose under the indicated conditions. 12B: Percentage of oscillating islets. Summary findings for the data are shown in 12C-F. 12C: Plateau fraction. 12D: Baseline values. 12E: oscillation frequency. 12F: oscillation amplitude. 12G and 12H: Insulin secretion was measured by acutely exposing 10 islets to 11 mM glucose for 30 minutes for each experimental condition. 12G: Both secreted insulin and insulin content and 12H: the percent insulin were quantified as described in Figure 2.7. All values shown are means ± SEM. ##, $p < 0.01$; n= at least 3 mice.

Figure 13

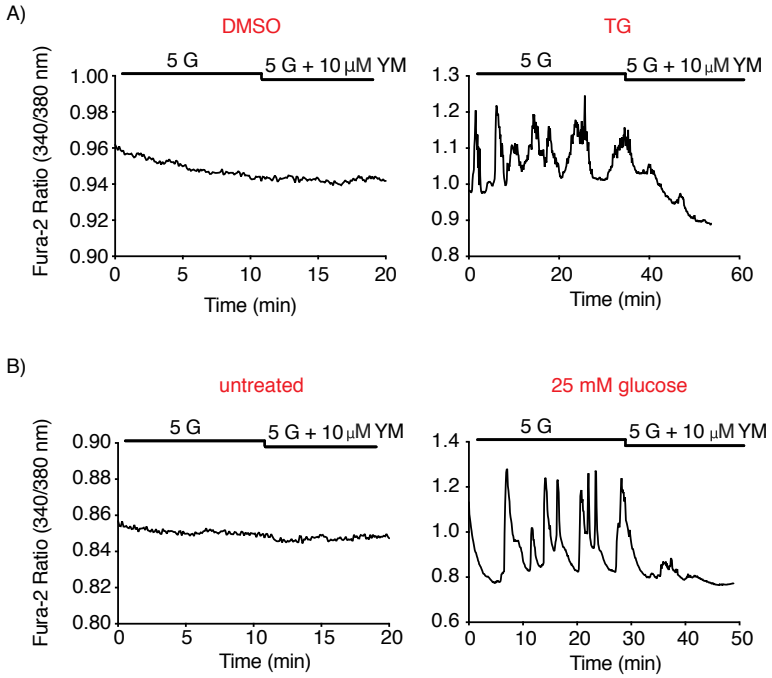


*Figure 2.13 Alternative ER stress inducers also increased cytosolic free $Ca^{2+}$ under sub-threshold glucose conditions*

13A: Isolated pancreatic mouse islets were treated with a vehicle control (DMSO) or thapsigargin (TG, 200 nM) in 11 mM glucose. 13B: Mouse islets were cultured in 11 mM glucose (untreated control) or 25 mM glucose for 16 hours. The responses of cytosolic free $Ca^{2+}$ to solution containing 5 mM glucose under the indicated conditions. n= at least 3 mice.

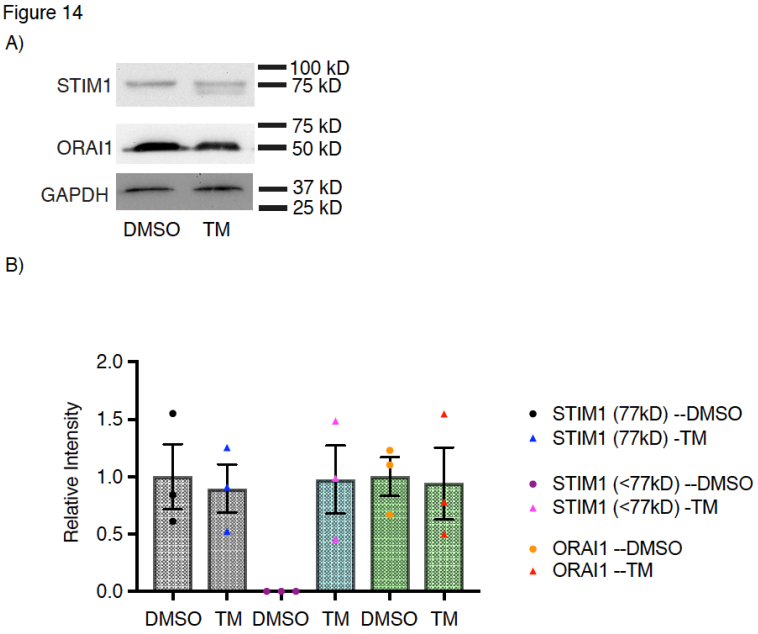


*Figure 2.14 The effect of tunicamycin on gene expression*

INS-1(832/13) cells were treated with a vehicle control (DMSO) or tunicamycin (TM, 10 µg/ml) for 16 hours in 11 mM glucose. 14A: Representative western blots show the level of STIM1 and ORAI1. GAPDH is shown as a loading control. 14B: Quantitative protein levels are shown graphically. All values shown are means ± SEM; n= 3 times repeated per condition.

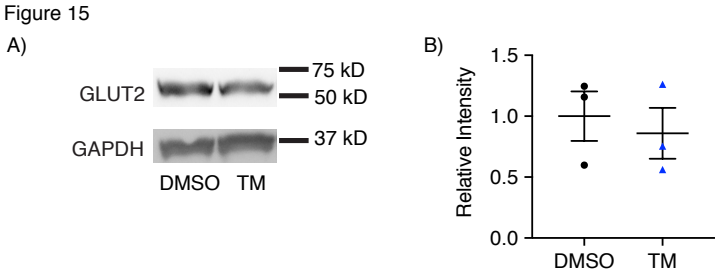


*Figure 2.15 Tunicamycin did not affect GLUT2 expression after 6 hours of TM exposure*

INS-1(832/13) cells were treated with a vehicle control (DMSO) or tunicamycin (TM, 10 µg/ml) for 6 hours in 11 mM glucose. 15A: Representative western blots showing the level of GLUT2. 15B: Quantitative protein levels are shown graphically. GAPDH is shown as a loading control. All values shown are means ± SEM; n= 3 times repeated per condition.

Figure 16

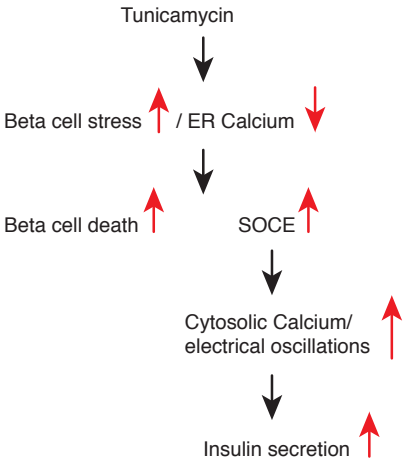


*Figure 2.16 Scheme of beta-cell death and increasing insulin secretion mediated by tunicamycin*

Table 1

A)

| Gene | forward | Reverse |
|---|---|---|
| Xbp1s (rat) | CTGAGTCCGAATCAGGTGCAG | ATCCATGGGAAGATGTTCTGG |
| Xbp1 total (rat) | GAGCAGCAAGTGGTGGAT | TCTCAATCACAAGCCCATG |
| Chop (rat) | AGAGTGGTCAGTGCGCAGC | CTCATTCTCCTGCTCCTTCTCC |
| Hprt1 | CTCATGGACTGATTATGGACAGGAC | GCAGGTCAGCAAAGAACTTATAGCC |
| Xbp1s (mouse) | CTGAGTCCGAATCAGGTGCAG | GTCCATGGGAAGATGTTCTGG |
| Stim1 (rat) | GGCCAGAGTCTCAGCCATAG | CATAGGTCCTCCACGCTGAT |

B)

| Antibodies | animal | Source and dilution |
|---|---|---|
| BiP | Rabbit | Arvan Lab at the University of Michigan, Ann Arbor, 1:5000 |
| PARP | Rabbit | Cell Signaling Technology, 1:1000 |
| STIM 1 | Rabbit | Cell Signaling Technology, 1:1000 |
| ORAI 1 | Mouse | SIGMA, 1:1000 |
| GLUT2 | Rabbit | EMD Millipore, 1:1000 |
| GAPDH | Rabbit | Cell Signaling Technology, 1:1000 |
| Tubulin | Mouse | Cell Signaling Technology, 1:1000 |
| HRP-conjugated mouse anti-rabbit | Mouse | Cell Signaling Technology, 1:5000 |
| HRP-conjugated goat anti-mouse | Goat | Cell Signaling Technology, 1:5000 |

*Table 1. Material table*

T1A: Oligonucleotide primers. T1B: Antibodies.

***References***


1. Topp, B. G., Atkinson, L. L., and Finegood, D. T. (2007) Dynamics of insulin sensitivity, β-cell function, and β-cell mass during the development of diabetes in fa/fa rats. *Am. J. Physiol.-Endocrinol. Metab.* **293**, E1730–E1735

2. Satin, L. S., Butler, P. C., Ha, J., and Sherman, A. S. (2015) Pulsatile insulin secretion, impaired glucose tolerance and type 2 diabetes. *Mol. Aspects Med.* **42**, 61–77

3. Kahn, S. E. (2003) The relative contributions of insulin resistance and beta-cell dysfunction to the pathophysiology of Type 2 diabetes. *Diabetologia*. **46**, 3–19

4. Gilon, P., Shepherd, R. M., and Henquin, J. C. (1993) Oscillations of secretion driven by oscillations of cytoplasmic Ca2+ as evidences in single pancreatic islets. *J. Biol. Chem.* **268**, 22265–22268

5. Fridlyand, L. E., Tamarina, N., and Philipson, L. H. (2010) Bursting and calcium oscillations in pancreatic β-cells: specific pacemakers for specific mechanisms. *Am. J. Physiol.-Endocrinol. Metab.* **299**, E517–E532

6. Ashcroft, F. M., and Rorsman, P. (1990) ATP-sensitive $K^+$ channels: a link between B-cell metabolism and insulin secretion. *Biochem. Soc. Trans.* **18**, 109–111

7. Beauvois, M. C., Merezak, C., Jonas, J.-C., Ravier, M. A., Henquin, J.-C., and Gilon, P. (2006) Glucose-induced mixed $[Ca^{2+}]_c$ oscillations in mouse β-cells are controlled by the membrane potential and the SERCA3 $Ca^{2+}$-ATPase of the endoplasmic reticulum. *Am. J. Physiol.-Cell Physiol.* **290**, C1503–C1511

8. Bergsten, P. (1995) Slow and fast oscillations of cytoplasmic Ca2+ in pancreatic islets correspond to pulsatile insulin release. *Am. J. Physiol.-Endocrinol. Metab.* **268**, E282–E287

9. Bergsten, P. (1998) Glucose-induced pulsatile insulin release from single islets at stable and oscillatory cytoplasmic Ca2+. *Am. J. Physiol.-Endocrinol. Metab.* **274**, E796–E800

10. Gilon, P., Ravier, M. A., Jonas, J.-C., and Henquin, J.-C. (2002) Control Mechanisms of the Oscillations of Insulin Secretion In Vitro and In Vivo. *Diabetes*. **51**, S144–S151

11. Gillon, A. D., Latham, C. F., and Miller, E. A. (2012) Vesicle-mediated ER export of proteins and lipids. *Biochim. Biophys. Acta BBA - Mol. Cell Biol. Lipids*. **1821**, 1040–1049

12. Qi, L., Tsai, B., and Arvan, P. (2017) New Insights into the Physiological Role of Endoplasmic Reticulum-Associated Degradation. *Trends Cell Biol.* **27**, 430–440

13. Lemaire, K., and Schuit, F. (2012) Integrating insulin secretion and ER stress in pancreatic β-cells. *Nat. Cell Biol.* **14**, 979–981

14. Berridge, M. J., Bootman, M. D., and Roderick, H. L. (2003) Calcium signalling: dynamics, homeostasis and remodelling: Calcium. *Nat. Rev. Mol. Cell Biol.* **4**, 517–529

15. Berridge, M. J. (2002) The endoplasmic reticulum: a multifunctional signaling organelle. *Cell Calcium*. **32**, 235–249

16. Mekahli, D., Bultynck, G., Parys, J. B., De Smedt, H., and Missiaen, L. (2011) Endoplasmic-Reticulum Calcium Depletion and Disease. *Cold Spring Harb. Perspect. Biol.* **3**, a004317–a004317

17. Kiviluoto, S., Vervliet, T., Ivanova, H., Decuypere, J.-P., De Smedt, H., Missiaen, L., Bultynck, G., and Parys, J. B. (2013) Regulation of inositol 1,4,5-trisphosphate receptors during endoplasmic reticulum stress. *Biochim. Biophys. Acta BBA - Mol. Cell Res.* **1833**, 1612–1624

18. Johnson, J. S., Kono, T., Tong, X., Yamamoto, W. R., Zarain-Herzberg, A., Merrins, M. J., Satin, L. S., Gilon, P., and Evans-Molina, C. (2014) Pancreatic and Duodenal Homeobox Protein 1 (Pdx-1) Maintains Endoplasmic Reticulum Calcium Levels through Transcriptional Regulation of Sarco-endoplasmic Reticulum Calcium ATPase 2b (SERCA2b) in the Islet β Cell. *J. Biol. Chem.* **289**, 32798–32810

19. Seo, M.-D., Enomoto, M., Ishiyama, N., Stathopulos, P. B., and Ikura, M. (2015) Structural insights into endoplasmic reticulum stored calcium regulation by inositol 1,4,5-trisphosphate and ryanodine receptors. *Biochim. Biophys. Acta BBA - Mol. Cell Res.* **1853**, 1980–1991

20. Carafoli, E. (2002) Calcium signaling: A tale for all seasons. *Proc. Natl. Acad. Sci.* **99**, 1115–1122

21. Ivanova, H., Vervliet, T., Missiaen, L., Parys, J. B., De Smedt, H., and Bultynck, G. (2014) Inositol 1,4,5-trisphosphate receptor-isoform diversity in cell death and survival. *Biochim. Biophys. Acta BBA - Mol. Cell Res.* **1843**, 2164–2183

22. Oslowski, C. M., and Urano, F. (2011) Measuring ER Stress and the Unfolded Protein Response Using Mammalian Tissue Culture System. in *Methods in Enzymology*, pp. 71–92, Elsevier, **490**, 71–92

23. Sano, R., and Reed, J. C. (2013) ER stress-induced cell death mechanisms. *Biochim. Biophys. Acta BBA - Mol. Cell Res.* **1833**, 3460–3470

24. Zhou, Y. P., Teng, D., Dralyuk, F., Ostrega, D., Roe, M. W., Philipson, L., and Polonsky, K. S. (1998) Apoptosis in insulin-secreting cells. Evidence for the role of intracellular Ca2+ stores and arachidonic acid metabolism. *J. Clin. Invest.* **101**, 1623–1632

25. Yang, G., Yang, W., Wu, L., and Wang, R. (2007) H $_2$ S, Endoplasmic Reticulum Stress, and Apoptosis of Insulin-secreting Beta Cells. *J. Biol. Chem.* **282**, 16567–16576

26. Kim, W.-H., Lee, J. W., Suh, Y. H., Hong, S. H., Choi, J. S., Lim, J. H., Song, J. H., Gao, B., and Jung, M. H. (2005) Exposure to Chronic High Glucose Induces -Cell Apoptosis Through Decreased Interaction of Glucokinase With Mitochondria: Downregulation of Glucokinase in Pancreatic -Cells. *Diabetes*. **54**, 2602–2611

27. Jeffrey, K. D., Alejandro, E. U., Luciani, D. S., Kalynyak, T. B., Hu, X., Li, H., Lin, Y., Townsend, R. R., Polonsky, K. S., and Johnson, J. D. (2008) Carboxypeptidase E mediates palmitate-induced -cell ER stress and apoptosis. *Proc. Natl. Acad. Sci.* **105**, 8452–8457

28. Yoo, J., Mashalidis, E. H., Kuk, A. C. Y., Yamamoto, K., Kaeser, B., Ichikawa, S., and Lee, S.-Y. (2018) GlcNAc-1-P-transferase–tunicamycin complex structure reveals basis for inhibition of N-glycosylation. *Nat. Struct. Mol. Biol.* **25**, 217–224

29. Meyerovich, K., Ortis, F., Allagnat, F., and Cardozo, A. K. (2016) Endoplasmic reticulum stress and the unfolded protein response in pancreatic islet inflammation. *J. Mol. Endocrinol.* **57**, R1–R17

30. Cunha, D. A., Hekerman, P., Ladriere, L., Bazarra-Castro, A., Ortis, F., Wakeham, M. C., Moore, F., Rasschaert, J., Cardozo, A. K., Bellomo, E., Overbergh, L., Mathieu, C., Lupi, R., Hai, T., Herchuelz, A., Marchetti, P., Rutter, G. A., Eizirik, D. L., and Cnop, M. (2008) Initiation and execution of lipotoxic ER stress in pancreatic -cells. *J. Cell Sci.* **121**, 2308–2318

31. Zhang, I. X., Raghavan, M., and Satin, L. S. (2020) The Endoplasmic Reticulum and Calcium Homeostasis in Pancreatic Beta Cells. *Endocrinology*. **161**, bqz028

32. Hetz, C., and Papa, F. R. (2018) The Unfolded Protein Response and Cell Fate Control. *Mol. Cell*. **69**, 169–181

33. Brandish, P. E., Kimura, K. I., Inukai, M., Southgate, R., Lonsdale, J. T., and Bugg, T. D. (1996) Modes of action of tunicamycin, liposidomycin B, and mureidomycin A: inhibition of phospho-N-acetylmuramyl-pentapeptide translocase from Escherichia coli. *Antimicrob. Agents Chemother.* **40**, 1640–1644

34. Zinszner, H., Kuroda, M., Wang, X., Batchvarova, N., Lightfoot, R. T., Remotti, H., Stevens, J. L., and Ron, D. (1998) CHOP is implicated in programmed cell death in response to impaired function of the endoplasmic reticulum. *Genes Dev.* **12**, 982–995

35. Guha, P., Kaptan, E., Gade, P., Kalvakolanu, D. V., and Ahmed, H. (2017) Tunicamycin induced endoplasmic reticulum stress promotes apoptosis of prostate cancer cells by activating mTORC1. *Oncotarget*. 10.18632/oncotarget.19277

36. Back, S. H., and Kaufman, R. J. (2012) Endoplasmic Reticulum Stress and Type 2 Diabetes. *Annu. Rev. Biochem.* **81**, 767–793

37. Walker, A. K., and Atkin, J. D. (2011) Stress signaling from the endoplasmic reticulum: A central player in the pathogenesis of amyotrophic lateral sclerosis. *IUBMB Life*. 10.1002/iub.520

38. Hara, T., Mahadevan, J., Kanekura, K., Hara, M., Lu, S., and Urano, F. (2014) Calcium Efflux From the Endoplasmic Reticulum Leads to β-Cell Death. *Endocrinology*. **155**, 758–768

39. Lu, S., Kanekura, K., Hara, T., Mahadevan, J., Spears, L. D., Oslowski, C. M., Martinez, R., Yamazaki-Inoue, M., Toyoda, M., Neilson, A., Blanner, P., Brown, C. M., Semenkovich, C. F., Marshall, B. A., Hershey, T., Umezawa, A., Greer, P. A., and Urano, F. (2014) A calcium-dependent protease as a potential therapeutic target for Wolfram syndrome. *Proc. Natl. Acad. Sci.* **111**, E5292–E5301

40. Shen, M., Wang, L., Guo, X., Xue, Q., Huo, C., Li, X., Fan, L., and Wang, X. (2015) A novel endoplasmic reticulum stress-induced apoptosis model using tunicamycin in primary cultured neonatal rat cardiomyocytes. *Mol. Med. Rep.* **12**, 5149–5154

41. Wang, X., Xiong, W., and Tang, Y. (2018) Tunicamycin suppresses breast cancer cell growth and metastasis via regulation of the protein kinase B/nuclear factor-κB signaling pathway. *Oncol. Lett.* 10.3892/ol.2018.7874

42. Shiraishi, H. (2006) ER stress-induced apoptosis and caspase-12 activation occurs downstream of mitochondrial apoptosis involving Apaf-1. *J. Cell Sci.* **119**, 3958–3966

43. Chaitanya, G., Alexander, J. S., and Babu, P. (2010) PARP-1 cleavage fragments: signatures of cell-death proteases in neurodegeneration. *Cell Commun. Signal.* **8**, 31

44. Boulares, A. H., Yakovlev, A. G., Ivanova, V., Stoica, B. A., Wang, G., Iyer, S., and Smulson, M. (1999) Role of Poly(ADP-ribose) Polymerase (PARP) Cleavage in Apoptosis. Caspase 3-resistant PARP mutant increases rates of apoptosis in transfected cells. *J. Biol. Chem.* **274**, 22932–22940

45. Braakman, I., and Bulleid, N. J. (2011) Protein Folding and Modification in the Mammalian Endoplasmic Reticulum. *Annu. Rev. Biochem.* **80**, 71–99

46. Brodsky, J. L., and Skach, W. R. (2011) Protein folding and quality control in the endoplasmic reticulum: Recent lessons from yeast and mammalian cell systems. *Curr. Opin. Cell Biol.* **23**, 464–475

47. McClellan, A. J., Tam, S., Kaganovich, D., and Frydman, J. (2005) Protein quality control: chaperones culling corrupt conformations. *Nat. Cell Biol.* **7**, 736–741

48. Hartl, F. U., Bracher, A., and Hayer-Hartl, M. (2011) Molecular chaperones in protein folding and proteostasis. *Nature*. **475**, 324–332

49. Sehgal, P., Szalai, P., Olesen, C., Praetorius, H. A., Nissen, P., Christensen, S. B., Engedal, N., and Møller, J. V. (2017) Inhibition of the sarco/endoplasmic reticulum (ER) $Ca^{2+}$-ATPase by thapsigargin analogs induces cell death via ER $Ca^{2+}$ depletion and the unfolded protein response. *J. Biol. Chem.* **292**, 19656–19673

50. Glynn, E., Thompson, B., Vadrevu, S., Lu, S., Kennedy, R. T., Ha, J., Sherman, A., and Satin, L. S. (2016) Chronic Glucose Exposure Systematically Shifts the Oscillatory Threshold of Mouse Islets: Experimental Evidence for an Early Intrinsic Mechanism of Compensation for Hyperglycemia. *Endocrinology*. **157**, 611–623

51. Bertram, R., Sherman, A., and Satin, L. S. (2010) Electrical Bursting, Calcium Oscillations, and Synchronization of Pancreatic Islets. in *The Islets of Langerhans* (Islam, Md. S. ed), pp. 261–279, Springer Netherlands, Dordrecht, **654**, 261–279

52. Nunemaker, C. S., Bertram, R., Sherman, A., Tsaneva-Atanasova, K., Daniel, C. R., and Satin, L. S. (2006) Glucose Modulates [Ca2+]i Oscillations in Pancreatic Islets via Ionic and Glycolytic Mechanisms. *Biophys. J.* **91**, 2082–2096

53. Ren, J., Sherman, A., Bertram, R., Goforth, P. B., Nunemaker, C. S., Waters, C. D., and Satin, L. S. (2013) Slow oscillations of $K_{ATP}$ conductance in mouse pancreatic islets provide support for electrical bursting driven by metabolic oscillations. *Am. J. Physiol.-Endocrinol. Metab.* **305**, E805–E817

54. Dahlgren, G. M., Kauri, L. M., and Kennedy, R. T. (2005) Substrate effects on oscillations in metabolism, calcium and secretion in single mouse islets of Langerhans. *Biochim. Biophys. Acta BBA - Gen. Subj.* **1724**, 23–36

55. Alonso, M. T., Manjarrés, I. M., and García-Sancho, J. (2012) Privileged coupling between Ca2+ entry through plasma membrane store-operated Ca2+ channels and the endoplasmic reticulum Ca2+ pump. *Mol. Cell. Endocrinol.* **353**, 37–44

56. Tamarina, N. A., Kuznetsov, A., and Philipson, L. H. (2008) Reversible translocation of EYFP-tagged STIM1 is coupled to calcium influx in insulin secreting β-cells. *Cell Calcium*. **44**, 533–544

57. Jairaman, A., and Prakriya, M. (2013) Molecular pharmacology of store-operated CRAC channels. *Channels*. **7**, 402–414

58. Ohga, K., Takezawa, R., Arakida, Y., Shimizu, Y., and Ishikawa, J. (2008) Characterization of YM-58483/BTP2, a novel store-operated Ca2+ entry blocker, on T cell-mediated immune responses in vivo. *Int. Immunopharmacol.* **8**, 1787–1792

59. González-Sánchez, P., del Arco, A., Esteban, J. A., and Satrústegui, J. (2017) Store-Operated Calcium Entry Is Required for mGluR-Dependent Long Term Depression in Cortical Neurons. *Front. Cell. Neurosci.* 10.3389/fncel.2017.00363

60. Zhang, B., Yan, J., Schmidt, S., Salker, M. S., Alexander, D., Föller, M., and Lang, F. (2015) Lithium- Sensitive Store-Operated $Ca^{2+}$ Entry in the Regulation of FGF23 Release. *Neurosignals*. **23**, 34–48

61. McKenna, J. P., and Bertram, R. (2018) Fast-slow analysis of the Integrated Oscillator Model for pancreatic β-cells. *J. Theor. Biol.* **457**, 152–162

62. Muik, M., Schindl, R., Fahrner, M., and Romanin, C. (2012) Ca2+ release-activated Ca2+ (CRAC) current, structure, and function. *Cell. Mol. Life Sci.* **69**, 4163–4176

63. Stathopulos, P. B., Schindl, R., Fahrner, M., Zheng, L., Gasmi-Seabrook, G. M., Muik, M., Romanin, C., and Ikura, M. (2013) STIM1/Orai1 coiled-coil interplay in the regulation of store-operated calcium entry. *Nat. Commun.* 10.1038/ncomms3963

64. Wei, M., Zhou, Y., Sun, A., Ma, G., He, L., Zhou, L., Zhang, S., Liu, J., Zhang, S. L., Gill, D. L., and Wang, Y. (2016) Molecular mechanisms underlying inhibition of STIM1-Orai1-mediated Ca2+ entry induced by 2-aminoethoxydiphenyl borate. *Pflüg. Arch. - Eur. J. Physiol.* **468**, 2061–2074

65. Bonilla, I. M., Belevych, A. E., Baine, S., Stepanov, A., Mezache, L., Bodnar, T., Liu, B., Volpe, P., Priori, S., Weisleder, N., Sakuta, G., Carnes, C. A., Radwański, P. B., Veeraraghavan, R., and Gyorke, S. (2019) Enhancement of Cardiac Store Operated Calcium Entry (SOCE) within Novel Intercalated Disk Microdomains in Arrhythmic Disease. *Sci. Rep.* **9**, 10179

66. Tian, C., Du, L., Zhou, Y., and Li, M. (2016) Store-operated CRAC channel inhibitors: opportunities and challenges. *Future Med. Chem.* **8**, 817–832

67. Huang, C., Gurlo, T., Haataja, L., Costes, S., Daval, M., Ryazantsev, S., Wu, X., Butler, A. E., and Butler, P. C. (2010) Calcium-activated Calpain-2 Is a Mediator of Beta Cell Dysfunction and Apoptosis in Type 2 Diabetes. *J. Biol. Chem.* **285**, 339–348

68. Kono, T., Tong, X., Taleb, S., Bone, R. N., Iida, H., Lee, C.-C., Sohn, P., Gilon, P., Roe, M. W., and Evans-Molina, C. (2018) Impaired Store-Operated Calcium Entry and STIM1 Loss Lead to Reduced Insulin Secretion and Increased Endoplasmic Reticulum Stress in the Diabetic β-Cell. *Diabetes*. **67**, 2293–2304

69. Shen, W.-W., Frieden, M., and Demaurex, N. (2011) Remodelling of the endoplasmic reticulum during store-operated calcium entry. *Biol. Cell*. **103**, 365–380

70. Yamamoto, W. R., Bone, R. N., Sohn, P., Syed, F., Reissaus, C. A., Mosley, A. L., Wijeratne, A. B., True, J. D., Tong, X., Kono, T., and Evans-Molina, C. (2019) Endoplasmic reticulum stress alters ryanodine receptor function in the murine pancreatic β cell. *J. Biol. Chem.* **294**, 168–181

71. Tong, X., Kono, T., Anderson-Baucum, E. K., Yamamoto, W., Gilon, P., Lebeche, D., Day, R. N., Shull, G. E., and Evans-Molina, C. (2016) SERCA2 Deficiency Impairs Pancreatic β-Cell Function in Response to Diet-Induced Obesity. *Diabetes*. **65**, 3039–3052

72. Sachdeva, M. M., Claiborn, K. C., Khoo, C., Yang, J., Groff, D. N., Mirmira, R. G., and Stoffers, D. A. (2009) Pdx1 ( *MODY4* ) regulates pancreatic beta cell susceptibility to ER stress. *Proc. Natl. Acad. Sci.* **106**, 19090–19095

73. Czyż, A., Brutkowski, W., Fronk, J., Duszyński, J., and Zabłocki, K. (2009) Tunicamycin desensitizes store-operated Ca2+ entry to ATP and mitochondrial potential. *Biochem. Biophys. Res. Commun.* **381**, 176–180

74. Choi, Y. J., Zhao, Y., Bhattacharya, M., and Stathopulos, P. B. (2017) Structural perturbations induced by Asn131 and Asn171 glycosylation converge within the EFSAM core and enhance stromal interaction molecule-1 mediated store operated calcium entry. *Biochim. Biophys. Acta BBA - Mol. Cell Res.* **1864**, 1054–1063

75. Skelin, M. (2010) Pancreatic beta cell lines and their applications in diabetes mellitus research. *ALTEX*. 10.14573/altex.2010.2.105

76. Tabák, A. G., Herder, C., Rathmann, W., Brunner, E. J., and Kivimäki, M. (2012) Prediabetes: a high-risk state for diabetes development. *The Lancet*. **379**, 2279–2290

77. Kassem, S. A., Ariel, I., Thornton, P. S., Scheimberg, I., and Glaser, B. (2000) Beta-cell proliferation and apoptosis in the developing normal human pancreas and in hyperinsulinism of infancy. *Diabetes*. **49**, 1325–1333

78. Zhang, M., Goforth, P., Bertram, R., Sherman, A., and Satin, L. (2003) The Ca2+ Dynamics of Isolated Mouse β-Cells and Islets: Implications for Mathematical Models. *Biophys. J.* **84**, 2852–2870

79. Ravier, M. A., Daro, D., Roma, L. P., Jonas, J.-C., Cheng-Xue, R., Schuit, F. C., and Gilon, P. (2011) Mechanisms of Control of the Free Ca2+ Concentration in the Endoplasmic Reticulum of Mouse Pancreatic -Cells: Interplay With Cell Metabolism and [Ca2+]c and Role of SERCA2b and SERCA3. *Diabetes*. **60**, 2533–2545

# Chapter 3 Differential Roles of Beta-cell IP3R and RyR ER $Ca^{2+}$ Channels in Tunicamycin-Induced Disruption of Beta-cell $Ca^{2+}$ Homeostasis

Irina X. Zhang, Vishal Parekh, Juan Leon and Leslie S. Satin

***Abstract***

Pancreatic beta cells maintain glucose homeostasis by secreting insulin following a rise in plasma glucose. Insulin secretion is pulsatile, which is brought about because of oscillations in the concentrations of beta-cell cytosolic $Ca^{2+}$. The endoplasmic reticulum (ER) helps to regulate the cytosolic $Ca^{2+}$ level, thereby playing a role in $Ca^{2+}$-induced insulin release. ER stress, triggered by the accumulation of unfolded proteins in the ER, can lead to the ER $Ca^{2+}$ depletion, which in turn can contribute to beta-cell deterioration and an increased risk of type-2 diabetes. We sought to determine the effects of tunicamycin (TM)-induced ER stress on ER $Ca^{2+}$ channels, inositol 1,4,5-triphosphate ($IP_3$) receptors (IP3Rs) and ryanodine receptors (RyRs), and subsequent alterations in beta-cell $Ca^{2+}$ homeostasis that result from these alterations. Treating INS-1 (832/13) cells with TM increased RyR1 and decreased IP3R1 and IP3R2 RNA transcripts. To determine the roles of these receptors in TM-induced beta-cell dysfunction, we treated mouse pancreatic islets with the RyR1 inhibitor dantrolene (Dan) or the IP3R inhibitor xestospongin C (XeC) along with TM. Beta cells treated with TM exhibited altered cytosolic and mitochondrial $Ca^{2+}$ when in sub-threshold glucose compared to vehicle controls. As TM treatment also depleted ER $Ca^{2+}$, this raised the possibility that the mitochondrial and cytosolic $Ca^{2+}$ oscillations of

stressed cells resulted from increased ER $Ca^{2+}$ efflux mediated by RyRs and IP3Rs. We found that TM-induced ER $Ca^{2+}$ depletion, as well as cytosolic and mitochondrial $Ca^{2+}$ oscillations were inhibited by co-treatment with Dan; whereas the inclusion of XeC was without effect. These results suggest that RyRs, and more specifically RyR1 may play a critical role in mediating the disturbed cellular $Ca^{2+}$ homeostasis seen in response to the induction of ER stress.

***Introduction***

Calcium ($Ca^{2+}$) is an essential second messenger in cellular signal transduction, and it plays a crucial role in many physiological processes (1, 2). In pancreatic beta cells, $Ca^{2+}$ mediates the exocytosis of insulin granules to maintain normal blood glucose after a meal (1). Once in the cell, $Ca^{2+}$ is primarily sequestered within the endoplasmic reticulum (ER), which is the organelle where the synthesis, correct folding and the sorting of proteins occurs, along with lipid synthesis and the maintenance of intracellular $Ca^{2+}$ homeostasis (3, 4). In beta cells, a properly functioning ER is extremely critical for the proper functioning and survival of the cell. (5–8) Malfunction in the ER potentially can lead to type 2 diabetes mellitus (T2D), and increasing evidence has emerged suggesting that the ER stress cascade (or UPR) is activated in islets obtained from T2D patients or animal models of diabetes (7, 9).

Decreased ER $Ca^{2+}$ has been associated with ER stress and apoptosis, which accompany many pathological conditions (7, 10, 11). We have previously shown that tunicamycin-induced ER stress partially depleted ER $Ca^{2+}$ in mouse beta cells (12). ER $Ca^{2+}$ is maintained through the concerted regulation of ER $Ca^{2+}$ uptake and release. The ER takes up $Ca^{2+}$ through the action of sarco/endoplasmic reticulum $Ca^{2+}$-ATPases (SERCA pumps) (2). Both inositol 1,4,5-

trisphosphate receptors (IP3Rs) and ryanodine receptors (RyRs) are two main families of intracellular $Ca^{2+}$ channels that can release ER $Ca^{2+}$ into the cytosol (2). More recently, $Ca^{2+}$-permeable ER translocons have been identified as ER $Ca^{2+}$ leak channels in beta cells (13, 14). Both IP3Rs and RyRs are gated by $Ca^{2+}$, and cytosolic $Ca^{2+}$ can activate both receptor types to trigger $Ca^{2+}$-induced $Ca^{2+}$ release (CICR) under certain conditions (15, 16). IP3Rs have been studied extensively in beta cells, and their role, for example in GPCR-coupled $Ca^{2+}$ release is well established (17). In contrast, the role of RyRs has been somewhat more controversial.

We wished here to test whether RyRs and IP3Rs are differentially regulated by ER stress conditions in beta cells. In addition, we sought to better define their respective roles in beta-cell function, such as in ER $Ca^{2+}$ handling, and in the production of cytosolic and mitochondrial $Ca^{2+}$ oscillations.

In the present study, we used TM treatment to experimentally induce ER stress in insulin-secreting INS-1(832/13) cells as well as isolated mouse islets. TM activates the unfolded protein response (UPR) by inhibiting N-acetylglucosamine phosphotransferase, the initial step in the N-linked protein glycosylation pathway following protein synthesis, which in turn leads to protein misfolding in the ER (18). We previously showed that this treatment increased cytosolic $Ca^{2+}$ signaling and insulin secretion even under sub-threshold glucose conditions by activating store-operated $Ca^{2+}$ entry (SOCE) (12). SOCE activation likely resulted from reduced ER $Ca^{2+}$, potentially occurring due to decreased SERCA activity (19), and/or increased RyR- or IP3R-mediated $Ca^{2+}$ release from the ER. In this report, we show that TM differentially regulated IP3Rs and RyRs such that RyR1 was selectively upregulated, which mediated ER $Ca^{2+}$ depletion,

and consequently increased cytosolic free $Ca^{2+}$ oscillations and mitochondrial $Ca^{2+}$ oscillations; IP3R1 and IP3R2 were downregulated, but blocking them showed no effect, suggesting they did not contribute to these processes.

## *Materials* and Methods

### ***Materials***

Tunicamycin (TM), cyclopiazonic acid (CPA) and YM58483 were obtained from Cayman Chemical, Ann Arbor, MI. Dantrolene (Dan) and xestospongin C (XeC) were purchased from Sigma-Aldrich Products. Rabbit antibody against phosphorylated IP3R1 (pIP3R1) and HRP-conjugated mouse anti-rabbit antibody were purchased from Cell Signaling Technology (1:1000 dilution). ECL reagents were obtained from Bio-Rad Laboratories.

The standard culture RPMI 1640 medium contained 11 mM glucose, 10% fetal bovine serum (FBS), 10 mM HEPES, 1% penicillin/streptomycin and 1% sodium pyruvate. The culture medium contained RPMI 1640 medium, 5 mM glucose, 10% fetal bovine serum (FBS), 10 mM HEPES, 1% penicillin/streptomycin and 1% sodium pyruvate. The imaging solution contained (in mM): 140 NaCl, 3 $CaCl_2$, 5 KCl, 2 $MgCl_2$, 10 HEPES and 5 glucose.

The RNeasy Mini Kit for qRT-PCR was from Qiagen. Superscript RT II was from Invitrogen. SYBR Green PCR master mix was from Applied Biosystems. Primers for qRT-PCR were from Integrated DNA Technologies. Primer sequences employed in this report were listed in Table 2.

### ***Isolation of pancreatic islets and islet pretreatments***

Pancreatic islets were isolated from male Swiss-Webster mice (3 months of age; 25-35 g) according to the regulations of the University of Michigan Committee on the Use and Care of Animals (UCUCA), using previously described methods (20) and with an approved protocol. Isolated mouse islets were pretreated with DMSO (control group), 10 µg/mL tunicamycin (TM), 10 µM dantrolene (Dan), 1 µM xestospongin C (XeC) or co-treated with TM and Dan/XeC. The islets were cultured in standard RPMI 1640 medium containing 11 mM glucose, 10% fetal bovine serum (FBS), 10 mM HEPES, 1% penicillin/streptomycin and 1% sodium pyruvate.

***Cell culture***

INS-1(832/13) cells were grown in RPMI 1640 containing 11 mM glucose, 10% fetal bovine serum (FBS), 1% penicillin/streptomycin, 10 mM HEPES and 1% sodium pyruvate. INS-1(832/13) cells were grown in 10 cm culture dishes or 6-well plates at 37°C in a 5% $CO_2$ humidified atmosphere. Cells obtained ~70% confluence before the initiation of experimentation.

***Real-Time PCR***

Total RNA was extracted from INS-1(832/13) cells and reverse transcribed to cDNA as described (12). Then qPCR was carried out using primers listed in Table 2, and data were analyzed as described (12) with expression presented relative to endogenous controls, HPRT1.

***Western blotting***

Total protein was obtained by treating INS-1(832/13) cells with KHEN lysis buffer (50 mM KCL, 50 mM HEPES, 10 mM EGTA, 1.92 mM $MgCl_2$; pH 7.2) and then separating proteins using 4-12% SDS-PAGE and transferring them to nitrocellulose membranes. Membranes were

blocked in 5% w/v nonfat dry milk in 1X TBST containing 50 mM Tris-HCl (pH 7.4), 150 mM NaCl and 0.1% Tween 20. Blots were incubated overnight with rabbit antibody against pIP3R1 diluted in 5% nonfat dry milk in 1X TBST at 4 °C. Blots were incubated with horseradish peroxidase (HRP)-conjugated mouse anti-rabbit antibody and then were visualized using ECL reagents.

***Fura-2/AM imaging***

Islets were loaded with Fura-2/AM (2.5 μM) for 45 min. in medium containing 5 mM glucose before imaging. Islets were then transferred to a 1 mL perfusion chamber containing 5 mM glucose imaging buffer for 6 min, followed by 10 to 30 min perfusion with this solution at approximately 1 mL/min. Imaging buffer contained (in mM): 140 NaCl, 3$CaCl_2$, 5 KCl, 2 $MgCl_2$, 10 HEPES and 5 glucose. Ratiometric Fura-2/AM imaging was carried out using 340/380 nm excitation and collecting 502 nm emission, as previously described (20). The fluorescence data were acquired using Metafluor software (Molecular Devices, Sunnyvale, CA, USA) and plotted using Prism (GraphPad Software Solutions).

***FRET imaging***

To measure ER [$Ca^{2+}$], we utilized a previously described ER-localized FRET biosensor, D4ER (21). D4ER was selectively expressed in beta cells by directing its expression by RIP2 (21). The same system described above for Fura-2/AM imaging was employed here. D4ER imaging was carried out using 430 nm excitation, and 470/535 nm ratiometric emission. The imaging solution used contained (in mM): 140 NaCl, 3 $CaCl_2$, 5 KCl, 2 $MgCl_2$, 10 HEPES, 5 glucose and 0.2 diazoxide (Dz). Dz was included to keep the $K_{ATP}$ channel in its open state to prevent oscillatory

$Ca^{2+}$ activity and improve the signal/noise ratio and stability of the ER $Ca^{2+}$ recordings. FRET ratios were acquired using Metafluor software, plotted using Prism, and mean values were calculated using Excel.

***Mito-pericam imaging***

To measure mitochondrial [$Ca^{2+}$], we utilized a previously described ratiometric mitochondrial pericam (mito-pericam; (22, 23)). The same system described above for Fura-2/AM and D4ER imaging was again employed here, except that the mito-pericam imaging was carried out using 485/400 nm excitation and with emission collected at 535 nm. The imaging solution used contained (in mM): 140 NaCl, 3 $CaCl_2$, 5 KCl, 2 $MgCl_2$, 10 HEPES and 5 glucose. The fluorescence data were acquired using Metafluor software and plotted using Prism.

***Assays of apoptosis***

INS-1(832/13) cells were harvested and prepared for sub-G1 apoptosis assay as described (12). The percentage of apoptotic cells was determined by calculating the percentage cells present in the sub-G1 phase in the DNA content histogram using a flow cytometer provided by the Flow Cytometry Core of the University of Michigan.

***Statistical analysis***

Data were expressed as means +/- SEM and were analyzed using an unpaired Student's t-test (Prism) when comparing two groups. Differences between two or more groups were analyzed using one-way ANOVA or two-way ANOVA (Prism) with post hoc multiple comparisons by

Tukey's procedure as specified in figure legends. Values of $p < 0.05$ were considered statistically significant.

***Results***

We recently reported that chemically inducing ER stress in beta cells with TM activated store-operated $Ca^{2+}$ entry (SOCE) and led to the appearance of cytosolic free $Ca^{2+}$ oscillations in parallel with oscillating membrane potential. The increasing cytosolic $Ca^{2+}$ oscillations concomitantly augmented insulin secretion under what would normally be sub-threshold glucose conditions, e.g., in medium containing 5 mM glucose (12). TM induced a reduction in ER $[Ca^{2+}]$, which we suggested was the proximal trigger for inducing extracellular $Ca^{2+}$ influx via SOCE. $Ca^{2+}$ leaves the ER down its concentration gradient through IP3Rs, RyRs or possibly the translocon (not addressed in this paper (7)). In the case of ER stress, IP3Rs and RyRs may become dysregulated, and ER $Ca^{2+}$ efflux enhanced as a result. As this possibility was not addressed in our previous paper, we decided here to investigate the respective roles of IP3Rs and RyRs in altered beta-cell function after ER stress. To do so, we took advantage of the selective ER $Ca^{2+}$ channel antagonists, xestospongin C (XeC; (24)) and dantrolene (Dan; (25)), to block IP3Rs and RyRs, respectively.

There are three known isoforms of IP3R : IP3R1, IP3R2 and IP3R3 (17, 26, 27), and several groups have reported that all three isoforms are expressed in beta cells, with IP3R1 being most abundant (27). The three isoforms exhibit 70% sequence homology (28), and in our hands they responded similarly to TM treatment. As shown in Figure 3.1A and 3.1B, the mRNA levels of both IP3R1 and IP3R2 decreased after 16 hours of TM treatment. Although the mRNA level of

IP3R3 was not significantly reduced, we did observe a trend towards lower levels of IP3R3 transcripts after TM treatment (Figure 3.1C). Phosphorylated IP3R1 protein was similarly found to decrease in TM-treated INS-1(832/13) cells (Figure 3.1F, preliminary data). RyRs are encoded by three genes, RyR1, RyR2 and RyR3 (17, 29), where RyR2 is the most abundant isoform expressed in beta cells (30). As shown in Figure 3.1D and 3.1E, RyR1 mRNA level was increased by TM treatment, while RyR2 transcript level was unchanged.

Activation of the unfolded protein response (UPR) occurs in response to TM-treatment in cells (12, 30, 31). We previously showed increased spliced XBP1, CHOP and BiP, canonical markers of the ER stress response occurred in both TM-treated INS-1(832/13) cells as well as isolated mouse pancreatic islets (12). To define better the respective roles of IP3Rs and RyRs in TM-induced ER stress in beta cells, INS-1(832/13) cells were treated with a vehicle control (DMSO) or TM (10 μg/ml) for 6 hours with or without XeC (1μM ) or Dan (10 μM) in 11 mM glucose-containing media and then total mRNA was extracted. The 6 hour time point was chosen for mRNA quantification because we previously observed that spliced XBP1 peaked after 6 hours of TM treatment (12). As shown in Figure 3.2A and 3.2B, XBP1 splicing increased after 6 hours of TM treatment in these cells, but neither XeC nor Dan produced any significant inhibition. Thus, blocking IP3Rs or RyR1 did not prevent UPR activation in TM-treated beta cells.

To test whether blocking IP3Rs or RyRs prevented TM-induced ER $Ca^{2+}$ loss, as was previously found in islets (12), the ER $Ca^{2+}$ probe D4ER was transiently expressed in islets using adenovirus. Islets were then treated with vehicle control (DMSO), TM, TM+XeC or TM+Dan for 16 hours, and then ER [$Ca^{2+}$] was measured in 5 mM glucose-containing recording solution.

Representative traces shown in Figures 3.3A and 3.4A are plots of ER [$Ca^{2+}$] expressed in arbitrary units as a function of time. The effect of cyclopiazonic acid (CPA, 50 μM) is shown near the end of each recording trace. CPA is a widely used SERCA blocker that, like thapsigargin, depletes ER $Ca^{2+}$ (32). As shown in Figures 3.3B and 3.4B, exposing islets to TM for 16 hours significantly reduced steady state ER [$Ca^{2+}$] compared to controls, and XeC as well as Dan both appeared to prevent this loss.

Mouse islets cultured overnight in media containing 11 mM glucose do not typically show oscillations in cytosolic free $Ca^{2+}$ when acutely exposed to sub-threshold glucose levels (i.e., glucose concentrations < 7 mM) (12, 33, 34). However, our previous study showed that TM-treated islets undergoing ER stress exhibit cytosolic free $Ca^{2+}$ oscillations in 5 mM glucose due to the activation of store-operated $Ca^{2+}$ entry (SOCE); note that SOCE channels are not a part of the mechanism mediating the normal oscillatory responses of islets to glucose (12, 35).

To determine the roles of IP3Rs and RyRs in the production of oscillations seen in sub-threshold glucose, mouse islets were exposed to a vehicle control (DMSO), TM, XeC, Dan, TM+ XeC or TM+ Dan in standard RPMI 1640 medium for 16 hours. Following these treatments, cytosolic islet $Ca^{2+}$ was recorded using an extracellular recording solution containing 5 mM glucose. As shown in Figures 3.5 and 3.6, the cytosolic free $Ca^{2+}$ of vehicle only control islets displayed little oscillatory activity (less than 5% on average) in 5 mM glucose solution, whereas approximately 80% of TM-treated islets exhibited $Ca^{2+}$ oscillations. These oscillations were abolished (Figure 3.6A), with the percentage of islets exhibiting oscillations reduced to < 5% (Figure 3.6B) in islets treated with TM containing Dan. In contrast, the inclusion of XeC with TM did not affect

the cytosolic [$Ca^{2+}$] oscillations seen in stressed islets (Figures 3.5A and 3.5B). In Dan or XeC-treated islets, as for DMSO-treated control islets, little or no oscillatory $Ca^{2+}$ activity was observed if TM was omitted (Figures 3.5 and 3.6).

Mitochondria generate ATP to fuel cellular biochemical reactions (36) and these organelles are also capable of storing $Ca^{2+}$ with a large capacity (37, 38). RyRs and IP3Rs have been proposed to gate $Ca^{2+}$ transport from the ER to mitochondria (37–39). Mouse islets cultured overnight in standard media do not typically exhibit oscillatory mitochondrial $Ca^{2+}$ activity when acutely exposed to sub-threshold glucose levels (22). As shown in Figure 3.7A, the mitochondrial $Ca^{2+}$ of control beta cells lacked oscillations in 5 mM glucose solution, as expected. In contrast, about 47% of TM-treated beta cells expressing the mito-pericam probe within intact islets exhibited mitochondrial $Ca^{2+}$ oscillations after 22-24 hours of TM exposure (Figure 3.7B). We also investigated the effect of blocking RyRs or IP3Rs on mitochondrial $Ca^{2+}$ oscillations in TM-treated islets. As shown in Figure 3.7B, the percentages of mitochondrial oscillations observed in beta cells in intact islets treated with TM+Dan or TM+XeC were 17% and 39%, respectively. Thus, Dan inclusion reduced the percentage of TM-treated beta cells exhibiting mitochondrial $Ca^{2+}$ oscillations more than did XeC.

Apoptosis has been shown to occur in beta-cells in response to prolonged ER stress (7, 12, 40, 41). Since we observed that inhibiting RyRs could affect beta-cell $Ca^{2+}$ signaling subjected to ER stress, we then analyzed the percentage of cells found to be in the sub-G1 phase of the cell cycle, indicating cell entry into a late stage of apoptosis, following 24 hours exposure to TM, with and without Dan present. As shown in Figure 3.8B, TM-treatment significantly increased in the

percentage of apoptotic cells in the sub-G1 phase compared to DMSO or Dan-treated controls. The application of Dan, together with TM thus considerably reduced beta-cell apoptosis to near control levels. In contrast, the co-application of TM with XeC was without effect (Figure 3.8A). Thus, beta-cell death in our hands appeared to be linked to RyR1 activation.

We previously demonstrated using islets that TM-triggered cytosolic free $Ca^{2+}$ oscillations were mediated by SOCE in 5 mM glucose, as the oscillations were acutely blocked by the SOCE blocker YM58483. Many studies emphasize the importance of ER-mitochondria contact and $Ca^{2+}$ flux from the ER into the mitochondria, but mitochondrial $Ca^{2+}$ may also increase due to influx from the cytosol due to the mitochondrial $Ca^{2+}$ uniporter (MCU), and mitochondrial ion exchangers (37, 42–44) to prevent cytosolic $Ca^{2+}$ overload. Therefore, to further investigate mitochondrial $Ca^{2+}$ regulation in the face of ER stress, we tested if the increased mitochondrial $Ca^{2+}$ oscillations we observed was due to increased SOCE. The representative trace shown in Figure 3.9 demonstrates that acute application of YM58483 in 5 mM glucose abolished mitochondrial $Ca^{2+}$ oscillations that were observed in a TM-treated beta-cell in an intact islet. Hence, SOCE activation in response to TM treatment also appeared to trigger mitochondrial as well as cytosolic $Ca^{2+}$ oscillations under sub-threshold glucose conditions.

### *Discussion*

In this study, we attempted to differentiate the roles of RyRs and IP3Rs in ER stress-mediated alterations in beta-cell function, specifically the maintenance of beta-cell $Ca^{2+}$ homeostasis. The studies were carried out by exposing INS-1(832/13) cells or mouse islets to the glycosylation inhibitor tunicamycin (TM) for up to 24 hours. We found that blocking RyRs using dantrolene

(Dan) in the presence of TM prevented ER $Ca^{2+}$ depletion and cytosolic as well as mitochondrial $Ca^{2+}$ oscillations. Dan also suppressed TM-induced cell apoptosis. In contrast, although inhibiting IP3Rs with xestospongin C (XeC) also reduced ER $Ca^{2+}$ loss, XeC failed to restore normal $Ca^{2+}$ homeostasis in the face of ER stress.

Yamamoto *et al*. also tested the involvement of RyRs and IP3Rs in TM-mediated ER stress conditions in beta cells (30). They proposed that TM decreased ER $Ca^{2+}$ by increasing RyR2 activity, which in turn elicited spontaneous cytosolic $Ca^{2+}$ transients that were seen after raising the extracellular $Ca^{2+}$ concentration (30). Our results agree with those of Yamamoto *et al.* that ryanodine receptors (RyRs) are indeed involved in TM-induced ER $Ca^{2+}$ loss, while IP3Rs are not (IP3Rs, in contrast, were proposed by those authors to be involved in cytokine-induced stress, something we did not test). As XeC did not suppress TM-induced cytosolic free $Ca^{2+}$ oscillations observed in 5 mM glucose (Figure 3.5), we also concluded that IP3Rs were not involved in TM-triggered cytosolic free $Ca^{2+}$ oscillations seen under sub-threshold conditions.

We previously suggested that the augmented cytosolic free $Ca^{2+}$ oscillations and insulin secretion we observed in stressed beta cells were mediated through SOCE channels under sub-threshold glucose conditions (12). In the present study, our data collectively support the hypothesis that the increased free $Ca^{2+}$ occurred secondary to RyR1-mediated ER $Ca^{2+}$ depletion in response to TM treatment. Yamamoto *et al.* inhibited RyRs using ryanodine, a commonly used antagonist targeting all three isoforms if present at sufficiently high concentrations (at least 100 μM). Because RyR2 is the dominant isoform of beta cells, they concluded the spontaneous free $Ca^{2+}$

transients they observed in TM-treated cells were directly due to the increased activity of RyR2 to release $Ca^{2+}$ into the cytosol.

Although we did not explicitly rule out RyR2 in our study, we proposed that the cytosolic $Ca^{2+}$ oscillations induced by TM that we observed in sub-threshold glucose occurred because of increased RyR1 expression, which in turn depleted ER $Ca^{2+}$ to the level that SOCE was activated, as Dan inclusion reduced the percentage of TM-treated islets exhibiting cytosolic $Ca^{2+}$ oscillations in sub-threshold glucose (Figure 3.6B).

Dan is selective for RyR1 over RyR2 (25). Although there was one piece of evidence demonstrating a putative dantrolene-binding site on RyR2, the site was found to not be approachable by Dan without a structural/post-translational modification (45). Unfortunately, we were unable to successfully blot RyR1 protein due to technical limitations. However, we did observe a significant increase in RyR1 mRNA (Figure 3.1D) using qPCR. Yamamoto *et al.* also tested Dan (1 μM) in their study, but they found no effect of the drug on TM-triggered cytosolic $Ca^{2+}$ activity, perhaps due to the concentration of Dan. We used 10 μM of Dan in our study and observed it had a substantial impact on cytosolic $Ca^{2+}$ activity and was able to restore ER $Ca^{2+}$. Other research groups have also found Dan to be effective (up to 30 μM) (46).

In parallel with observing cytosolic free $Ca^{2+}$ oscillations in stressed cells, we saw that mitochondrial $Ca^{2+}$ concentration also oscillated in TM-treated islets under sub-threshold glucose conditions, and further that these oscillations appeared to depend on SOCE activation (Figure 3.9). However, the most profound mitochondrial $Ca^{2+}$ oscillations we observed occurred after

somewhat longer TM treatment (e.g., 22 hours rather than 16 hours) (Figure 3.7A). Moreover, as we found for cytosolic $Ca^{2+}$ oscillations, Dan inclusion prevented these mitochondrial oscillations while XeC inclusion did not (Figure 3.7A and 3.7B). After 16 hours of TM exposure, a very small percentage of islets (~5%) exhibited mitochondrial oscillations. We at present have no explanation for why this extra time of exposure was necessary. However, unlike measurements made using Fura-2/AM, the fluorescent dye we used to image cytosolic $Ca^{2+}$, ratiometric changes monitored using mito-pericam probe are much smaller in amplitude. Hence, we might have underestimated the percentages displayed in Figure 3.7B by missing islets with weak oscillations that were buried in signal noise.

Both disrupted ER homeostasis and mitochondrial homeostasis can result in beta-cell apoptosis (7, 37, 39, 41, 47, 48). As shown in Figure 3.8A, TM treatment led to increased apoptosis, as indicated by the percentage of cells found in the sub-G1 phase in INS-1(832-13) cells. XeC-treatment, in the presence of TM, did not affect the percentage of the cells undergoing apoptosis. In contrast, restoring ER $Ca^{2+}$ levels in TM-treated islets using Dan was found to protect INS-1(832/13) cells from death, as the percentage of cells experiencing apoptosis was reduced after Dan+TM compared to TM treatment alone (Figure 3.8B). However, the percentage of oscillations we recorded was still greater than those of control (DMSO) islets. Mitochondrial $Ca^{2+}$ overload and consequent mitochondrial swelling and permeabilization can cause mitochondria to release pro-apoptotic factors into the cytosol, resulting in apoptosis (39). Therefore, the oscillations in mitochondrial $Ca^{2+}$ may account for the cells that progressed to apoptosis after Dan+TM treatment, as shown in Figure 3.8B.

If any of the changes reported here indeed reflect the importance of ER $Ca^{2+}$ in the downstream effects of ER stress, then it is peculiar that IP3Rs, while capable of blunting ER $Ca^{2+}$ loss, seemed to be unable to reproduce the efficacy of RyR blockade, which also prevented ER $Ca^{2+}$ release. Why might this be the case? While we have no definitive answer, the data are consistent with two possibilities. First, regionalization of the ER might occur so that the depletion of $Ca^{2+}$ within different domains of the ER result in different consequences for the cell. Resolving this question will require higher resolution imaging approaches to assay distinct ER subdomains and their potentially differentially localized $Ca^{2+}$ pools. We do not know whether the different types of ER $Ca^{2+}$ channels indeed may also be differentially localized within these different subdomains of the ER (49, 50).

Secondly, there could be direct roles of the RyRs themselves in the signaling that is linked to the downstream events associated with ER stress. What other molecules do these proteins interact with, and do they also perhaps generate additional signals through these interactions? In this case, lowering ER $Ca^{2+}$ could be but one component of the response to ER stress involving RyRs and IP3Rs. Further research will need to be carried out to answer these questions.

In summary, this report demonstrates that the RyR1 is a critical player in TM-induced ER $Ca^{2+}$ loss, cytosolic and mitochondrial $Ca^{2+}$ oscillations and beta-cell apoptosis, as described in Figure 3.10. Inhibiting RyR1 using Dan blocked both the cytosolic $Ca^{2+}$ oscillations seen under sub-threshold glucose conditions and cell apoptosis seen in response to TM. Hence, merging our findings with existing knowledge on RyRs and IP3Rs, we suggest that RyR1 could be a potentially useful therapeutic target in T2DM and prediabetes.

## *Figures and legends*

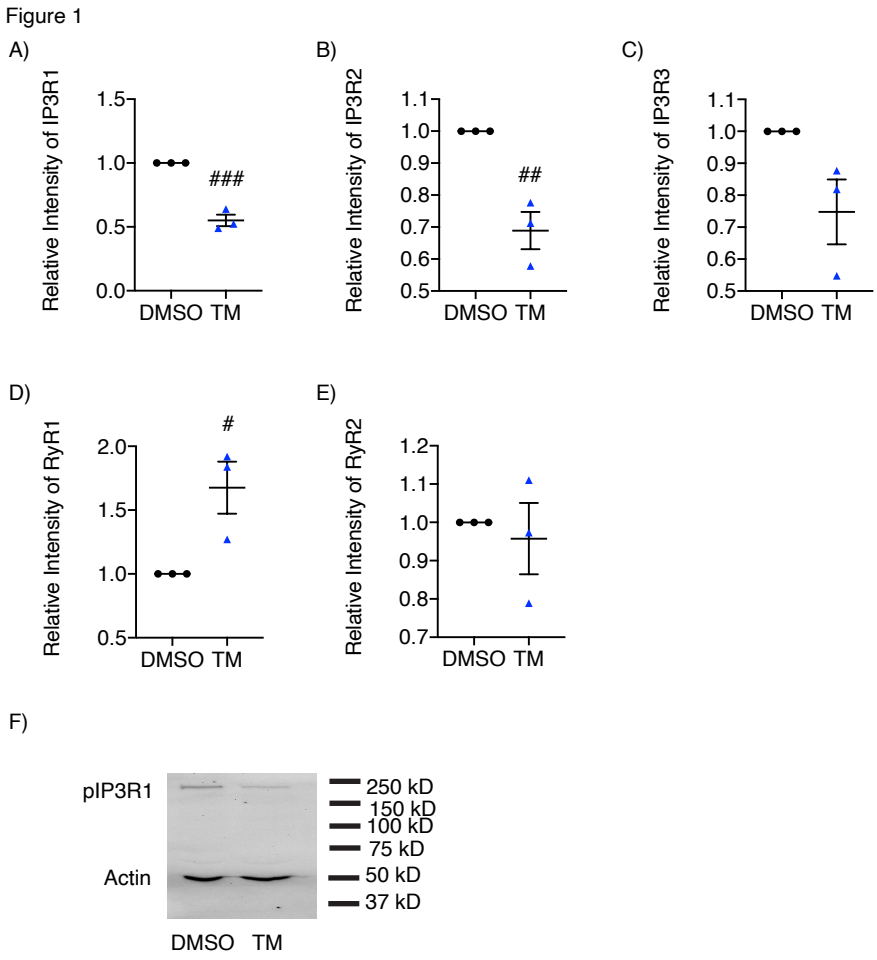


*Figure 3.1 Tunicamycin altered IP3Rs and RyRs expression*

INS-1(832/13) cells were treated with vehicle control (DMSO) or tunicamycin (TM, 10 µg/ml) for 16 hours in 11 mM glucose. 1A-1C: IP3R isoforms mRNA levels were measured. 1A: IP3R1. 1B: IP3R2. 1C: IP3R3. 1D-1E: RyR isoforms mRNA levels were measured. 1D: RyR1. 1E: RyR2. All values shown are means ± SEM, #, $p< 0.05$, ##, $p< 0.01$, ###, $p< 0.005$; n= 3 times repeated per condition, by student's t-test. 1F: Representative western blots showing the expression of phosphorylated IP3R1 (n=1).

Figure 2

A)

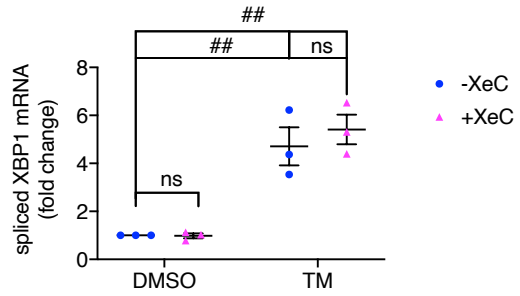


B)

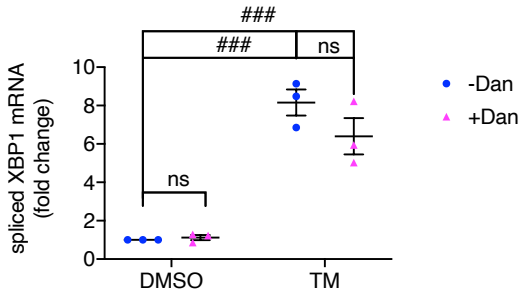


*Figure 3.2 Inhibiting IP3Rs or RyRs did not prevent UPR activation*

2A: INS-1(832/13) cells were treated with vehicle control (DMSO), tunicamycin (TM, 10 µg/ml), xestospongin C (XeC, 1 µM) or TM+XeC for 6 hours in 11 mM glucose containing culture medium. Expression level of spliced XBP1 mRNA. Row Factor F(1, 8)= 64.85, p< 0.0001, Column Factor F(1, 8)= 0.4599, p=0.5168, Interaction F(1, 8)= 0.5129, p= 0.4943, by two-way ANOVA. 2B: INS-1(832/13) cells were treated with vehicle control (DMSO), tunicamycin (TM, 10 µg/ml), dantrolene (Dan, 10 µM) or TM+Dan for 6 hours in 11 mM glucose containing culture medium. Expression level of spliced XBP1 mRNA. Row Factor F(1, 8)= 112.3, p< 0.0001, Column Factor F(1, 8)= 1.937, p=0.2015, Interaction F(1, 8)= 2.568, p= 0.1477, by two-way ANOVA. All values shown are means ± SEM. ##, p< 0.01; ###, p< 0.005; ns= not significant; n= 3 times repeated per condition, by two-way ANOVA with post hoc multiple comparison by Tukey's procedure.

Figure 3

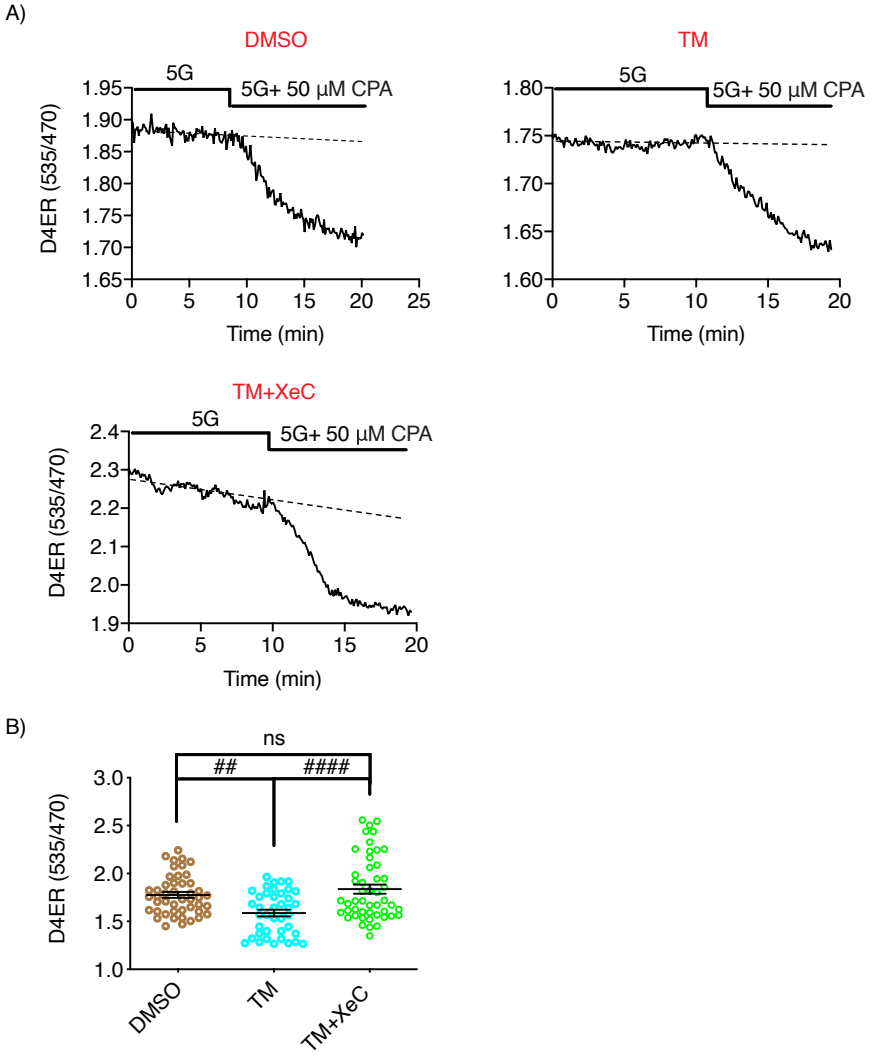


*Figure 3.3 Xestospongin C treatment restored basal ER $Ca^{2+}$ level*

Mouse pancreatic islets were infected with an adenovirus expressing a beta-cell directed D4ER probe for three hours, followed by a 48-hour recovery period. Islets were then treated with vehicle control (DMSO), tunicamycin (TM, 10 µg/ml) or TM+ xestospongin C (XeC, 1 µM) for 16 hours in 11 mM glucose islet culture medium. 3A: Basal ER $Ca^{2+}$ traces for each condition obtained in 5 mM glucose solution before and after cyclopiazonic acid (CPA, 50 µM). 3B: The raw data showing resting ER $Ca^{2+}$ level from mouse islets in 5 mM glucose solution. Each data point shown was a D4ER ratio obtained for one selected region of interest, a single cell or small group of cells. All values shown are means ± SEM. ##, $p< 0.01$; ####, $p< 0.0001$; ns= not significant; n= at least 3 mice, by one-way ANOVA with post hoc multiple comparison by Tukey's procedure.

Figure 4

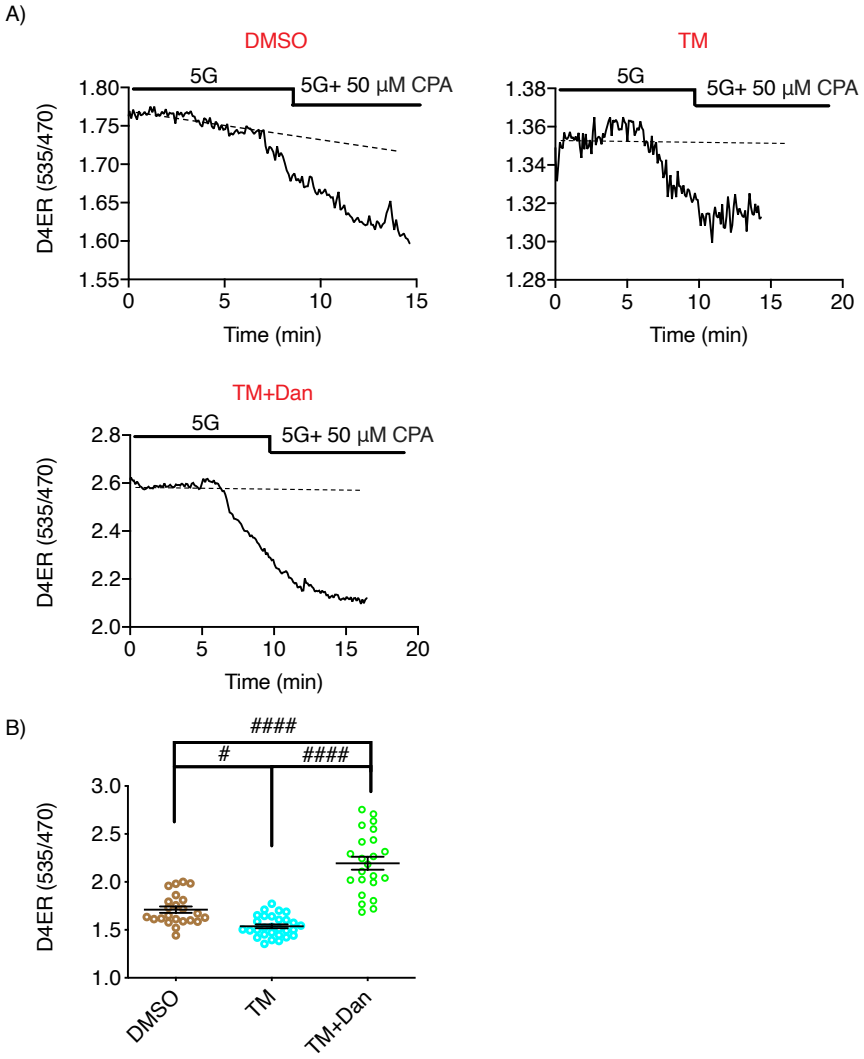


*Figure 3.4 Dantrolene treatment increased basal ER $Ca^{2+}$ level*

Mouse pancreatic islets were infected with an adenovirus expressing a beta-cell directed D4ER probe for three hours, followed by a 48-hour recovery period. Islets were then treated with vehicle control (DMSO), tunicamycin (TM, 10 µg/ml) or TM+ dantrolene (Dan, 10 µM) for 16 hours in 11 mM glucose islet culture medium. 3A: Basal ER $Ca^{2+}$ traces for each condition obtained in 5 mM glucose solution before and after cyclopiazonic acid (CPA, 50 µM). 3B: The raw data showing resting ER $Ca^{2+}$ level from mouse islets in 5 mM glucose solution. Each data point shown was a D4ER ratio obtained for one selected region of interest, a single cell or small group of cells. All values shown are means ± SEM. #, $p< 0.05$; ####, $p< 0.0001$; n= at least 3 mice, by one-way ANOVA with post hoc multiple comparison by Tukey's procedure.

Figure 5

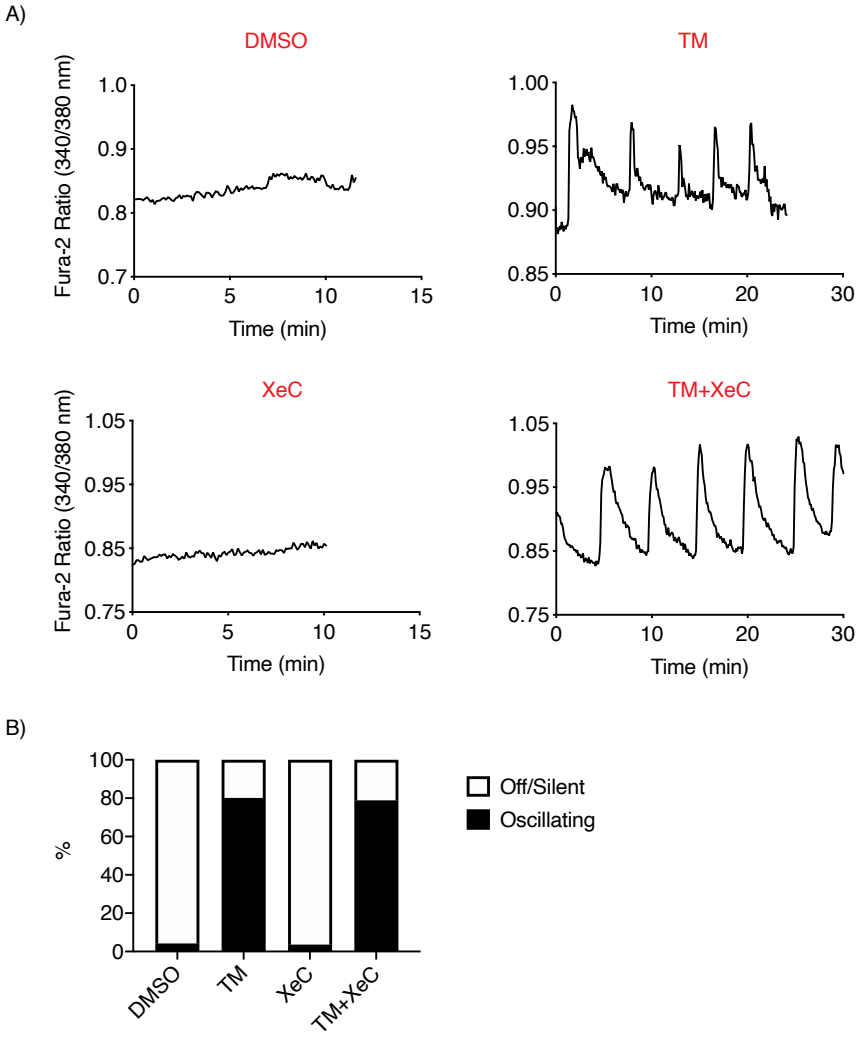


*Figure 3.5 Xestospongin C did not affect cytosolic free $Ca^{2+}$ oscillations under sub-threshold glucose conditions*

Isolated pancreatic mouse islets were treated with a vehicle control (DMSO), tunicamycin (TM, 10 µg/ml), xestospongin C (XeC, 1 µM) or TM+XeC for 16 hours in 11 mM glucose. 3A: The responses of cytosolic free $Ca^{2+}$ to the solution containing 5 mM glucose under the indicated conditions. 3B: Percentage of oscillating islets; n= at least 3 mice.

Figure 6

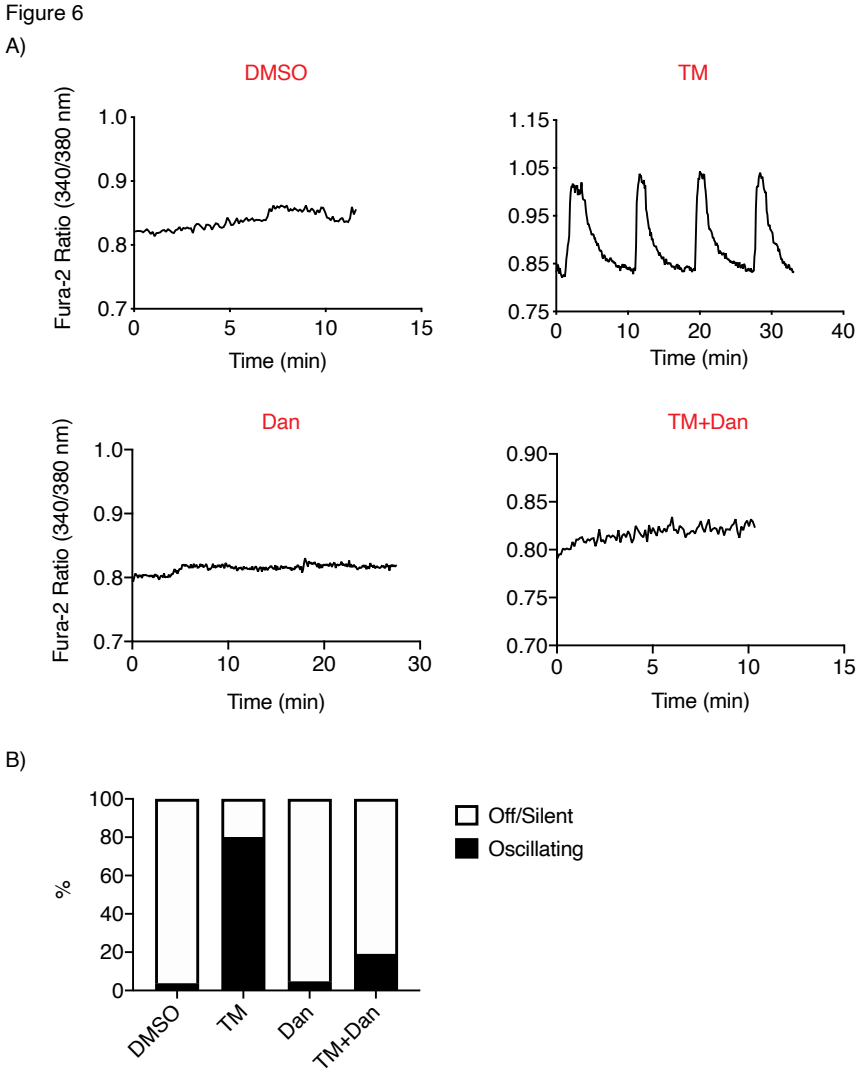


*Figure 3.6 Dantrolene suppressed cytosolic free $Ca^{2+}$ oscillations under sub-threshold glucose conditions*

Isolated pancreatic mouse islets were treated with a vehicle control (DMSO), tunicamycin (TM, 10 µg/ml), dantrolene (Dan, 10 µM) or TM+Dan for 16 hours in 11 mM glucose. 3A: The responses of cytosolic free $Ca^{2+}$ to the solution containing 5 mM glucose under the indicated conditions. 3B: Percentage of oscillating islets; n= at least 3 mice.

Figure 7

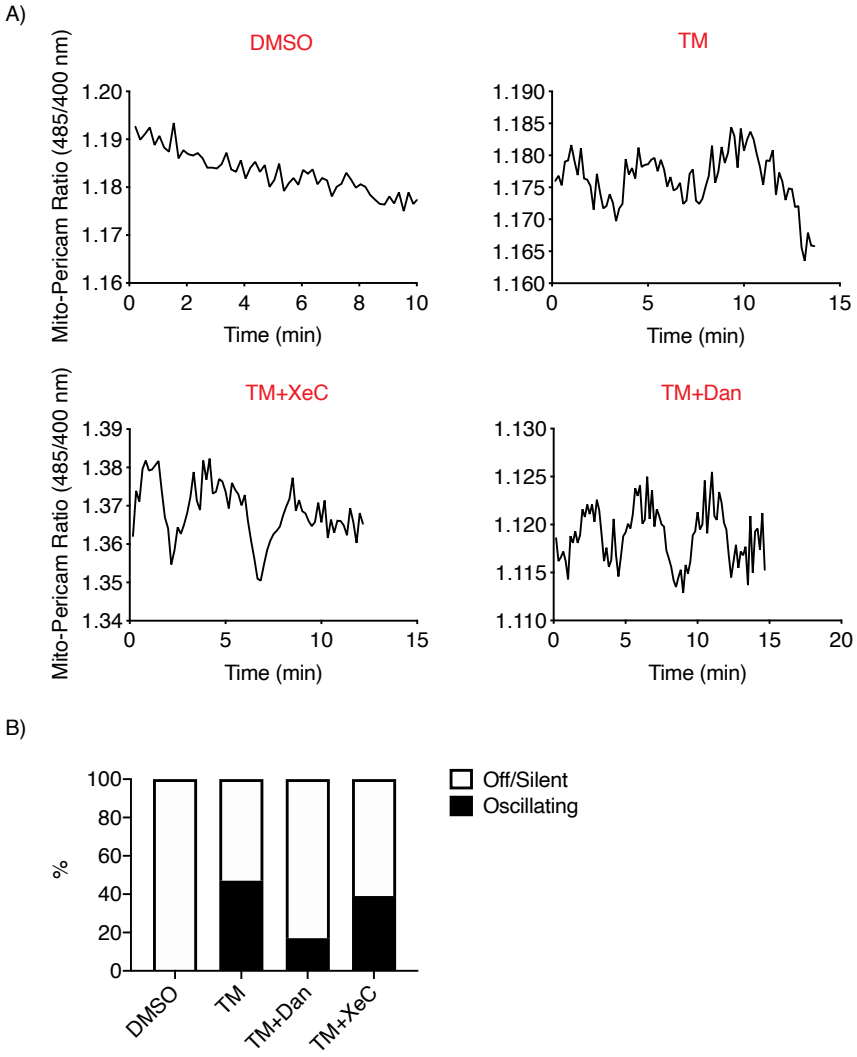


*Figure 3.7 Differential effects of xestospongin C and dantrolene on mitochondrial $Ca^{2+}$ oscillations under sub-threshold glucose conditions*

Mouse pancreatic islets were infected with an adenovirus expressing the mito-pericam probe for 6 hours, followed by a 72-hour recovery period prior to imaging. Within the last 16 hours period, islets were treated with vehicle control (DMSO), tunicamycin (TM, 10 µg/ml), TM+ xestospongin C (XeC, 1 µM) or TM+dantrolene (Dan, 10 µM) in 11 mM glucose islet culture medium. 7A: Representative traces of basal mitochondrial $Ca^{2+}$ in the solution containing 5 mM glucose under the indicated conditions. 7B: Percentage of oscillating beta cells within intact islets; n= at least 3 mice.

Figure 8

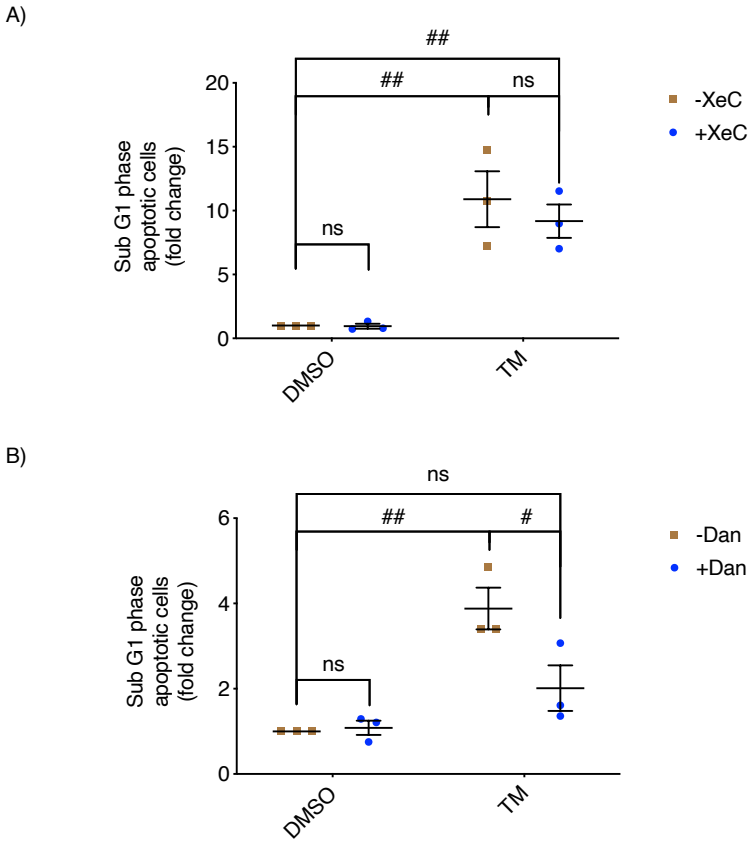


*Figure 3.8 Differential effects of xestospongin C and dantrolene on beta-cell apoptosis under sub-threshold glucose conditions*

INS-1(832/13) cells were treated with vehicle control (DMSO), tunicamycin (TM, 10 µg/ml), 8A: xestospongin C (XeC, 1 µM), or TM+XeC; 8B: dantrolene (Dan, 10 µM) or TM+Dan for 24 hours in 11 mM glucose containing cell culture medium. Late stage apoptotic INS-1(832/13) cells is shown using the sub-G1 assay measured by flow cytometry. Fold change was derived by comparing to DMSO group. 8A: Row Factor $F(1, 8)= 50.25$, $p= 0.0001$, Column Factor $F(1, 8)= 0.4793$, $p=0.5083$, Interaction $F(1, 8)= 0.4267$, $p= 0.5319$, by two-way ANOVA. 8B: Row Factor $F(1, 8)= 26.26$, $p= 0.0009$, Column Factor $F(1, 8)= 5.753$, $p=0.0433$, Interaction $F(1, 8)= 6.879$, $p= 0.0305$, by two-way ANOVA. All values shown are means ± SEM. #, $p< 0.05$, ##, $p< 0.01$, ns= not significant; n= 3 times repeated per condition, by two-way ANOVA with post hoc multiple comparison by Tukey's procedure.

Figure 9

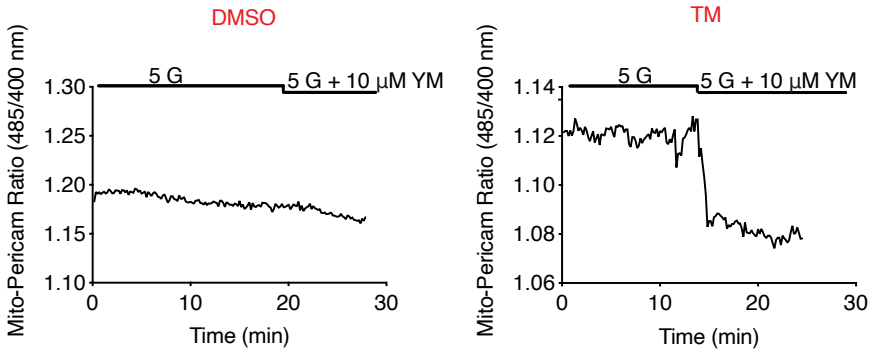


*Figure 3.9 Increased mitochondrial $Ca^{2}$ was mediated by store-operated $Ca^{2+}$ entry (SOCE)*

Mouse pancreatic islets were infected with an adenovirus expressing the mito-pericam probe, as described in Figure 3.7. Islets were treated with vehicle control (DMSO), tunicamycin (TM, 10 µg/ml) for 16 hours in 11 mM glucose islet culture medium. Islets were then acutely exposed to 5 mM glucose containing solution with or without YM58483 (YM, 10 µM).

Figure 10

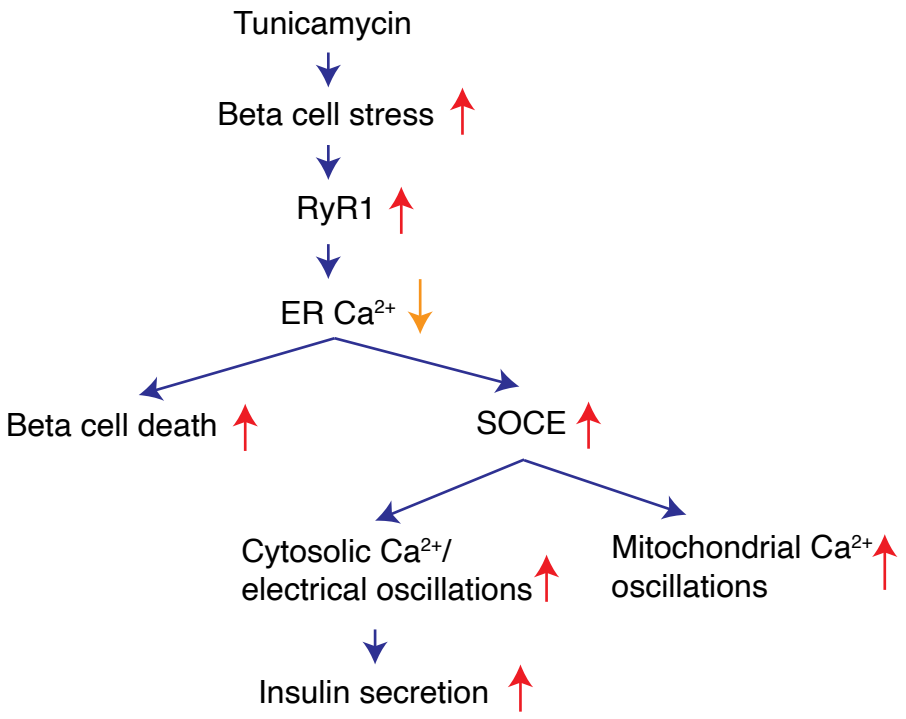


*Figure 3.10 Scheme of beta-cell death and increasing insulin secretion mediated by tunicamycin*

Table 1

A)

| Gene | Forward | Reward |
|---|---|---|
| Xbp1s (rat) | CTGAGTCCGAATCAGGTGCAG | ATCCATGGGAAGATGTTCTGG |
| Ryr1 (rat) | CGTAGACAACAACAGGGCAC | AGATTTCTCCCACCATCCTGA |
| Ryr2 (rat) | ACGGCGACCATCCACAAAG | AAAGTCTGTTGCCAAATCCTTCT |
| IP3R1 (rat) | CAACCGTTACTATGGAAACATC | TCAGCCAGGCTCATCTCAC |
| IP3R2 (rat) | CGATGCCAGGATACGATGT | CACCCTTGAAGTACCGATT |
| IP3R3 (rat) | AGGAGCTGGTGGACGTGAT | TGCTTGTTGTGCCTGGAAA |
| Hprt1 (rat) | CTCATGGACTGATTATGGACAGGAC | GCAGGTCAGCAAAGAACTTATAGCC |

*Table 2 Oligonucleotide primers*

***References***


1. Howell, S. L., Jones, P. M., and Persaud, S. J. (1994) Regulation of insulin secretion: the role of second messengers. *Diabetologia*. **37**, S30–S35

2. Clapham, D. E. (2007) Calcium Signaling. *Cell*. **131**, 1047–1058

3. Berridge, M. J. (2002) The endoplasmic reticulum: a multifunctional signaling organelle. *Cell Calcium*. **32**, 235–249

4. Anelli, T., and Sitia, R. (2008) Protein quality control in the early secretory pathway. *EMBO J.* **27**, 315–327

5. Fonseca, S. G., Gromada, J., and Urano, F. (2011) Endoplasmic reticulum stress and pancreatic β-cell death. *Trends Endocrinol. Metab.* **22**, 266–274

6. Hasnain, S. Z., Prins, J. B., and McGuckin, M. A. (2016) Oxidative and endoplasmic reticulum stress in β-cell dysfunction in diabetes. *J. Mol. Endocrinol.* **56**, R33–R54

7. Zhang, I. X., Raghavan, M., and Satin, L. S. (2020) The Endoplasmic Reticulum and Calcium Homeostasis in Pancreatic Beta Cells. *Endocrinology*. **161**, bqz028

8. Arunagiri, A., Haataja, L., Pottekat, A., Pamenan, F., Kim, S., Zeltser, L. M., Paton, A. W., Paton, J. C., Tsai, B., Itkin-Ansari, P., Kaufman, R. J., Liu, M., and Arvan, P. (2019) Proinsulin misfolding is an early event in the progression to type 2 diabetes. *eLife*. **8**, e44532

9. Back, S. H., and Kaufman, R. J. (2012) Endoplasmic Reticulum Stress and Type 2 Diabetes. *Annu. Rev. Biochem.* **81**, 767–793

10. Sammels, E., Parys, J. B., Missiaen, L., De Smedt, H., and Bultynck, G. (2010) Intracellular Ca2+ storage in health and disease: A dynamic equilibrium. *Cell Calcium*. **47**, 297–314

11. Mekahli, D., Bultynck, G., Parys, J. B., De Smedt, H., and Missiaen, L. (2011) Endoplasmic-Reticulum Calcium Depletion and Disease. *Cold Spring Harb. Perspect. Biol.* **3**, a004317–a004317

12. Zhang, I. X., Ren, J., Vadrevu, S., Raghavan, M., and Satin, L. S. (2020) ER stress increases store-operated $Ca^{2+}$ entry (SOCE) and augments basal insulin secretion in pancreatic β cells. *J. Biol. Chem.* 10.1074/jbc.RA120.012721

13. Flourakis, M., Van Coppenolle, F., Lehen'kyi, V., Beck, B., Skryma, R., and Prevarskaya, N. (2006) Passive calcium leak via translocon is a first step for $iPLA_2$ -pathway regulated store operated channels activation. *FASEB J.* **20**, 1215–1217

14. Van Coppenolle, F. (2004) Ribosome-translocon complex mediates calcium leakage from endoplasmic reticulum stores. *J. Cell Sci.* **117**, 4135–4142

15. Graves, T. K., and Hinkle, P. M. (2003) Ca $^{2+}$ -Induced Ca $^{2+}$ Release in the Pancreatic β-Cell: Direct Evidence of Endoplasmic Reticulum Ca $^{2+}$ Release. *Endocrinology*. **144**, 3565–3574

16. Dyachok, O., Tufveson, G., and Gylfe, E. (2004) Ca2+-induced Ca2+ release by activation of inositol 1,4,5-trisphosphate receptors in primary pancreatic β-cells. *Cell Calcium*. **36**, 1–9

17. Santulli, G., Nakashima, R., Yuan, Q., and Marks, A. R. (2017) Intracellular calcium release channels: an update: RyRs *vs* . IP $_3$ Rs. *J. Physiol.* **595**, 3041–3051

18. Yoo, J., Mashalidis, E. H., Kuk, A. C. Y., Yamamoto, K., Kaeser, B., Ichikawa, S., and Lee, S.-Y. (2018) GlcNAc-1-P-transferase–tunicamycin complex structure reveals basis for inhibition of N-glycosylation. *Nat. Struct. Mol. Biol.* **25**, 217–224

19. Tong, X., Kono, T., Anderson-Baucum, E. K., Yamamoto, W., Gilon, P., Lebeche, D., Day, R. N., Shull, G. E., and Evans-Molina, C. (2016) SERCA2 Deficiency Impairs Pancreatic β-Cell Function in Response to Diet-Induced Obesity. *Diabetes*. **65**, 3039–3052

20. Zhang, M., Goforth, P., Bertram, R., Sherman, A., and Satin, L. (2003) The Ca2+ Dynamics of Isolated Mouse β-Cells and Islets: Implications for Mathematical Models. *Biophys. J.* **84**, 2852–2870

21. Ravier, M. A., Daro, D., Roma, L. P., Jonas, J.-C., Cheng-Xue, R., Schuit, F. C., and Gilon, P. (2011) Mechanisms of Control of the Free Ca2+ Concentration in the Endoplasmic Reticulum of Mouse Pancreatic -Cells: Interplay With Cell Metabolism and [Ca2+]c and Role of SERCA2b and SERCA3. *Diabetes*. **60**, 2533–2545

22. Montemurro, C., Nomoto, H., Pei, L., Parekh, V. S., Vongbunyong, K. E., Vadrevu, S., Gurlo, T., Butler, A. E., Subramaniam, R., Ritou, E., Shirihai, O. S., Satin, L. S., Butler, P. C., and Tudzarova, S. (2019) IAPP toxicity activates HIF1α/PFKFB3 signaling delaying β-cell loss at the expense of β-cell function. *Nat. Commun.* **10**, 2679

23. Nagai, T., Sawano, A., Park, E. S., and Miyawaki, A. (2001) Circularly permuted green fluorescent proteins engineered to sense Ca2+. *Proc. Natl. Acad. Sci.* **98**, 3197–3202

24. Gafni, J., Munsch, J. A., Lam, T. H., Catlin, M. C., Costa, L. G., Molinski, T. F., and Pessah, I. N. (1997) Xestospongins: Potent Membrane Permeable Blockers of the Inositol 1,4,5-Trisphosphate Receptor. *Neuron*. **19**, 723–733

25. Zhao, F., Li, P., Chen, S. R. W., Louis, C. F., and Fruen, B. R. (2001) Dantrolene Inhibition of Ryanodine Receptor Ca $^{2+}$ Release Channels: MOLECULAR MECHANISM AND ISOFORM SELECTIVITY. *J. Biol. Chem.* **276**, 13810–13816

26. Mataragka, S., and Taylor, C. W. (2018) All three IP $_3$ receptor subtypes generate Ca $^{2+}$ puffs, the universal building blocks of IP $_3$ -evoked Ca $^{2+}$ signals. *J. Cell Sci.* **131**, jcs220848

27. Ye, R., Ni, M., Wang, M., Luo, S., Zhu, G., Chow, R. H., and Lee, A. S. (2011) Inositol 1,4,5-trisphosphate receptor 1 mutation perturbs glucose homeostasis and enhances susceptibility to diet-induced diabetes. *J. Endocrinol.* **210**, 209–217

28. Baker, M. R., Fan, G., and Serysheva, I. I. (2017) Structure of IP3R channel: high-resolution insights from cryo-EM. *Curr. Opin. Struct. Biol.* **46**, 38–47

29. Santulli, G., Pagano, G., Sardu, C., Xie, W., Reiken, S., D'Ascia, S. L., Cannone, M., Marziliano, N., Trimarco, B., Guise, T. A., Lacampagne, A., and Marks, A. R. (2015) Calcium release channel RyR2 regulates insulin release and glucose homeostasis. *J. Clin. Invest.* **125**, 1968–1978

30. Yamamoto, W. R., Bone, R. N., Sohn, P., Syed, F., Reissaus, C. A., Mosley, A. L., Wijeratne, A. B., True, J. D., Tong, X., Kono, T., and Evans-Molina, C. (2019) Endoplasmic reticulum stress alters ryanodine receptor function in the murine pancreatic β cell. *J. Biol. Chem.* **294**, 168–181

31. Collett, G. P., Redman, C. W., Sargent, I. L., and Vatish, M. (2018) Endoplasmic reticulum stress stimulates the release of extracellular vesicles carrying danger-associated molecular pattern (DAMP) molecules. *Oncotarget*. 10.18632/oncotarget.24158

32. Laursen, M., Bublitz, M., Moncoq, K., Olesen, C., Møller, J. V., Young, H. S., Nissen, P., and Morth, J. P. (2009) Cyclopiazonic acid is complexed to a divalent metal ion when bound to the sarcoplasmic reticulum Ca2+-ATPase. *J. Biol. Chem.* **284**, 13513–13518

33. Satin, L. S., Butler, P. C., Ha, J., and Sherman, A. S. (2015) Pulsatile insulin secretion, impaired glucose tolerance and type 2 diabetes. *Mol. Aspects Med.* **42**, 61–77

34. Glynn, E., Thompson, B., Vadrevu, S., Lu, S., Kennedy, R. T., Ha, J., Sherman, A., and Satin, L. S. (2016) Chronic Glucose Exposure Systematically Shifts the Oscillatory Threshold of Mouse Islets: Experimental Evidence for an Early Intrinsic Mechanism of Compensation for Hyperglycemia. *Endocrinology*. **157**, 611–623

35. Bertram, R., Satin, L. S., and Sherman, A. S. (2018) Closing in on the Mechanisms of Pulsatile Insulin Secretion. *Diabetes*. **67**, 351–359

36. Tait, S. W. G., and Green, D. R. (2010) Mitochondria and cell death: outer membrane permeabilization and beyond. *Nat. Rev. Mol. Cell Biol.* **11**, 621–632

37. Wacquier, B., Combettes, L., Van Nhieu, G. T., and Dupont, G. (2016) Interplay Between Intracellular Ca2+ Oscillations and Ca2+-stimulated Mitochondrial Metabolism. *Sci. Rep.* **6**, 19316

38. Idevall-Hagren, O., and Tengholm, A. (2020) Metabolic regulation of calcium signaling in beta cells. *Semin. Cell Dev. Biol.* 10.1016/j.semcdb.2020.01.008

39. Hajnóczky, G., Csordás, G., Das, S., Garcia-Perez, C., Saotome, M., Sinha Roy, S., and Yi, M. (2006) Mitochondrial calcium signalling and cell death: Approaches for assessing the role of mitochondrial Ca2+ uptake in apoptosis. *Cell Calcium*. **40**, 553–560

40. Oslowski, C. M., and Urano, F. (2011) Measuring ER Stress and the Unfolded Protein Response Using Mammalian Tissue Culture System. in *Methods in Enzymology*, pp. 71–92, **490**, 71–92

41. Sano, R., and Reed, J. C. (2013) ER stress-induced cell death mechanisms. *Biochim. Biophys. Acta BBA - Mol. Cell Res.* **1833**, 3460–3470

42. Wacquier, B., Combettes, L., and Dupont, G. (2019) Cytoplasmic and Mitochondrial Calcium Signaling: A Two-Way Relationship. *Cold Spring Harb. Perspect. Biol.* **11**, a035139

43. Lee, K.-S., Huh, S., Lee, S., Wu, Z., Kim, A.-K., Kang, H.-Y., and Lu, B. (2018) Altered ER–mitochondria contact impacts mitochondria calcium homeostasis and contributes to neurodegeneration in vivo in disease models. *Proc. Natl. Acad. Sci.* **115**, E8844–E8853

44. Calvo-Rodriguez, M., Hou, S. S., Snyder, A. C., Kharitonova, E. K., Russ, A. N., Das, S., Fan, Z., Muzikansky, A., Garcia-Alloza, M., Serrano-Pozo, A., Hudry, E., and Bacskai, B. J. (2020) Increased mitochondrial calcium levels associated with neuronal death in a mouse model of Alzheimer's disease. *Nat. Commun.* **11**, 2146

45. Paul-Pletzer, K., Yamamoto, T., Ikemoto, N., Jimenez, L. S., Morimoto, H., Williams, P. G., Ma, J., and Parness, J. (2005) Probing a putative dantrolene-binding site on the cardiac ryanodine receptor. *Biochem. J.* **387**, 905–909

46. Luciani, D. S., Gwiazda, K. S., Yang, T.-L. B., Kalynyak, T. B., Bychkivska, Y., Frey, M. H. Z., Jeffrey, K. D., Sampaio, A. V., Underhill, T. M., and Johnson, J. D. (2009) Roles of IP3R and RyR Ca2+ Channels in Endoplasmic Reticulum Stress and -Cell Death. *Diabetes*. **58**, 422–432

47. Rojas, J., Bermudez, V., Palmar, J., Martínez, M. S., Olivar, L. C., Nava, M., Tomey, D., Rojas, M., Salazar, J., Garicano, C., and Velasco, M. (2018) Pancreatic Beta Cell Death: Novel Potential Mechanisms in Diabetes Therapy. *J. Diabetes Res.* **2018**, 1–19

48. Chan, J. Y., Luzuriaga, J., Maxwell, E. L., West, P. K., Bensellam, M., and Laybutt, D. R. (2015) The balance between adaptive and apoptotic unfolded protein responses regulates β-cell death under ER stress conditions through XBP1, CHOP and JNK. *Mol. Cell. Endocrinol.* **413**, 189–201

49. Sitia, R., and Meldolesi, J. (1992) Endoplasmic reticulum: a dynamic patchwork of specialized subregions. *Mol. Biol. Cell*. **3**, 1067–1072

50. Hobman, T. C., Zhao, B., Chan, H., and Farquhar, M. G. (1998) Immunoisolation and Characterization of a Subdomain of the Endoplasmic Reticulum That Concentrates Proteins Involved in COPII Vesicle Biogenesis. *Mol. Biol. Cell*. **9**, 1265–1278

# Chapter 4 ER Stress Activates $K_{ir}2.1$ and Enhances Free $Ca^{2+}$ Oscillations in Pancreatic Beta Cells

Irina X. Zhang, Suryakiran Vadrevu, and Leslie S. Satin

***Abstract***

Accumulating evidence demonstrates an essential role for ER stress in T2DM pathogenesis. In a previous study from our laboratory, store-operated $Ca^{2+}$ entry (SOCE) was shown to be activated by the stress-inducing agent tunicamycin (TM; 10 μg/ml) in insulin-secreting INS-1 (832/13) cells or isolated mouse islets. As a result, oscillations in cytosolic $Ca^{2+}$, membrane potential and insulin secretion were observed even in normally sub-threshold glucose (e.g., 5 mM glucose). Our laboratory has proposed that islets from $K_{ATP}$ (SUR1) deficient mice, which are well known to display relatively normal cytosolic $Ca^{2+}$ oscillations because compensatory activation of the inward rectifier $K^+$ channel $K_{ir}2.1$. To investigate whether $K_{ir}2.1$ is also involved in ER stress-induced beta-cell dysfunction, as in other cell types (1, 2) we tested the $K_{ir}2.1$-selective inhibitor ML133 (10 μM). We found that the TM-induced cytosolic $Ca^{2+}$ oscillations of mouse islets were blocked following overnight exposure to ML133, as was TM-induced beta-cell apoptosis. ML133 also alleviated ER stress, as evidenced by decreased XBP1 splicing in TM-treated cells, while it enhanced BiP expression. The induction of ER stress, in addition, resulted in reduced trafficking of $K_{ATP}$ (SUR1) to the plasma membrane in INS-1 (832/13) cells. These results suggest that $K_{ir}2.1$ channels may represent a novel target for increasing insulin secretion under

conditions of ER stress.

### *Introduction*

Diabetes affects approximately 1 in 10 Americans, and type 2 diabetes mellitus (T2DM) accounts for 90% to 95% of the population with diabetes overall (3). T2DM is a chronic disorder which is characterized by hyperglycemia due to deficient beta cell insulin secretion and insulin resistance of target tissues, causing a failure of the body to maintain normal blood glucose levels (4, 5). Insulin secretion is a $Ca^{2+}$- dependent process. In mouse beta cells, elevated blood glucose is taken up by type 2 glucose transporters (GLUT-2) and then metabolized to generate ATP. The ratio of ATP/ADP being thus enhanced, ATP-gated $K^+$ channels ($K_{ATP}$) close, leading to plasma membrane depolarization. The voltage-gated $Ca^{2+}$ channel (VGCC), which is gated by plasma membrane depolarization thus allows $Ca^{2+}$ influx into the cytosol (6–10). $Ca^{2+}$ is sequestered within the endoplasmic reticulum (ER) and released into the cytosol in response to various physiological stimuli, such as occur when beta cell plasma membrane GPCRs activate (11).

The ER plays a vital role in intracellular $Ca^{2+}$ signaling, protein folding and trafficking and cell apoptosis. Disrupted ER homeostasis triggers the activation of the unfolded protein response (UPR), an adaptive signaling pathway in which cells strive to survive, or they undergo apoptosis after unresolved ER stress (12). Disturbed ER homeostasis and ER stress are believed to be an essential part of the pathogenesis of T2DM (9, 13), and increasing evidence suggests the activation of UPR occurs in beta cells from T2DM patients and T2DM animal models (13–17).

The $K_{ATP}$ channel consists of four pairs of $K_{ir}6.2$ and SUR1 subunits that together form an octameric arrangement (18, 19). The inward-rectifier $K_{ir}6.2$ is the pore-forming subunit that is bound by ATP. SUR1 is a high-affinity sulfonylurea receptor belonging to the ATP-binding cassette superfamily (ABC transporters;17). The $K_{ATP}$ channel requires both subunits in order to function (19, 21). However, paradoxically the SUR1-/- mouse which lacks SUR1 subunit and functional $K_{ATP}$ has been shown by several labs to maintain relatively normal oscillations in both membrane potential and cytosolic free $Ca^{2+}$ in 11 mM glucose. Yildirim et al (19) from our group, using mainly mathematical modeling and some key experimental data and a companion experimental study (Vadrevu et al., in preparation) demonstrated a compensatory mechanism that can account for the puzzling results seen in SUR1-/- islets based on the hypothesis that upregulation of another inward rectifier channel, $K_{ir}2.1$ occurs in SUR1-/- mice (19).

$K_{ir}2.1$ is encoded by the KCNJ2 gene (22) and $K_{ir}2.1$ currents have been observed in human beta cells (23). However, few studies have addressed their possible role in beta cells. To better understand the role of $K_{ir}2.1$ channels in beta cells, we aimed to characterize it in INS-1(832/13) cells and isolated mouse islets under normal as well as stressed conditions. In this study, we used TM, which inhibited N-glycosylation to trigger ER stress in INS-1(832/13) cells or isolated mouse islets. ER stress response markers, cytosolic $Ca^{2+}$ activity and beta-cell apoptosis were measured after exposing islets or cells to TM with and without ML133, a selective and potent inhibitor of $K_{ir}2.1$ channels that was found in an unbiased screen of a large library of compounds (24). TM treatment increased cytosolic free $Ca^{2+}$ oscillations even in sub-threshold glucose (e.g., 5 mM glucose), as we reported previously (25). We found that the aberrant $Ca^{2+}$ signaling seen upon ER stress was suppressed by an overnight exposure to ML133. ML133 also inhibited UPR

activation and prevented the apoptosis induced in TM-treated INS-1(832/13) cells. ML133 acutely triggered a weak increase in cytosolic $Ca^{2+}$ in wildtype islets. Together, our results suggest that $K_{ir}2.1$ channels may represent a novel target of increasing insulin secretion under ER stress conditions.

## Materials and Methods

### *Materials*

Tunicamycin (TM) and thapsigargin (TG) were obtained from Cayman Chemical. ML133 and $BaCl_2$ were purchased from Sigma-Aldrich Products. RIPA lysis buffer was obtained from ThermoFisher Scientific. Signal Fire ECL reagents were purchased from Bio-Rad Laboratories. Rabbit anti-$K_{ir}2.1$ antibody (1:1000), Rabbit anti-GAPDH (1:1000), Mouse anti-KDEL (1:1000), horseradish peroxidase (HRP)-conjugated mouse anti-rabbit antibody (1:5000) and HPR-conjugated horse anti-mouse antibody (1:5000) were purchased from Cell Signaling Technology.

The standard culture RPMI 1640 medium contained 11 mM glucose, 10% fetal bovine serum (FBS), 10 mM HEPES, 1% penicillin/streptomycin and 1% sodium pyruvate. The culture medium contained RPMI 1640 medium, 5 mM glucose, 10% fetal bovine serum (FBS), 10 mM HEPES, 1% penicillin/streptomycin and 1% sodium pyruvate. The imaging solution contained 5 mM glucose, 140 mM NaCl, 3 mM $CaCl_2$, 5 mM KCl, 2mM $MgCl_2$ and 10 mM HEPES.

The RNeasy Mini Kit for qRT-PCR was from Qiagen. Superscript RT II was from Invitrogen. SYBR Green PCR master mix was from Applied Biosystems. Primers for qRT-PCR were from Integrated DNA Technologies with the sequences listed in Table 3.

***Preparation of pancreatic islets***

Pancreatic islets were prepared as described (25). Islets were isolated from wildtype male Swiss-Webster mice followed by culturing in standard RPMI 1640 medium. The islets were treated with 0.1% DMSO, 10 μM ML133, 10 μg/mL tunicamycin (TM) or 20 μM $BaCl_2$.

***Cell culture***

INS-1(832/13) cells were grown in the standard culture RPMI 1640 medium containing 11 mM glucose in 10 cm culture dishes at 37 °C in a 5% $CO_2$ humidified atmosphere. Cells were treated for experiments after reaching 70% confluency.

***Real-Time PCR***

Total RNA was extracted from INS-1(832/13) cells using the RNeasy Mini Kit and one μg of total RNA was reverse-transcribed using Superscript RT II according to the manufacturer's instructions. Genes of interest were amplified using the SYBR Green PCR master mix with primer sequences listed above. Data were presented as RQ values ($2^{-\Delta\Delta CT}$) with expression showed relative to an endogenous control HPRT1. The threshold-cycle (CT) values were obtained using the Step One software.

***Surface labeling assay***

Cell surface biotinylation assay was performed using a Pierce cell surface protein isolation kit following manufacturer's instructions (Pierce, ThermoFisher Scientific). Surface protein was

eluted in sample buffer containing DTT before resolving on an SDS-PAGE gel and analyzed by immunoblotting.

***Western blotting***

INS-1(832/13) cells were lysed with RIPA buffer, and total protein was extracted before separating using 4-12% SDS-PAGE and transferring to nitrocellulose membranes. Membranes were blocked in 5% w/v nonfat dry milk in 1X TBST buffer before overnight incubating with primary antibodies diluted in 5% nonfat dry milk in 1X TBST at 4 °C. Blots were incubated with HRP-conjugated secondary antibodies and then visualized using ECL reagents.

***Fura-2/AM imaging***

Islets were loaded with Fura-2/AM (2.5 $\mu$M) in the culture RPMI medium containing 5 mM glucose for 45 minutes at 37 °C before imaging. During imaging, the islets were fused with warm imaging solution containing 5 mM glucose at 1 mL/min, and ratiometric 340/380 nm excitation and 502 emission were carried out as previously described (26). The fluorescence data were acquired using Metafluor, and the traces were derived from Excel and presented in Prism.

***Statistical analysis***

Data were expressed as means +/- SEM. They were analyzed using an unpaired Student's t-test (Prism, GraphPad Software Solutions) when comparing two groups, and two-way ANOVA (Prism) with post hoc multiple comparisons by Tukey's procedure when comparing more two groups. Values of $p<0.05$ were considered statistically significant.

***Results***

$K_{ir}2.1$ channels play an essential role in cardiac cells, and $K_{ir}2.1$ is also expressed in beta cells, as evidenced by western blotting (23). To investigate the role of the channel in beta cells, we measured cytosolic free $Ca^{2+}$ in parallel with UPR markers to characterize the role of the channel in normal as well as stressed conditions. TM was used to trigger ER stress, and ML133 or $BaCl_2$ were used to inhibit the $K_{ir}2.1$ channels (27).

We first confirmed that $K_{ir}2.1$ channel protein was expressed in INS-1(832/13) cells and mouse islets (Figure 4.1A and 4.1B), and then whether protein levels were modulated under ER stress conditions. Measured levels of $K_{ir}2.1$ mRNA or protein in control (DMSO vehicle) or TM-treated INS-1(832/13) cells or mouse islets after 16 hours of exposure are shown in Figure 4.1A and 4.1B. As can be seen, $K_{ir}2.1$ mRNA levels were decreased by 45% and 75% compared to controls in INS-1(832/13) cells and mouse islets, respectively, in preparations treated with TM. In Figure 4.1C and 4.1D, it can be further seen that TM significantly reduced $K_{ir}2.1$ protein by ~50% in INS-1(832/13) cells.

The cytosolic $Ca^{2+}$ concentration of mouse islets does not typically exhibit oscillations when acutely exposed to glucose concentrations $<$7 mM (4). We previously reported that TM-treated mouse islets exhibited cytosolic $Ca^{2+}$ oscillations in 5 mM glucose, however, and that this leads to increased insulin secretion (25). As shown in Figure 4.2A, about 50% of islets exhibited $Ca^{2+}$ oscillations after overnight TM treatment (Figure 4.2B). As shown in Figure 4.2A, treating islets with ML133 overnight along with TM, prevented the oscillations seen in 5 mM glucose. Baseline $Ca^{2+}$ levels (Figure 4.3A) of all islets tested were analyzed, and they did not differ

between control and TM-treated islets, with or without ML133 being present during TM treatment (Figure 4.3A). The plateau fraction (Figure 4.3B), frequency (Figure 4.3C) and amplitude (Figure 4.3D) of the oscillations in TM-treated islets were analyzed. $Ba^{2+}$ (or $BaCl_2$) is a well-known ion blocker of $K_{ir}2.1$ channels (28). As with ML133, overnight treatment of $BaCl_2$ also inhibited the $Ca^{2+}$ oscillations that were triggered by TM exposure and observed acutely in 5 mM glucose (Figure 4.4).

To test if the increased cytosolic $Ca^{2+}$ activity required the activity of $K_{ir}2.1$ channels, ML133 was applied acutely to islets during recordings made in 5 mM glucose. As shown in Figure 4.5, ML133 slightly increased cytosolic $Ca^{2+}$ without causing oscillations in control islets. In TM-treated islets, ML133 acutely increased baseline $Ca^{2+}$ in 5 mM glucose, but oscillations persisted (Figure 4.5). Like $K_{ATP}$ channels, Kir2.1 channels conduct small outward $K^+$ currents at membrane potentials that are depolarized from -70 mV, but unlike $K_{ATP}$ they are not ATP-sensitive (29). Blocking the $K_{ir}2.1$ channels prevents the outward flow of $K^+$, and in theory can depolarize the cell membrane potential and lead to increased $Ca^{2+}$ influx if the blockade is sufficiently large. This may explain the increased baseline $Ca^{2+}$ in islets that were acutely exposed to ML133.

When glucose concentration is raised to 11 mM, the voltage-gated $Ca^{2+}$ channel is activated, and islets exhibit cytosolic $Ca^{2+}$ oscillations (30). We previously showed that these oscillations were not affected by TM treatment, except that TM tended to increase oscillation frequency (31). As shown in Figure 4.6A, control, ML133, TM and TM+ML133 treated islets all exhibited cytosolic $Ca^{2+}$ oscillations. The percentage of oscillations seen among all conditions were similar (Figure

4.6B). The frequency of the oscillations was higher in TM-treated islets than control, and the addition of ML133 decreased the frequency of TM-treated islets. The differences observed in the baseline, plateau fraction or amplitude among the groups, however, were not significant (Figure 4.7).

The change in XBP1 splicing, a canonical ER stress response marker, was determined at the mRNA level after treating INS-1(832/13) cells with DMSO, TM, ML133 or TM+ML133 in 11 mM glucose. As shown in Figure 4.8A, XBP1 splicing increased 7-fold after 6 hours of TM treatment in INS-1(832/13) cells. ML133 applied alone did not increase XBP1 splicing. Interestingly, when cells were treated with TM and ML133 together for 6 hours, the spliced XBP1 transcripts were reduced. Similarly, blocking $K_{ir}2.1$ channels using $BaCl_2$ also repressed the increasing spliced XBP1 level in TM-treated cells (Figure 4.8B, preliminary data). BiP is another ER stress response marker. As shown in Figure 4.8C and 4.8D, TM and ML133 both upregulated BiP protein expression after 16 hours of treatment. When cells were treated with TM and ML133 together overnight, the BiP protein level was higher compared to other groups (n=2).

Apoptosis has been shown to occur as a consequence of TM-induced ER stress (14, 25). Cleaved PARP protein was used here as a marker of apoptosis (32, 33). As shown in Figure 4.9 (preliminary data), cleaved PARP at 89 kDa was found in TM-treated INS-1(832/13) cells overnight, but not under conditions of control, ML133 or TM+ML133.

We further investigated the mechanism of TM stimulating $K_{ir}2.1$ channels activity in beta-cell. SUR1-deficient mice exhibited increased activity of $K_{ir}2.1$ channels (19). Therefore, we

examined whether SUR1 was regulated as an intermediary in this study. As shown in Figure 4.10, INS-1(832/13) cells treated with tunicamycin (TM) demonstrated a diminished level of SUR1 protein (seen at 170 kDa) on the plasma membrane, while total SUR1 expression remained unchanged. TM halted SUR1 proteins from trafficking to the plasma membrane and retained them within the ER lumen. Therefore, ER stress may activate $K_{ir}2.1$ channels as compensation for the reduced SUR1 protein on the plasma membrane.

***Discussion***

A previous modeling paper (19) and an unpublished experimental work (Vadrevu et al.) indicated compensation of SUR1 by $K_{ir}2.1$ channels to give normal free $Ca^{2+}$ oscillations in SUR1-deficient mice. In this study, we aimed to characterize $K_{ir}2.1$ channels in stressed conditions by exposing INS-1(832/13) cells or mouse islets to ER stress inducer TM overnight with and without $K_{ir}2.1$ channel inhibitors ML133 or $BaCl_2$. We found that overnight blockade of $K_{ir}2.1$ channels by ML133 or $BaCl_2$ suppressed TM-induced cytosolic $Ca^{2+}$ oscillations in 5 mM glucose (Figure 4.2 and Figure 4.4).

Acute inhibition of $K_{ir}2.1$ channels by ML133 or $BaCl_2$ did not abolish the cytosolic $Ca^{2+}$ oscillations in TM-treated islets (Figure 4.2 and Figure 4.4), so the influx of $Ca^{2+}$ might not be directly through $K_{ir}2.1$ channels. Our previous studies have reported increased cytosolic $Ca^{2+}$ and insulin secretion in TM-treated islets or beta cells resulted from the activation of store-operated $Ca^{2+}$ entry (SOCE). Therefore, $K_{ir}2.1$ channels may facilitate SOCE activation, which has been observed in other cell types. In microglia, blocking $K_{ir}2.1$ channels with ML133 has been shown to decrease $Ca^{2+}$ influx via SOCE (34). In brain capillary endothelial cells, inhibiting $K_{ir}2.1$

channels with $Ba^{2+}$ has been demonstrated to suppress cytosolic $Ca^{2+}$ increase through SOCE under hypoxic conditions (1). However, the mechanism underlying $K_{ir}2.1$ channels assisting SOCE activation remains uncovered.

Blocking $K_{ir}2.1$ channels by ML133 or $BaCl_2$ suppressed UPR activation that was evidenced by reduced sXBP1 mRNA levels in TM-treated INS-1(832/13) cells (Figure 4.8A and 4.8B). In addition, inhibiting $K_{ir}2.1$ channels by ML133 reversed cell apoptosis, as shown in Figure 4.9. (Please note that I intend to repeat the experiments when I return to the lab.) BiP is also a marker of the ER stress response. However, ML133 tends to increase BiP expression with and without TM treatment. Therefore, BiP, as a chaperone, may be increased to bind to $K_{ir}2.1$ and assist its folding and suppress UPR activation in response to TM-mediated reduced $K_{ir}2.1$ expression (This will be discussed in Chapter 5). Overexpression of BiP has been shown to alleviate ER stress in hIAPP-expressing beta cells (35) and high-fat-diet-induced diabetic mice (36).

The total protein expression and mRNA level of $K_{ir}2.1$ were both downregulated by TM in INS-1(832/13) cells (Figure 4.1). Therefore, $K_{ir}2.1$ channels activity may be enhanced to compensate for the partial loss of the channel expression. Whereas, there is another potential mechanism explaining TM-mediated enhanced $K_{ir}2.1$ channels activity. As shown in Figure 4.10, TM, as well as other well-known ER stress inducers, palmitate and thapsigargin, all halted SUR1 trafficking to the plasma membrane in INS 832/12 cells. Thus, we herein suggest a possibility that $K_{ir}2.1$ channels activity was increased to compensate for the loss of SUR1 under ER stress conditions.

This report appears to be the first demonstrating the involvement of $K_{ir}2.1$ channels in $Ca^{2+}$ oscillations in beta cells under ER stress conditions. We showed that inhibiting $K_{ir}2.1$ channels while inducing ER stress using TM in beta cells suppressed TM-induced cytosolic $Ca^{2+}$ oscillations in 5 mM glucose. We view this study as the first step in characterizing $K_{ir}2.1$ channels in beta cells. Future studies, such as $K_{ir}2.1$ trafficking, $K_{ir}2.1$ interaction with SOCE components and $K_{ir}2.1$ localization in beta cells under ER stress conditions and diabetic models are warranted.

## *Figures and legends*

Figure 1

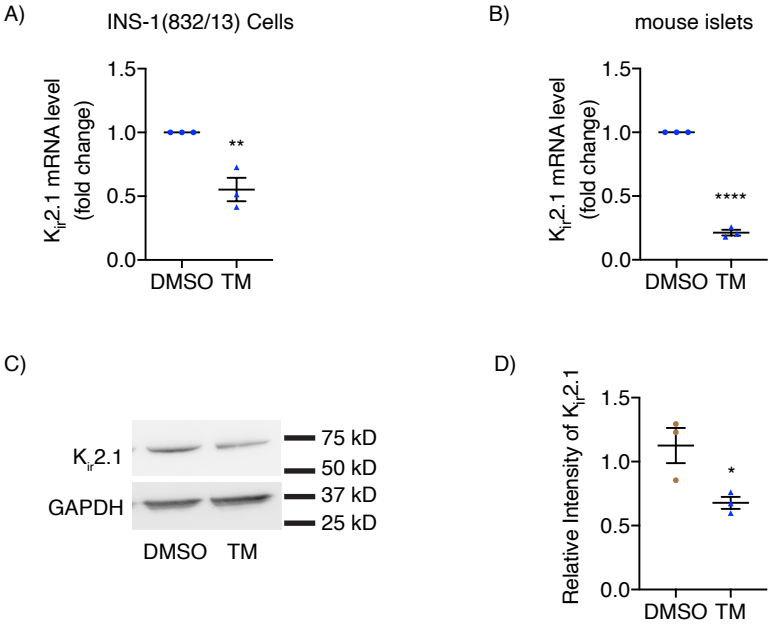


*Figure 4.1 Tunicamycin decreased $K_{ir}$2.1 expression*

INS-1(832/13) cells or isolated mouse islets were treated with vehicle control (DMSO) or tunicamycin (TM, 10 μg/ml) for 1A: 6 hours and 1B-C: 16 hours. 1A: Expression level of $K_{ir}$2.1 mRNA in INS-1(832/13) cells. 1B: Expression level of $K_{ir}$2.1 mRNA in mouse islets. 1C: Representative western blot showing the level of $K_{ir}$2.1 in INS-1(832/13) cells. GAPDH is a loading control. Quantitative protein levels are shown graphically in 1D. All values shown are means ± SEM, *, $p< 0.05$, **, $p< 0.01$, ****, $p<0.001$; n= at least 3 times repeated per condition, by student's t-test.

Figure 2

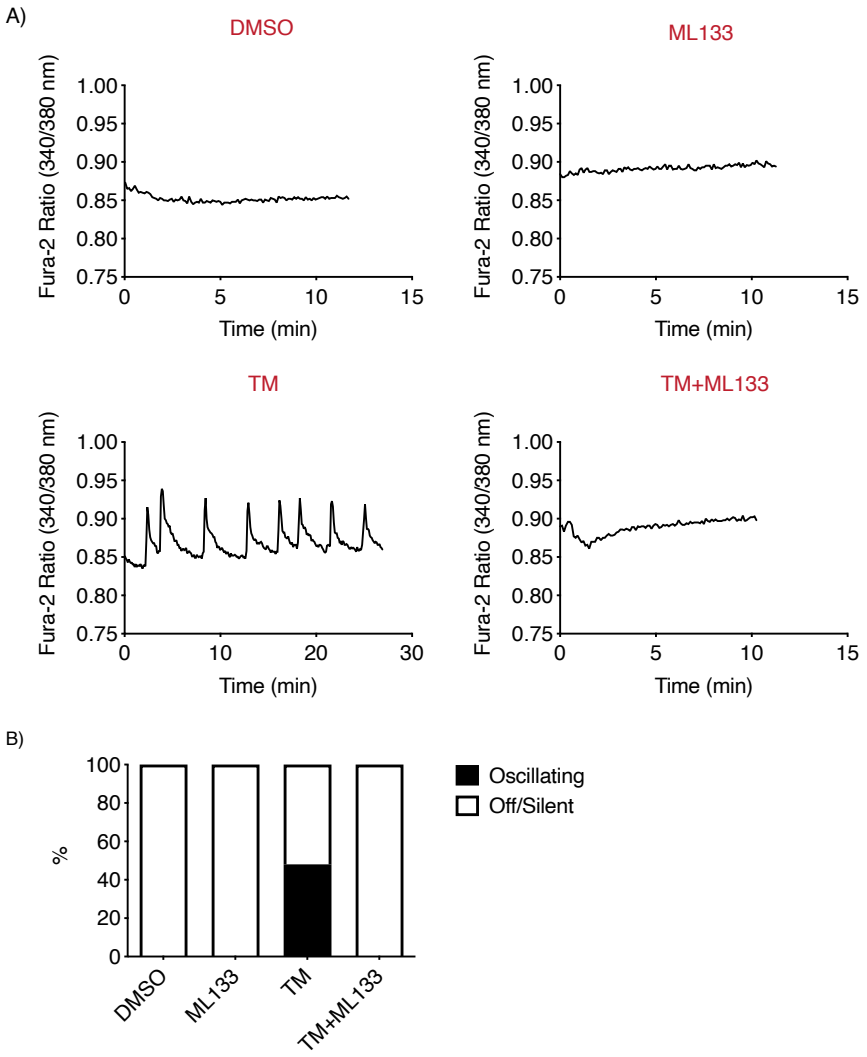


*Figure 4.2 ML133 prevented tunicamycin-induced increased cytosolic free $Ca^{2+}$ under sub-threshold glucose conditions*

Isolated pancreatic mouse islets were treated with a vehicle control (DMSO), ML133 (10 μM), tunicamycin (TM, 10 μg/ml) or ML133+TM for 16 hours in 11 mM glucose. 2A: The responses of cytosolic free $Ca^{2+}$ to the solution containing 5 mM glucose under the indicated conditions. 3B: Percentage of oscillating islets; n= at least 3 mice.

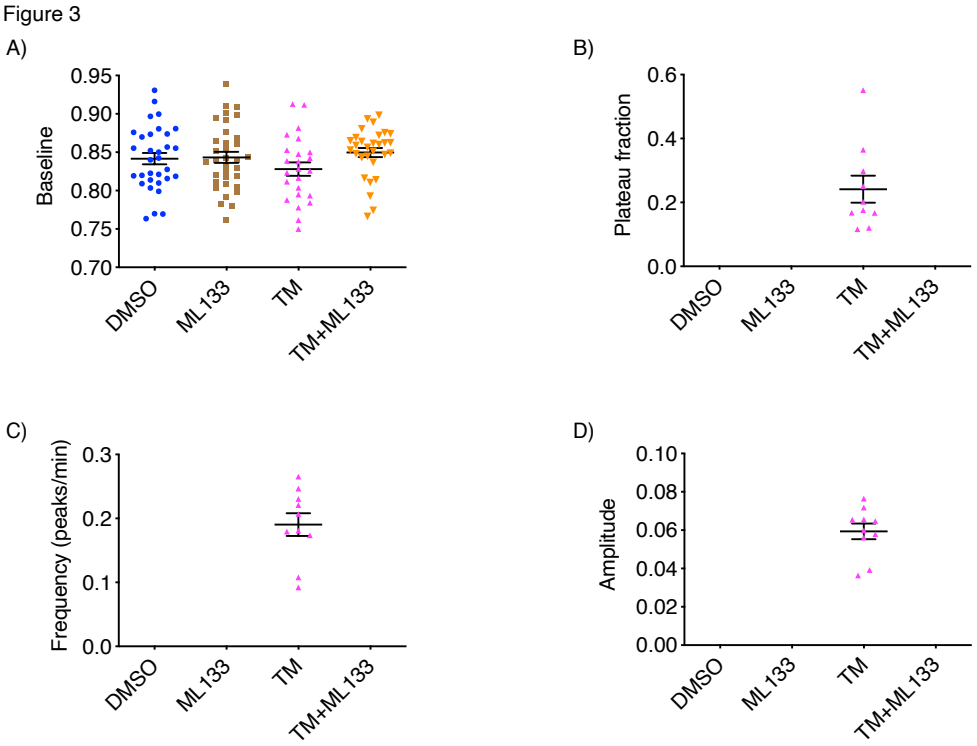


*Figure 4.3 Cytosolic free $Ca^{2+}$ imaging analysis*

Summary findings for the cytosolic free $Ca^{2+}$ traces shown in 2. 2A: Baseline values. 2B: Plateau fraction. 2C: oscillation frequency. 2D: oscillation amplitude. n= at least 3 mice.

Figure 4

A)

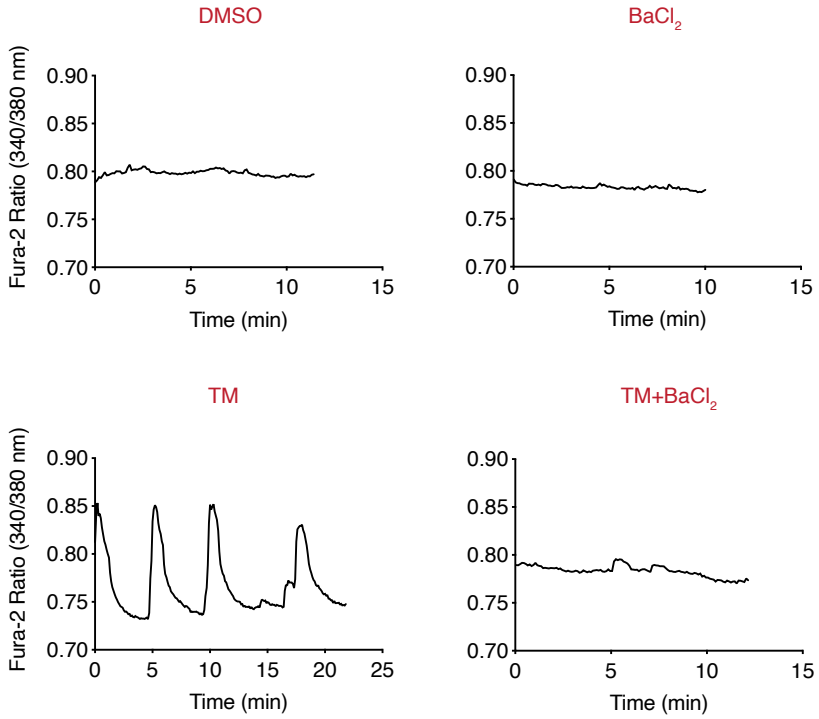


*Figure 4.4 $BaCl_2$ prevented tunicamycin-induced increased cytosolic free $Ca^{2+}$ under sub-threshold glucose conditions*

Isolated pancreatic mouse islets were treated with a vehicle control (DMSO), $BaCl_2$ (20 μM), tunicamycin (TM, 10 μg/ml) or $BaCl_2$+TM for 16 hours in 11 mM glucose. The responses of cytosolic free $Ca^{2+}$ to solution containing 5 mM glucose under the indicated conditions.

Figure 5

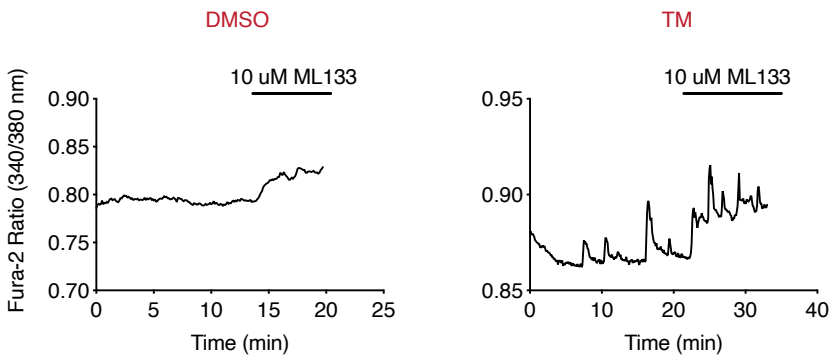


*Figure 4.5 Acute effect of ML133 on cytosolic free $Ca^{2+}$ under sub-threshold glucose conditions*

Isolated pancreatic mouse islets were treated with vehicle control (DMSO) or tunicamycin (TM, 10 μg/ml) for 16 hours in 11 mM glucose. The responses of cytosolic free $Ca^{2+}$ to the solution containing 5 mM glucose containing solution with or without ML133 (10 μM) under the indicated conditions.

Figure 6

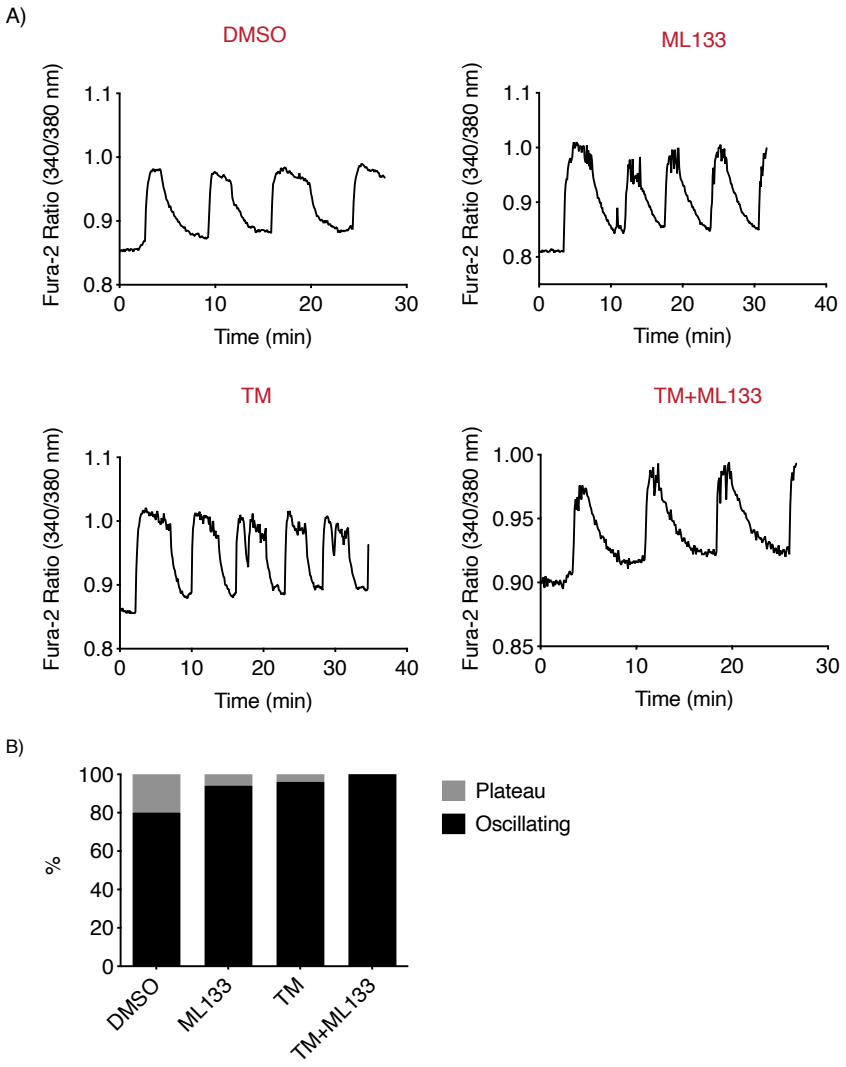


*Figure 4.6 Tunicamycin or ML133 did not affect cytosolic free $Ca^{2+}$ under suprathreshold glucose conditions*

Isolated pancreatic mouse islets were treated with a vehicle control (DMSO), ML133 (10 μM), tunicamycin (TM, 10 μg/ml) or ML133+TM for 16 hours in 11 mM glucose. 2A: The responses of cytosolic free $Ca^{2+}$ to the solution containing 11 mM glucose under the indicated conditions. 3B: Percentage of oscillating islets; n= at least 3 mice.

Figure 7

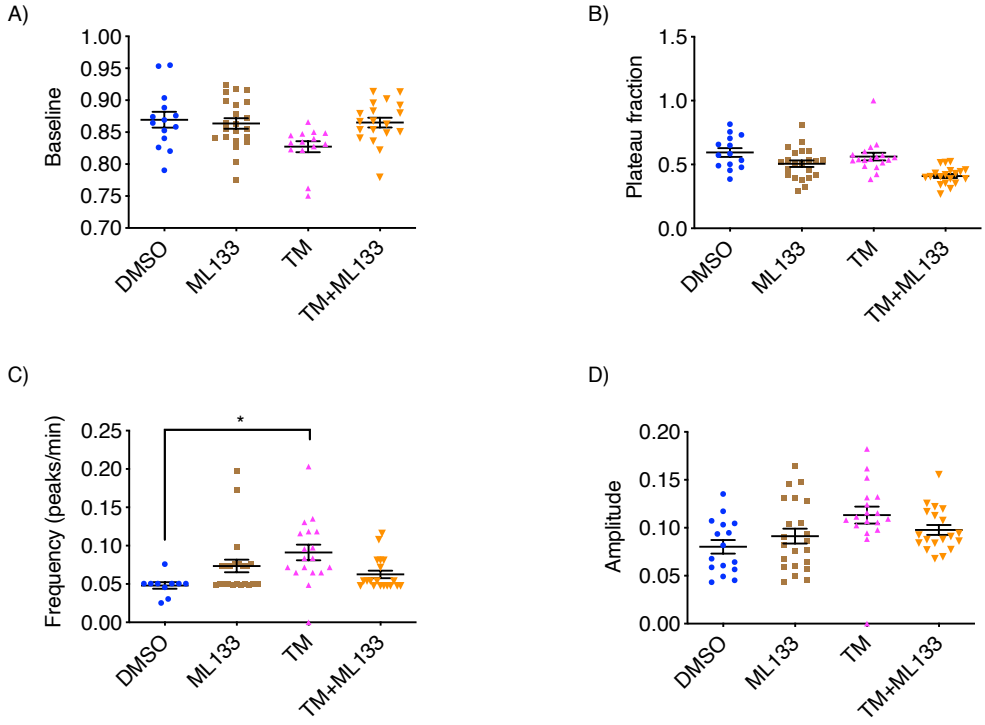


*Figure 4.7 Cytosolic free $Ca^{2+}$ imaging analysis under suprathreshold glucose conditions*

Summary findings for the cytosolic free $Ca^{2+}$ traces shown in 6. 6A: Baseline values. 6B: Plateau fraction. 6C: oscillation frequency. 6D: oscillation amplitude. #, $p< 0.05$; n= at least 3 mice.

Figure 8

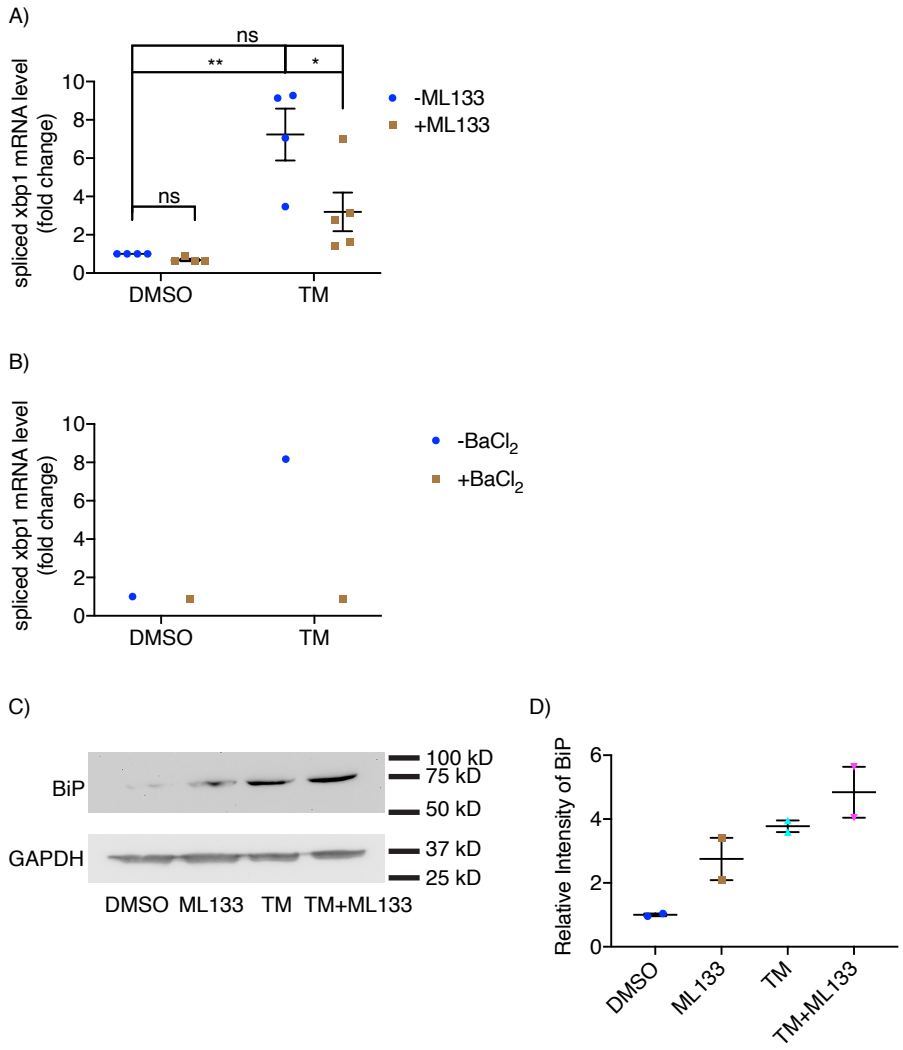


*Figure 4.8 Effects of $K_{ir}2.1$ inhibitor on UPR activation*

8A and 8C-D: INS-1(832/13) cells were treated with vehicle control (DMSO), ML133 (10 μM), tunicamycin (TM, 10 μg/ml) or ML133+TM for 16 hours in 11 mM glucose. 8A: Expression level of spliced XBP1 mRNA. Row Factor F(1, 13)= 24.75, p= 0.0003, Column Factor F(1, 13)= 6.147, p=0.0276, Interaction F(1, 13)= 4.478, p= 0.0542, by two-way ANOVA, n=3 times repeated per condition. 8B: INS-1(832/13) cells were treated with vehicle control (DMSO), $BaCl_2$ (20 μM), tunicamycin (TM, 10 μg/ml) or $BaCl_2$+TM for 16 hours in 11 mM glucose. Expression level of spliced XBP1 mRNA. n=1, preliminary data. 8C: Representative western blot showing the level of BiP in INS-1(832/13) cells. GAPDH is loading control. Quantitative protein levels are shown graphically in 8D. n=2 times repeated per condition.

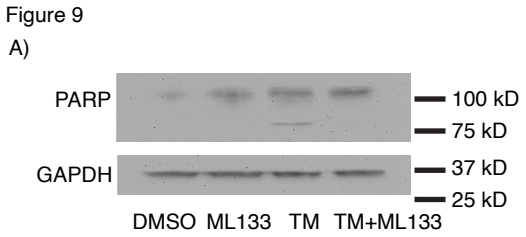


*Figure 4.9 ML133 prevented tunicamycin-induced beta-cell apoptosis*

INS-1(832/13) cells were treated with vehicle control (DMSO), ML133 (10 μM), tunicamycin (TM, 10 μg/ml) or ML133+TM for 16 hours in 11 mM glucose. Representative western blot showing the level of total PARP at 116 kDa and cleaved PARP at 89 kDa in INS-1(832/13) cells. GAPDH is shown as a loading control. n=1, preliminary data.

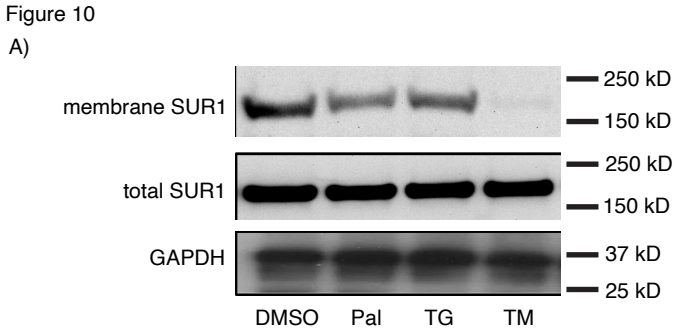


*Figure 4.10 ER stress inducers decreased SUR1 expression on the plasma membrane*

INS-1(832/13) cells were treated with vehicle control (DMSO), palmitate (Pal, 250 μM), thapsigargin (TG, 200 nM) or tunicamycin (TM, 10 μg/ml) for 16 hours in 11 mM glucose. 9A: Representative western blot showing the level of SUR1 in INS-1(832/13) cells. GAPDH is shown as loading control. n= 3 times repeated per condition.

Table 1

A)

| Gene | Forward | Reward |
|---|---|---|
| Xbp1s (rat) | CTGAGTCCGAATCAGGTGCAG | ATCCATGGGAAGATGTTCTGG |
| $K_{ir}2.1$ (rat) | TGCCCGATTGCTGTTTC | GGCTGTCTTCGTCTATTT |
| $K_{ir}2.1$ (mouse) | CACAGCTTCTCAAATCTAGGATCA | CTATTTCGTGAACGATAGTGATGG |
| Hprt1 (rat and mouse) | CTCATGGACTGATTATGGACAGGAC | GCAGGTCAGCAAAGAACTTATAGCC |

*Table 3 Primer sequences*

***References***


1. Yamamura, H., Suzuki, Y., Yamamura, H., Asai, K., and Imaizumi, Y. (2016) Hypoxic stress up-regulates Kir2.1 expression and facilitates cell proliferation in brain capillary endothelial cells. *Biochem. Biophys. Res. Commun.* **476**, 386–392

2. Yamamura, H., Suzuki, Y., Yamamura, H., Asai, K., Giles, W., and Imaizumi, Y. (2018) Hypoxic stress upregulates $K_{ir}$ 2.1 expression by a pathway including hypoxic-inducible factor-1α and dynamin2 in brain capillary endothelial cells. *Am. J. Physiol.-Cell Physiol.* **315**, C202–C213

3. CDC National diabetes statistics report, 2017

4. Satin, L. S., Butler, P. C., Ha, J., and Sherman, A. S. (2015) Pulsatile insulin secretion, impaired glucose tolerance and type 2 diabetes. *Mol. Aspects Med.* **42**, 61–77

5. Kahn, S. E. (2003) The relative contributions of insulin resistance and beta-cell dysfunction to the pathophysiology of Type 2 diabetes. *Diabetologia*. **46**, 3–19

6. Sabatini, P. V., Speckmann, T., and Lynn, F. C. (2019) Friend and foe: β-cell Ca2+ signaling and the development of diabetes. *Mol. Metab.* **21**, 1–12

7. Khan, F. A., Goforth, P. B., Zhang, M., and Satin, L. S. (2001) Insulin Activates ATP-Sensitive K+ Channels in Pancreatic -Cells Through a Phosphatidylinositol 3-Kinase-Dependent Pathway. *Diabetes*. **50**, 2192–2198

8. Ashcroft, F. M., and Rorsman, P. (2013) KATP channels and islet hormone secretion: new insights and controversies. *Nat. Rev. Endocrinol.* **9**, 660–669

9. Berridge, M. J., Bootman, M. D., and Roderick, H. L. (2003) Calcium signalling: dynamics, homeostasis and remodelling. *Nat. Rev. Mol. Cell Biol.* **4**, 517–529

10. Görlach, A., Klappa, P., and Kietzmann, Dr. T. (2006) The Endoplasmic Reticulum: Folding, Calcium Homeostasis, Signaling, and Redox Control. *Antioxid. Redox Signal.* **8**, 1391–1418

11. Fridlyand, L. E., and Philipson, L. H. (2016) Pancreatic Beta Cell G-Protein Coupled Receptors and Second Messenger Interactions: A Systems Biology Computational Analysis. *PloS One*. **11**, e0152869

12. Oslowski, C. M., and Urano, F. (2011) The binary switch that controls the life and death decisions of ER stressed β cells. *Curr. Opin. Cell Biol.* **23**, 207–215

13. Engin, F., Nguyen, T., Yermalovich, A., and Hotamisligil, G. S. (2015) Aberrant islet unfolded protein response in type 2 diabetes. *Sci. Rep.* **4**, 4054

14. Sano, R., and Reed, J. C. (2013) ER stress-induced cell death mechanisms. *Biochim. Biophys. Acta BBA - Mol. Cell Res.* **1833**, 3460–3470

15. Meyerovich, K., Ortis, F., Allagnat, F., and Cardozo, A. K. (2016) Endoplasmic reticulum stress and the unfolded protein response in pancreatic islet inflammation. *J. Mol. Endocrinol.* **57**, R1–R17

16. Cunha, D. A., Hekerman, P., Ladriere, L., Bazarra-Castro, A., Ortis, F., Wakeham, M. C., Moore, F., Rasschaert, J., Cardozo, A. K., Bellomo, E., Overbergh, L., Mathieu, C., Lupi, R., Hai, T., Herchuelz, A., Marchetti, P., Rutter, G. A., Eizirik, D. L., and Cnop, M. (2008) Initiation and execution of lipotoxic ER stress in pancreatic -cells. *J. Cell Sci.* **121**, 2308–2318

17. Back, S. H., and Kaufman, R. J. (2012) Endoplasmic Reticulum Stress and Type 2 Diabetes. *Annu. Rev. Biochem.* **81**, 767–793

18. Shyng, S., and Nichols, C. G. (1997) Octameric stoichiometry of the KATP channel complex. *J. Gen. Physiol.* **110**, 655–664

19. Yildirim, V., Vadrevu, S., Thompson, B., Satin, L. S., and Bertram, R. (2017) Upregulation of an inward rectifying K+ channel can rescue slow Ca2+ oscillations in K(ATP) channel deficient pancreatic islets. *PLoS Comput. Biol.* **13**, e1005686

20. Aittoniemi, J., Fotinou, C., Craig, T. J., de Wet, H., Proks, P., and Ashcroft, F. M. (2009) Review. SUR1: a unique ATP-binding cassette protein that functions as an ion channel regulator. *Philos. Trans. R. Soc. Lond. B. Biol. Sci.* **364**, 257–267

21. Hattersley, A. T., and Ashcroft, F. M. (2005) Activating Mutations in Kir6.2 and Neonatal Diabetes: New Clinical Syndromes, New Scientific Insights, and New Therapy. *Diabetes*. **54**, 2503–2513

22. Derst, C., Karschin, C., Wischmeyer, E., Hirsch, J. R., Preisig-Müller, R., Rajan, S., Engel, H., Grzeschik, K.-H., Daut, J., and Karschin, A. (2001) Genetic and functional linkage of Kir5.1 and Kir2.1 channel subunits. *FEBS Lett.* **491**, 305–311

23. Riz, M., Braun, M., Wu, X., and Pedersen, M. G. (2015) Inwardly rectifying Kir2.1 currents in human β-cells control electrical activity: Characterisation and mathematical modelling. *Biochem. Biophys. Res. Commun.* **459**, 284–287

24. Wang, H.-R., Wu, M., Yu, H., Long, S., Stevens, A., Engers, D. W., Sackin, H., Daniels, J. S., Dawson, E. S., Hopkins, C. R., Lindsley, C. W., Li, M., and McManus, O. B. (2011) Selective Inhibition of the $K_{ir}$ 2 Family of Inward Rectifier Potassium Channels by a Small Molecule Probe: The Discovery, SAR, and Pharmacological Characterization of ML133. *ACS Chem. Biol.* **6**, 845–856

25. Zhang, I. X., Ren, J., Vadrevu, S., Raghavan, M., and Satin, L. S. (2020) ER stress increases store-operated $Ca^{2+}$ entry (SOCE) and augments basal insulin secretion in pancreatic β cells. *J. Biol. Chem.* 10.1074/jbc.RA120.012721

26. Zhang, M., Goforth, P., Bertram, R., Sherman, A., and Satin, L. (2003) The Ca2+ Dynamics of Isolated Mouse β-Cells and Islets: Implications for Mathematical Models. *Biophys. J.* **84**, 2852–2870

27. Shen, N., Zheng, J., Liu, H., Xu, K., Chen, Q., Chen, Y., Shen, Y., Jiang, L., and Chen, Y. (2014) Barium chloride impaired Kir2.1 inward rectification in its stably transfected HEK 293 cell lines. *Eur. J. Pharmacol.* **730**, 164–170

28. Alagem, N., Dvir, M., and Reuveny, E. (2001) Mechanism of $Ba^{2+}$ block of a mouse inwardly rectifying $K^{+}$ channel: differential contribution by two discrete residues. *J. Physiol.* **534**, 381–393

29. Hodge, J. J. L. (2009) Ion channels to inactivate neurons in Drosophila. *Front. Mol. Neurosci.* **2**, 13

30. Bertram, R., Sherman, A., and Satin, L. S. (2010) Electrical Bursting, Calcium Oscillations, and Synchronization of Pancreatic Islets. in *The Islets of Langerhans* (Islam, Md. S. ed), pp. 261–279, Springer Netherlands, Dordrecht, **654**, 261–279

31. Nunemaker, C. S., Bertram, R., Sherman, A., Tsaneva-Atanasova, K., Daniel, C. R., and Satin, L. S. (2006) Glucose Modulates [Ca2+]i Oscillations in Pancreatic Islets via Ionic and Glycolytic Mechanisms. *Biophys. J.* **91**, 2082–2096

32. Boulares, A. H., Yakovlev, A. G., Ivanova, V., Stoica, B. A., Wang, G., Iyer, S., and Smulson, M. (1999) Role of Poly(ADP-ribose) Polymerase (PARP) Cleavage in Apoptosis: CASPASE 3-RESISTANT PARP MUTANT INCREASES RATES OF APOPTOSIS IN TRANSFECTED CELLS. *J. Biol. Chem.* **274**, 22932–22940

33. Chaitanya, G., Alexander, J. S., and Babu, P. (2010) PARP-1 cleavage fragments: signatures of cell-death proteases in neurodegeneration. *Cell Commun. Signal.* **8**, 31

34. Lam, D., and Schlichter, L. C. (2015) Expression and contributions of the Kir2.1 inward-rectifier K+ channel to proliferation, migration and chemotaxis of microglia in unstimulated and anti-inflammatory states. *Front. Cell. Neurosci.* 10.3389/fncel.2015.00185

35. Cadavez, L., Montane, J., Alcarraz-Vizán, G., Visa, M., Vidal-Fàbrega, L., Servitja, J.-M., and Novials, A. (2014) Chaperones ameliorate beta cell dysfunction associated with human islet amyloid polypeptide overexpression. *PloS One*. **9**, e101797

36. Teodoro-Morrison, T., Schuiki, I., Zhang, L., Belsham, D. D., and Volchuk, A. (2013) GRP78 overproduction in pancreatic beta cells protects against high-fat-diet-induced diabetes in mice. *Diabetologia*. **56**, 1057–1067

# Chapter 5 Concluding Remarks, Limitations and Future Directions

## *Conclusions*

Diabetes has been acknowledged as a medical problem for thousands of years. Scientists have been determinedly exploring treatment for T2DM, for instance, by gaining knowledge on the function and viability of the insulin-secreting pancreatic beta-cell. Recently, an increasing body of evidence has suggested the involvement of ER stress in causing T2DM (1–4) (and T1DM (3, 5, 6)), but the underlying mechanism remains largely unclear and requires additional studies. Therefore, this dissertation aims to define the interrelationship between ER stress and beta-cell function as well as beta-cell viability.

We mainly used the ER stress inducer TM to trigger ER stress in insulin-secreting INS-1(832/13) cells or isolated pancreatic mouse islets. As shown in chapter 2, we found that TM resulted in decreased ER [$Ca^{2+}$], increased cytosolic free $Ca^{2+}$ oscillations, membrane potential oscillations and insulin secretion even in sub-threshold glucose (e.g., 5 mM glucose) via SOCE activation. All these activities were abolished by the application of SOCE inhibitor YM58483 acutely.

Since we saw lowered ER [$Ca^{2+}$] as a result of TM treatment in islets, we then sought to determine through what mechanism TM depleted ER $Ca^{2+}$. The $IP_3$Rs and RyRs are known to gate $Ca^{2+}$ release from the ER to the cytosol and mitochondria (7–11). Therefore, we

pursued to determine their roles in altering beta-cell $Ca^{2+}$ homeostasis, particularly in mediating ER $Ca^{2+}$ release and disrupting $Ca^{2+}$ oscillations in the cytosol as well as mitochondria in the context of TM-induced ER stress. In chapter 3, we used XeC and Dan to block IP3Rs and RyR1, respectively, to treat INS-1(832/13) cells or mouse islets in the presence or absence of TM overnight. We saw that blocking RyR1 using Dan prevented TM-induced ER $Ca^{2+}$ depletion and increased $Ca^{2+}$ oscillations in the cytosol and mitochondria in 5 mM glucose. Nevertheless, inhibiting IP3Rs with XeC maintained ER [$Ca^{2+}$] but failed to affect TM- triggered $Ca^{2+}$ oscillations both in the cytosol as well as mitochondria. We also analyzed the effects of TM on IP3Rs and RyRs. RyR1 transcripts were upregulated, while RyR2 remained unchanged. In contrast, IP3R1 and IP3R2 transcripts were downregulated, and IP3R3 transcripts were unaffected.

Although SOCE was the downstream mechanism of TM-triggered increasing cytosolic $Ca^{2+}$ oscillations in 5 mM glucose, blocking these oscillations did not affect cell death. Therefore, we proposed that TM-triggered beta-cell death occurred via a separate pathway (Figure 2.16). As shown in Figure 1.2, reducing ER $Ca^{2+}$ can activate calpain 2, which is known to trigger beta-cell apoptosis through activating caspase 12 and JNK. Thus, we proposed that TM-induced beta-cell apoptosis was a result of ER $Ca^{2+}$ depletion. Since we suggested RyR1 to be a mechanism of TM-induced ER $Ca^{2+}$ loss, we further tested the role of RyR1 in TM-induced beta-cell apoptosis and found a preventive effect of Dan. XeC showed no impact on TM-induced apoptosis. In summary, we propose that increasing RyR1 is likely the mechanism of TM depleting ER $Ca^{2+}$ and, in turn, increasing cytosolic $Ca^{2+}$ oscillations, membrane potential oscillations, mitochondrial $Ca^{2+}$ oscillations, insulin secretion and beta-

cell apoptosis in normal sub-threshold glucose (Figure 3.10). However, more studies are needed to fully support the statement, as discussed in the next section.

Finally, we studied the inward rectifier $K^+$ channel $K_{ir}2.1$, a normally inactive surface $K^+$ channel in beta cells, in the context of ER stress. We tested the $K_{ir}2.1$-selective inhibitor ML133 and found that TM-induced cytosolic $Ca^{2+}$ oscillations were blocked by overnight exposure to ML133. ML133 also alleviated ER stress, evidenced by decreased spliced XBP1 and reduced apoptosis in TM-treated INS-1(832/13) cells. Besides, we observed a decrease in the trafficking of $K_{ATP}$ (SUR1) to the plasma membrane by TM. Thus, these results imply a possibility of TM triggering cytosolic $Ca^{2+}$ oscillations by switching from $K_{ATP}$ to $K_{ir}2.1$ channels, although more works are needed to conclude.

This dissertation mapped the mechanism of TM-induced ER stress disrupting beta-cell function and promoting beta-cell apoptosis. Three potential novel targets-- SOCE, RyR1 and $K_{ir}2.1$ channels, were identified as potential therapeutic strategies for T2DM and prediabetes. However, there are caveats present in the study.

### *Limitations and future directions*

There has been a concern of the D4ER $Ca^{2+}$ probe. In Figure 2.3B, although TM-induced decrease in ER [$Ca^{2+}$] was statistically significant, the data points between control and TM groups somewhat overlapped. The influx of $Ca^{2+}$ due to SOCE may have been too small to cause a detectable change in ER $Ca^{2+}$ due to limits in the $Ca^{2+}$ sensitivity of the D4ER probe. So far, the probe has not been calibrated. A subtle change in the ratio of D4ER (535/470)

may reflect a significant difference in ER [$Ca^{2+}$]. Recently, another genetically ER-targeted $Ca^{2+}$ sensor, GCEPIA1-$SNAP_{ER}$, has been made (12). Also, a genetically sarcoplasmic reticulum-targeted $Ca^{2+}$ sensor, R-CEPIA1er, has been used to measure ER [$Ca^{2+}$] (13). Therefore, we will test different ER $Ca^{2+}$ probes in the future.

In chapter 3, we showed that TM increased RyR1 messenger levels, but we failed to measure protein expression due to the lack of a practical antibody showing the requisite sensitivity of RyR1. We will need to test other antibodies from different suppliers, or we will seek collaborators who are experts on blotting RyRs in respect to the specialty of their considerable molecular weight (550 kDa).

The study relied on Dan to selectively block RyR1. Dan has been shown to inhibit RyR3, although the expression level of RyR3 in beta cells is very low compared to the other two isoforms (14, 15). Individually silencing RyR1 and RyR2 using siRNAs will determine which isoform mediates TM-induced ER $Ca^{2+}$ loss and subsequent activation of SOCE and disruption in intracellular $Ca^{2+}$ homeostasis. We hypothesize that RyR1 mediates ER $Ca^{2+}$ release. Therefore, we expect to see that silencing RyR1 would prevent TM-induced increased in cytosolic/mitochondrial $Ca^{2+}$ oscillations, membrane potential oscillations, insulin secretion in sub-threshold glucose (e.g., 5 mM glucose) and beta-cell apoptosis. Whereas, silencing RyR2 would not affect these alterations. Besides, it is important to use other ER stress inducers, such as palmitate, high glucose (25 mM glucose) or TG. Silencing IP3Rs is also a valuable approach, and we would expect these alterations to persist.

In chapter 4, we used $BaCl_2$ to block $K_{ir}2.1$ channels as an alternative to ML133. As with ML133, overnight exposure to $BaCl_2$ abolished cytosolic free $Ca^{2+}$ oscillations in TM-treated islets in 5 mM glucose. When studying the impact of inhibiting $K_{ir}2.1$ channels on Xbp1 splicing, we used both ML133 and $BaCl_2$. The data from $BaCl_2$ are preliminary so that additional repeats will be performed for publication. Besides Xbp1 splicing, we should test other ER stress response markers, such as PERK, CHOP, and ATF6. Silencing $K_{ir}2.1$ and then record cytosolic $Ca^{2+}$ oscillations and analyze insulin secretion are also fundamental approaches to confirm that $K_{ir}2.1$ is required for TM-induced ER stress to trigger cytosolic free $Ca^{2+}$ oscillations in 5 mM glucose. In addition to TM, Pal and TG both resulted in decreased surface SUR1 expression in INS-1(832/13) cells; however, they have not been used together with ML133 to measure cytosolic $Ca^{2+}$ oscillations and insulin secretion.

Figures 4.8C and 4.8D presented a trend of increasing BiP expression in ML133-treated INS-1(832/13) cells. Nevertheless, ML133 did not increase XBP1 splicing (Figure 4.8A) or beta-cell apoptosis (Figure 4.9). There are several possibilities: (1) ML133 has an off-target effect that enhances BiP expression; (2) Blocking $K_{ir}2.1$ channels causing protein misfolding, and in turn, BiP upregulates and corrects the misfolding without activating IRE1$\alpha$ and pro-apoptotic factors. (3) $K_{ir}2.1$ interacts with BiP and regulates BiP expression. Replacing ML133 with $BaCl_2$ or silencing $K_{ir}2.1$ and then measure BiP expression in INS-1(832/13) cells will shed some light on these questions.

In beta cells as well as other cells, cytosolic $Ca^{2+}$ rises and passes through the outer mitochondrial membrane (OMM) into the inner membrane space (IMS) through the voltage-

dependent anion-selective channel (VDAC) (10, 16, 17). $Ca^{2+}$ is then transferred from the IMS into the mitochondrial matrix via transporters, for instance, the mitochondrial $Ca^{2+}$ uniporter (MCU). MCU is found on the inner mitochondrial membrane (IMM) (10, 16, 17). Uptake of $Ca^{2+}$ by MCU is regulated by the mitochondrial $Ca^{2+}$ uptake 1 and 2 (MICU1 and MICU2) (17, 18). Mitochondrial $Ca^{2+}$ is released into the cytosol via the electrogenic mitochondrial $Na^{+}/Ca^{2+}$ exchanger (NCLX) and an $H^{+}/Ca^{2+}$ exchanger (10). The ER and mitochondria are two functionally and morphologically connected organelles, and the contacting area (mitochondria-associated membranes, MAMs) is critical for coordinating $Ca^{2+}$ signaling transmission. It has been proposed that the two organelles come even closer in the face of ER stress conditions in other cell types (19, 20). Therefore, it is important to study mitochondria function and particularly mitochondrial $Ca^{2+}$ regulation under ER stress conditions to fully understand beta-cell function. In chapter 2, we demonstrated increasing cytosolic $Ca^{2+}$ oscillations in 5 mM glucose occurred in 25 mM glucose or TG-treated islets. However, we haven't yet tested mitochondrial $Ca^{2+}$ oscillations in islets treated with alternative ER stress inducers.

The purpose of SOCE activation in response to ER $Ca^{2+}$ depletion is believed to refill $Ca^{2+}$ so that ER homeostasis is eventually restored. However, blocking SOCE in TM-treated islets did not restore ER [$Ca^{2+}$] (Figure 2.11A), which was unexpected. There are two possible explanations: 1. RyRs act as a leaky faucet and continuously gate $Ca^{2+}$ release from the ER, which is possible as ER [$Ca^{2+}$] was able to be restored (even increased) by Dan in TM-treated islets (Figure 3.4B). 2. It has been shown that SERCA2b is downregulated (21) so that it cannot pump as much $Ca^{2+}$ into the ER from the cytosol.

RyRs and IP3Rs both mediate ER $Ca^{2+}$ release into the cytosol and mitochondria (9–11). In chapter 3, we showed that inhibiting RyRs with Dan blocked TM-induced $Ca^{2+}$ oscillations in the cytosol as well as mitochondria in 5 mM glucose; whereas, inhibiting IP3Rs with XeC showed no effect on the oscillations. These results generally agreed with Yamamoto *et al.,* where they showed RyRs were activated in response to TM, but IP3Rs were not activated (although we proposed an utterly different mechanism of ER stress-inducing cytosolic $Ca^{2+}$ oscillations). They reported the activation of IP3Rs after beta cells being exposed to proinflammatory cytokines (15). It is puzzling why the two receptors have different preferences for chemicals. One possibility is that the two receptors manage different pools of ER $Ca^{2+}$, and these pools have distinct downstream signaling effects. Studying the localization of IP3Rs and RyRs, and their distance SOCE components and mitochondria, under ER stress conditions, may clarify the question. Another possibility is that RyRs, but not IP3Rs, regulate ER stress independently of handling ER $Ca^{2+}$. We only measured XBP1 splicing, but there are three pathways within the UPR signaling cascade. Therefore, we need to look at multiple ER stress response markers and other components in the UPR pathway. In addition, it is essential to differentiate IP3Rs and RyRs in diabetic animal models, and even in diabetic human islets.

In response to blood glucose elevation (>7 mM glucose), $K_{ATP}$ channels close and result in depolarization of the plasma membrane, which triggers the opening of the voltage-gated-$Ca^{2+}$ channels (VGCC) and mediates $Ca^{2+}$ influx (22, 23). In fact, these are high voltage-activated L-type VGCC, and they are considered the most critical $Ca^{2+}$ entry pathway regulating

insulin release in beta cells (24). There are other inward voltage-dependent $Ca^{2+}$ channels in human pancreatic beta cells, such as P/Q-type $Ca^{2+}$ channels, N-type $Ca^{2+}$ channels and low-voltage-activated T-type $Ca^{2+}$ channels (24). For example, in rat INS-1 cells, T-type $Ca^{2+}$ currents have been recorded using whole-cell patch-clamp techniques, and they've been shown to facilitate insulin secretion in 11 mM glucose (25). $NiCl_2$ is a T-type $Ca^{2+}$ channel inhibitor, and it blocked the channel current and decreased insulin secretion in INS-1 cells (25). T-type $Ca^{2+}$ channels are activated and contribute to increases in cytosolic $Ca^{2+}$ and cell death in beta cells after exposing the cells to cytokines (26). T-type $Ca^{2+}$ currents have also been found to be enhanced in streptozocin-induced diabetic rats (27). Therefore, expanding our focus on other $Ca^{2+}$ channels and incorporate our findings into a broader scope will be useful for a more comprehensive understanding of beta-cell function.

In summary, this dissertation advances the understanding of the beta-cell function and beta-cell apoptosis, particularly in the face of ER stress. It not only proposes three potential therapeutic targets, which are SOCE, RyR1 and $K_{ir}2.1$ channels, for T2DM and prediabetics but also points out new directions for future beta-cell studies.

***References***


1. Sabatini, P. V., Speckmann, T., and Lynn, F. C. (2019) Friend and foe: β-cell Ca2+ signaling and the development of diabetes. *Mol. Metab.* **21**, 1–12

2. Hetz, C., and Papa, F. R. (2018) The Unfolded Protein Response and Cell Fate Control. *Mol. Cell*. **69**, 169–181

3. Meyerovich, K., Ortis, F., Allagnat, F., and Cardozo, A. K. (2016) Endoplasmic reticulum stress and the unfolded protein response in pancreatic islet inflammation. *J. Mol. Endocrinol.* **57**, R1–R17

4. Arunagiri, A., Haataja, L., Pottekat, A., Pamenan, F., Kim, S., Zeltser, L. M., Paton, A. W., Paton, J. C., Tsai, B., Itkin-Ansari, P., Kaufman, R. J., Liu, M., and Arvan, P. (2019) Proinsulin misfolding is an early event in the progression to type 2 diabetes. *eLife*. **8**, e44532

5. Clark, A. L., and Urano, F. (2016) Endoplasmic reticulum stress in beta cells and autoimmune diabetes. *Curr. Opin. Immunol.* **43**, 60–66

6. Engin, F. (2016) ER stress and development of type 1 diabetes. *J. Investig. Med.* **64**, 2–6

7. Graves, T. K., and Hinkle, P. M. (2003) $Ca^{2+}$ -Induced $Ca^{2+}$ Release in the Pancreatic β-Cell: Direct Evidence of Endoplasmic Reticulum $Ca^{2+}$ Release. *Endocrinology*. **144**, 3565–3574

8. Dyachok, O., Tufveson, G., and Gylfe, E. (2004) Ca2+-induced Ca2+ release by activation of inositol 1,4,5-trisphosphate receptors in primary pancreatic β-cells. *Cell Calcium*. **36**, 1–9

9. Wacquier, B., Combettes, L., Van Nhieu, G. T., and Dupont, G. (2016) Interplay Between Intracellular Ca2+ Oscillations and Ca2+-stimulated Mitochondrial Metabolism. *Sci. Rep.* **6**, 19316

10. Idevall-Hagren, O., and Tengholm, A. (2020) Metabolic regulation of calcium signaling in beta cells. *Semin. Cell Dev. Biol.* 10.1016/j.semcdb.2020.01.008

11. Hajnóczky, G., Csordás, G., Das, S., Garcia-Perez, C., Saotome, M., Sinha Roy, S., and Yi, M. (2006) Mitochondrial calcium signalling and cell death: Approaches for assessing the role of mitochondrial Ca2+ uptake in apoptosis. *Cell Calcium*. **40**, 553–560

12. Luo, C., Wang, H., Liu, Q., He, W., Yuan, L., and Xu, P. (2019) A genetically encoded ratiometric calcium sensor enables quantitative measurement of the local calcium microdomain in the endoplasmic reticulum. *Biophys. Rep.* **5**, 31–42

13. Bovo, E., Martin, J. L., Tyryfter, J., de Tombe, P. P., and Zima, A. V. (2016) R-CEPIA1er as a new tool to directly measure sarcoplasmic reticulum [Ca] in ventricular myocytes. *Am. J. Physiol.-Heart Circ. Physiol.* **311**, H268–H275

14. Zhao, F., Li, P., Chen, S. R. W., Louis, C. F., and Fruen, B. R. (2001) Dantrolene Inhibition of Ryanodine Receptor Ca $^{2+}$ Release Channels: MOLECULAR MECHANISM AND ISOFORM SELECTIVITY. *J. Biol. Chem.* **276**, 13810–13816

15. Yamamoto, W. R., Bone, R. N., Sohn, P., Syed, F., Reissaus, C. A., Mosley, A. L., Wijeratne, A. B., True, J. D., Tong, X., Kono, T., and Evans-Molina, C. (2019) Endoplasmic reticulum stress alters ryanodine receptor function in the murine pancreatic β cell. *J. Biol. Chem.* **294**, 168–181

16. Wacquier, B., Combettes, L., and Dupont, G. (2019) Cytoplasmic and Mitochondrial Calcium Signaling: A Two-Way Relationship. *Cold Spring Harb. Perspect. Biol.* **11**, a035139

17. Xu, Z., Zhang, D., He, X., Huang, Y., and Shao, H. (2016) Transport of Calcium Ions into Mitochondria. *Curr. Genomics*. **17**, 215–219

18. Plovanich, M., Bogorad, R. L., Sancak, Y., Kamer, K. J., Strittmatter, L., Li, A. A., Girgis, H. S., Kuchimanchi, S., De Groot, J., Speciner, L., Taneja, N., OShea, J., Koteliansky, V., and Mootha, V. K. (2013) MICU2, a Paralog of MICU1, Resides within the Mitochondrial Uniporter Complex to Regulate Calcium Handling. *PLoS ONE*. **8**, e55785

19. Prasad, M., Walker, A. N., Kaur, J., Thomas, J. L., Powell, S. A., Pandey, A. V., Whittal, R. M., Burak, W. E., Petruzzelli, G., and Bose, H. S. (2016) Endoplasmic Reticulum Stress Enhances Mitochondrial Metabolic Activity in Mammalian Adrenals and Gonads. *Mol. Cell. Biol.* **36**, 3058–3074

20. Li, J., Zhang, D., Brundel, B. J. J. M., and Wiersma, M. (2019) Imbalance of ER and Mitochondria Interactions: Prelude to Cardiac Ageing and Disease? *Cells*. **8**, 1617

21. Tong, X., Kono, T., Anderson-Baucum, E. K., Yamamoto, W., Gilon, P., Lebeche, D., Day, R. N., Shull, G. E., and Evans-Molina, C. (2016) SERCA2 Deficiency Impairs Pancreatic β-Cell Function in Response to Diet-Induced Obesity. *Diabetes*. **65**, 3039–3052

22. Khan, F. A., Goforth, P. B., Zhang, M., and Satin, L. S. (2001) Insulin Activates ATP-Sensitive K+ Channels in Pancreatic -Cells Through a Phosphatidylinositol 3-Kinase-Dependent Pathway. *Diabetes*. **50**, 2192–2198

23. Ashcroft, F. M., and Rorsman, P. (2013) KATP channels and islet hormone secretion: new insights and controversies. *Nat. Rev. Endocrinol.* **9**, 660–669

24. Sher, E., Giovannini, F., Codignola, A., Passafaro, M., Giorgi-Rossi, P., Volsen, S., Craig, P., Davalli, A., and Carrera, P. (2003) Voltage-Operated Calcium Channel Heterogeneity in Pancreatic Cells: Physiopathological Implications. *J. Bioenerg. Biomembr.* **35**, 687–696

25. Bhattacharjee, A., Whitehurst, R. M., Zhang, M., Wang, L., and Li, M. (1997) T-Type Calcium Channels Facilitate Insulin Secretion by Enhancing General Excitability in the Insulin-Secreting β-Cell Line, INS-1*. *Endocrinology*. **138**, 3735–3740

26. Wang, L., Bhattacharjee, A., Zuo, Z., Hu, F., Honkanen, R. E., Berggren, P.-O., and Li, M. (1999) A Low Voltage-Activated Ca2+ Current Mediates Cytokine-Induced Pancreatic β-Cell Death*. *Endocrinology*. **140**, 1200–1204

27. Kato, S., Ishida, H., Tsuura, Y., Okamoto, Y., Tsuji, K., Horie, M., Okada, Y., and Seino, Y. (1994) Increased calcium-channel currents of pancreatic β cells in neonatally streptozocin-induced diabetic rats. *Metabolism*. **43**, 1395–1400